Supporting Information

Small bite-angle phosphinophosphinine ligands enable rhodium catalysed hydroboration of carbonyls

Robert. J. Newland, Jason M. Lynam and Stephen. M. Mansell*

Contents

Experimental

General experimental details

All reactions were performed under an oxygen-free nitrogen atmosphere using standard Schlenk line techniques or by using an MBRAUN UNIlab Plus glovebox unless otherwise noted. Anhydrous toluene and dichloromethane were obtained from an MBRAUN SPS-800, 40-60 petroleum ether was distilled from sodium wire. $CDCl_3$ was dried over calcium hydride, C_6D_6 was dried over molten potassium then trap-to-trap distilled under a static vacuum. All anhydrous solvents were degassed before use and stored over activated 4 Å MS, non-dry solvents were used as received from Fisher Scientific. Catecholborane was trap-to-trap distilled under a static vacuum before being stored at -25°C in the glovebox freezer. [{Rh(COD)Cl}$_2$], **2**, **4**, PCy_3 and [$Rh(PPh_3)_3Cl$] were stored under nitrogen. Air sensitive samples for NMR spectroscopy were prepared in NMR tubes equipped with a Young's tap. NMR spectra were recorded on a Bruker AVIII300 (300 MHz), AVI400 (400 MHz) or AVIII400 (400 MHz) spectrometer at 25°C unless otherwise noted. ^{1}H and ^{13}C NMR spectra were referenced to internal residual protio-solvent resonances, ^{11}B, ^{29}Si, ^{19}F and ^{31}P were referenced to external samples of $BF_3.OEt_2$, $SiMe_4$, $CFCl_3$ and 85% H_3PO_4 in H_2O respectively as 0 ppm. 2-diphenylphosphino-3-methyl-6-trimethylsilyl phosphinine (**1**), [Ru(**1**)$_2$Cl$_2$] (**4**),[1] [{Rh(CO)$_2$Cl}$_2$],[2] Na[BAr^F],[3] [$Rh(PPh_3)_3Cl$],[4] [{Rh(COD)Cl}$_2$],[5] [Rh(COD)$_2$][BAr^F],[6] phenyl (1-phenylethylidene)amine, phenyl (1-{4-fluorophenyl}ethylidene)amine, phenyl (1-{4-methylphenyl}ethylidene)amine and 4-nitrophenyl (1-phenylethylidene)amine[7] were prepared according to the literature methods. All other reagents were commercially available. Mass spectrometry data, using an Atmospheric-Pressure Solids Analysis Probe, was obtained on a Waters Xevo G2-S instrument at the EPSRC UK National Mass Spectrometry Facility at Swansea University (compounds **2** and **3**). FTIR was performed on a Thermo Scientific Nicolet iS5/iD5 ATR spectrometer. Elemental analyses were conducted using an Exeter CE-440 elemental analyser at Heriot-Watt University or by Mr Stephen Boyer at London Metropolitan University.

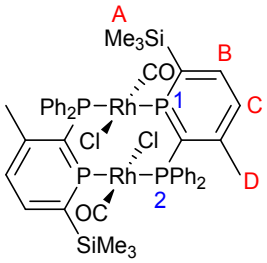

Compound 2

A Schlenk flask was charged with proligand **1** (186 mg, 0.5 mmol) and [{Rh(CO)$_2$Cl}$_2$] (99 mg, 0.25 mmol, 0.5 equiv). With efficient stirring, toluene (5 cm^3) was added, affording a deep purple solution with concomitant evolution of carbon monoxide. The reaction was stirred for 5 minutes at room temperature before concentration of the heterogeneous mixture to ~1 cm^3. The reaction mixture was stored at -25°C for 48h before the product was separated by cold cannula filtration and dried under high vacuum, yielding analytically pure **2.PhMe** as an air-sensitive deep purple crystalline powder (181 mg 0.16 mmol, 63 %). The filtrate still held a purple colour, however no further pure material could be obtained. Crystals suitable for X-ray diffraction were grown from slow diffusion of 40-60 petrol into a C_6D_6 solution (~5:1) of the complex.

^{1}H-NMR (400 MHz, 25 °C, $CDCl_3$): δ = 8.10-7.19 (m, 29H, 2x (*H$_B$*, *H$_C$*, P*Ph$_2$*), and *Ph*Me solvate), 2.40 (s, 3H, Ph*Me*), 2.00 (s, 6H, 2x *H$_D$*), 0.57 (s, 18H, 2x *H$_A$*); **^{31}P{^{1}H}-NMR (162 MHz, 25 °C, $CDCl_3$):** δ = 250.6 (app. dt, *P$_1$* $^2J_{P1\text{-}P2}$ = 137.3 Hz, $^1J_{P1\text{-}Rh}$ = -143.6 Hz, $^2J_{P1\text{-}P4}$ = -430.3 Hz), 25.5 (app. dt, *P$_2$*, $^2J_{P2\text{-}P1}$ = 137.3 Hz, $^1J_{P2\text{-}Rh}$ = -138.7 Hz, $^2J_{P1\text{-}P4}$ = -430.3 Hz); **^{13}C{^{1}H}-NMR (100 MHz, 25 °C, $CDCl_3$):** δ = 187.2-186.2 (m, 2x *C*O), 159.3-158.6 (m, 2x phosphinine *C*, *J* = 14.7 Hz), 154.3 (d, 2x phosphinine *C*), 148.4-147.6 (m, 2x phosphinine *C*), 144.0 (d, 2x *C$_B$*, $^2J_{CB\text{-}P1}$ = 18.4 Hz), 137.9 (s, *Ph*Me), 133.8-132.0 (m, 2x P*Ph$_2$*), 130.3 (dd, 2x *C$_C$*, $^3J_{CC\text{-}P1}$ = 32.2 Hz, $^3J_{CC\text{-}P2}$ = 4.6 Hz), 129.7-127.7 (m, *Ph*Me, 2x P*Ph$_2$*), 125.4 (s, *Ph*Me), 27.1 (s, 2x *C$_D$*), 21.5 (s, Ph*Me*) 1.1 (d, 2x *C$_A$*, $^3J_{CA\text{-}P1}$ = 2.8 Hz); **^{29}Si{^{1}H}-NMR (79 MHz, 25 °C, $CDCl_3$):** δ = 1.5 (d, $^2J_{Si\text{-}P1}$ = 25.0 Hz); **HRMS (ASAP/QTof)** *m/z*: ([M-Cl-2CO]$^+$) Calcd. for $C_{42}H_{49}P_4Rh_2Si_2$: 973.0043; Found: 973.0040; **FTIR (ATR):** ν(cm^{-1}) 1977 (CO); **Elemental Analysis:** Anal. Calcd. for $C_{44}H_{48}Cl_2O_2P_4Rh_2Si_2$: C 49.58, H 4.54; Found: C 49.04, H 4.57.

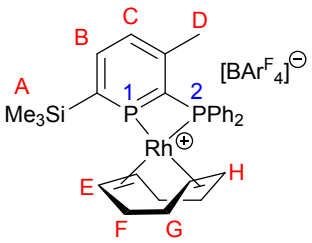

Compound 3

A Schlenk flask was charged with proligand **1** (149 mg, 0.41 mmol) and [Rh(COD)$_2$][BAr$^F_4$] (482 mg, 0.41 mmol, 1 equiv). CH_2Cl_2 (5 cm^3) was added and the resulting dark red solution stirred for 10 minutes before being concentrated to ~1 cm^3. 40-60 petrol ether (20 cm^3) was added and the resulting biphasic system stirred at high speed overnight. The pale red top layer was then removed by cannulation and discarded, leaving a sticky red oil. The contents of the flask were slowly subjected to high vacuum, and the resulting solid dried thoroughly under high vacuum to leave analytically pure **3** as an air-stable orange crystalline powder (473 mg, 0.33 mmol, 80%). Crystals suitable for X-ray diffraction were grown from slow diffusion of pentane into a concentrated $CDCl_3$ solution (~10:1) of the complex at -25°C.

^{1}H-NMR (400 MHz, 25 °C, $CDCl_3$): δ = 8.15 (ddd, 1H, *H$_B$*, $^4J_{HC\text{-}P1}$ = 24.94 Hz, $^3J_{HC\text{-}HB}$ = 8.51 Hz, $^4J_{HB\text{-}P2}$ = 0.88 Hz), 7.76-7.55 (m, 22H, B*Ar*^{F} & P*Ph*$_2$), 7.45-7.41 (m, 1H, *H$_B$*), 5.90 (bs, 2H, *H$_E$*), 5.02 (bs, 2H, *H$_H$*), 2.56-2.28 (m, 8H, *H$_F$* & *H$_G$*), 2.10 (s, 3H, *H$_D$*), 0.40 (s, 9H, *H$_A$*); **^{31}P{^{1}H}-NMR (162 MHz, 25 °C, $CDCl_3$):** δ = 189.4 (app. dd, *P$_1$*, $^2J_{P1\text{-}P2}$ = 16.0 Hz, $^1J_{P1\text{-}Rh}$ = 122.9 Hz), -6.8 (app. dd, *P$_2$*, $^2J_{P2\text{-}P1}$ = 16.0 Hz, $^1J_{P2\text{-}Rh}$ = 148.2 Hz); **^{13}C{^{1}H}-NMR (100 MHz, 25 °C, $CDCl_3$):** δ = 167.2 (d, phosphinine C, *J* = 24.8 Hz), 161.7 (q, 4x *C*-B, $^1J_{C\text{-}B}$ = 49.5 Hz), 153.6-152.7 (m, phosphinine *C*), 151.5-151.2 (m, phosphinine *C*), 145.0 (d,*C$_B$*, $^2J_{CB\text{-}P1}$ = 18.4 Hz), 134.8 (s, BAr$^F_4$), 132.9-132.5 (m, P*Ph$_2$*), 131.9 (dd, *C$_C$*, $^3J_{CC\text{-}P1}$ = 38.4 Hz, $^3J_{CC\text{-}P2}$ = 8.0 Hz), 129.9 (d, P*Ph$_2$*, *J* = 11.2 Hz), 128.9 (qq, BAr$^F_4$, $^2J_{F\text{-}C}$ = 32.0 Hz, $^3J_{C\text{-}B}$ = 3.2 Hz), 126.4 (dd, P*Ph$_2$*, J = 43.1 Hz, 5.6 Hz), 117.5 (t, BAr$^F_4$ $^3J_{C\text{-}F}$ = 3.2 Hz), 100.8 (dd, *C$_E$*, J = 9.6, 6.4 Hz), 95.4 (t, *C$_H$*, J = 9.6 Hz), 30.9 (s, *C$_E$*), 29.7 (s, *C$_H$*), 21.4 (t, *C$_D$*, $^3J_{CD\text{-}P1}$ = 6.4 Hz), 124.5 (q, BAr$^F_4$, $^1J_{C\text{-}F}$ =273.2 Hz), 134.33 (dd, P*Ph$_2$*), 130.48 (dd, *C$_D$*, $^2J_{CD\text{-}P1}$ = 20.8 Hz, $^4J_{CD\text{-}P2}$ = 4.0 Hz), -0.7 (d, *C$_A$*, $^3J_{C\text{-}P1}$ = 3.2 Hz); **^{19}F-NMR (376 MHz, 25°C, $CDCl_3$):** -62.4 (s, 24F, BAr$^F_4$); **^{11}B{^{1}H}-NMR (128 MHz, 25°C, $CDCl_3$):** δ = 6.6 (s, 1B, BAr$^F_4$); **^{29}Si{^{1}H}-NMR (79 MHz, 25 °C, $CDCl_3$):** δ = 0.2 (dd, $^2J_{Si\text{-}P1}$ = 20.5 Hz, $^4J_{Si\text{-}P2}$ = 2.6 Hz); **HRMS (ASAP/Qtof)** *m/z*: ([M-BAr^F]$^+$) Calcd. for $C_{29}H_{36}P_2RhSi$: 577.1116; Found : 577.1127; **Elemental Analysis:** Anal. Calcd. for $C_{61}H_{48}BF_{24}P_2RhSi$: C 50.85, H 3.36; Found: C 50.94, H 3.24.

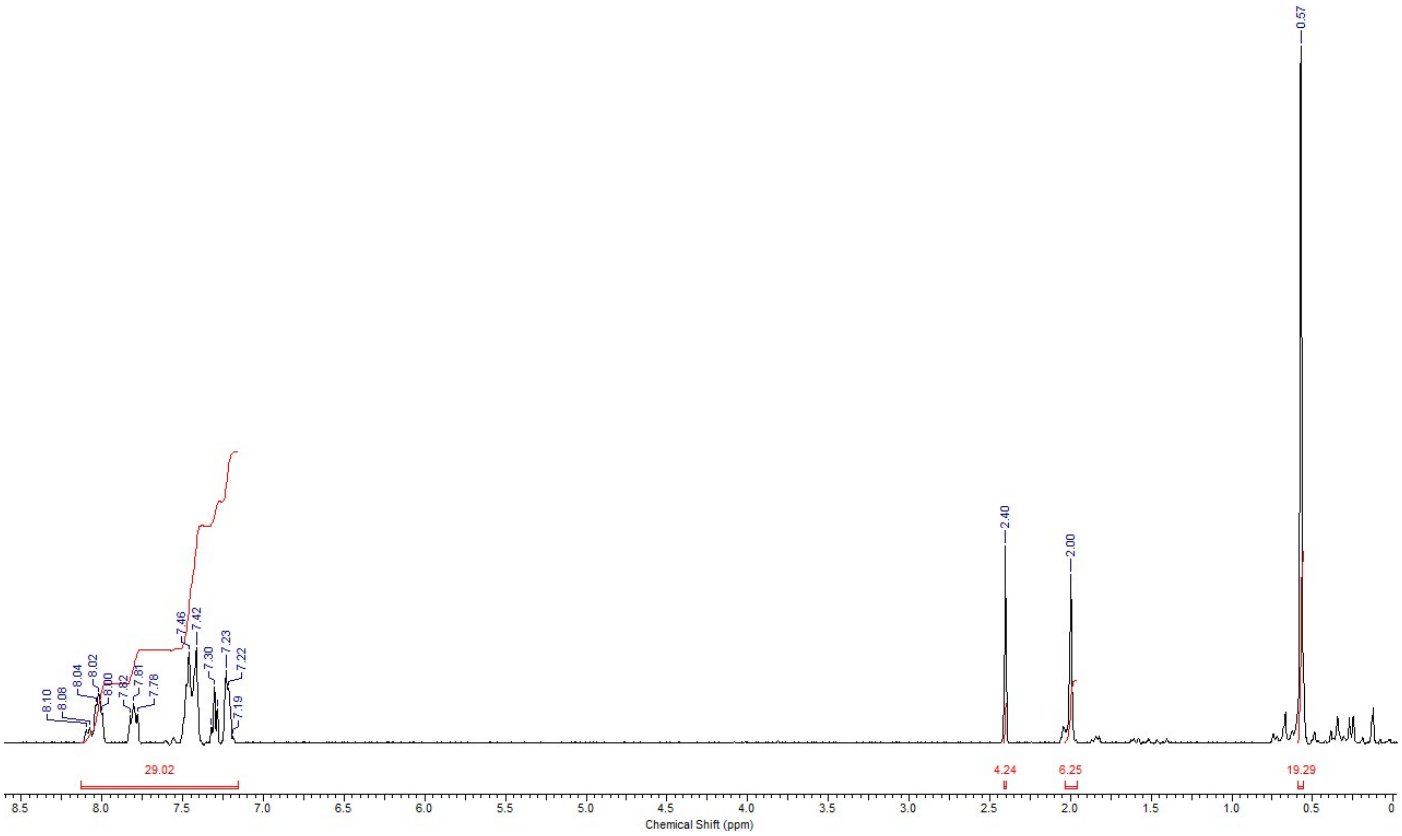

Figure S1A. ^{1}H-NMR spectrum (400 MHz, $CDCl_3$) of **2**

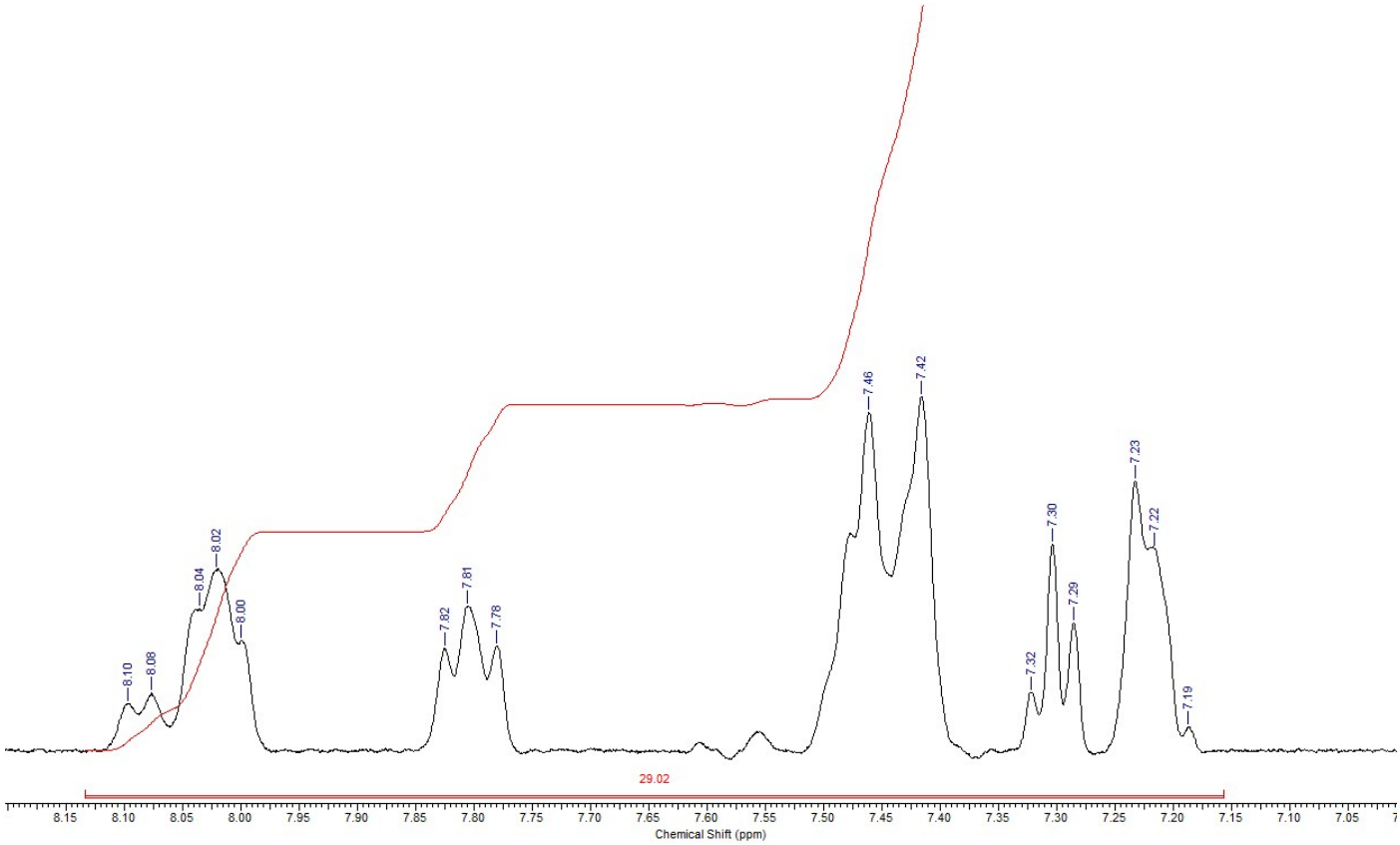

Figure S1B. ^{1}H-NMR spectrum (aromatic region) (400 MHz, $CDCl_3$) of **2**

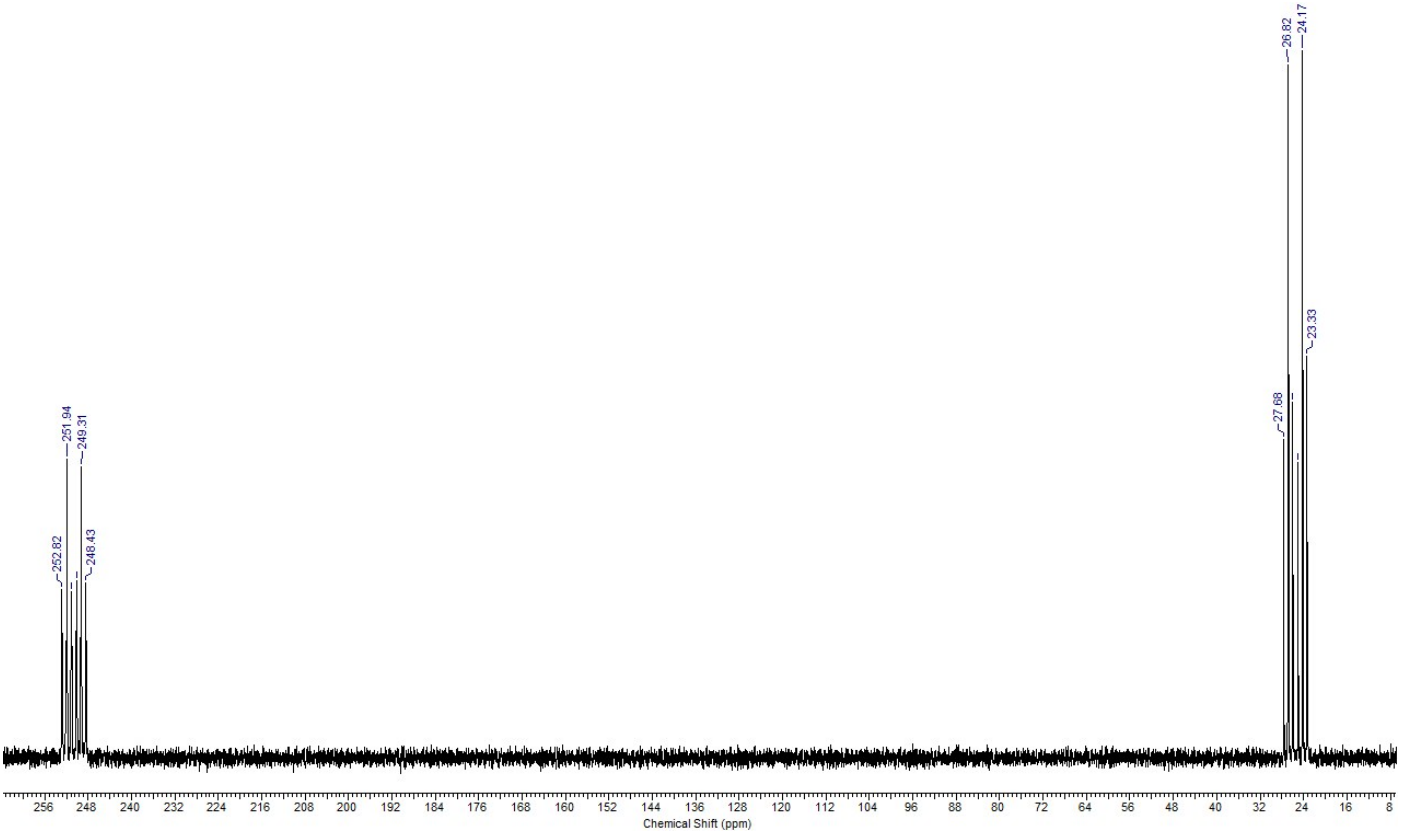

Figure S2. $^{31}P\{^{1}H\}$-NMR spectrum (162 MHz, $CDCl_3$) of **2**

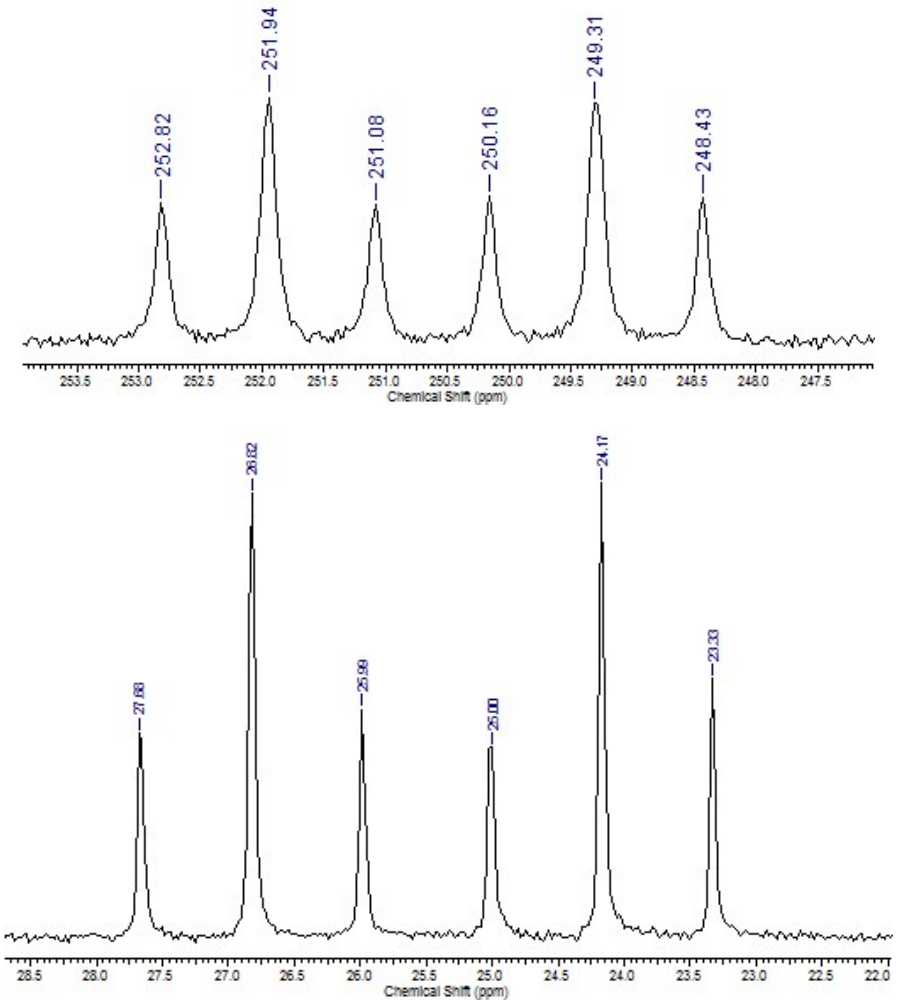

Figure S3. ^{31}P-NMR spectra: phosphinine (top) and phosphine (bottom) regions of **2**

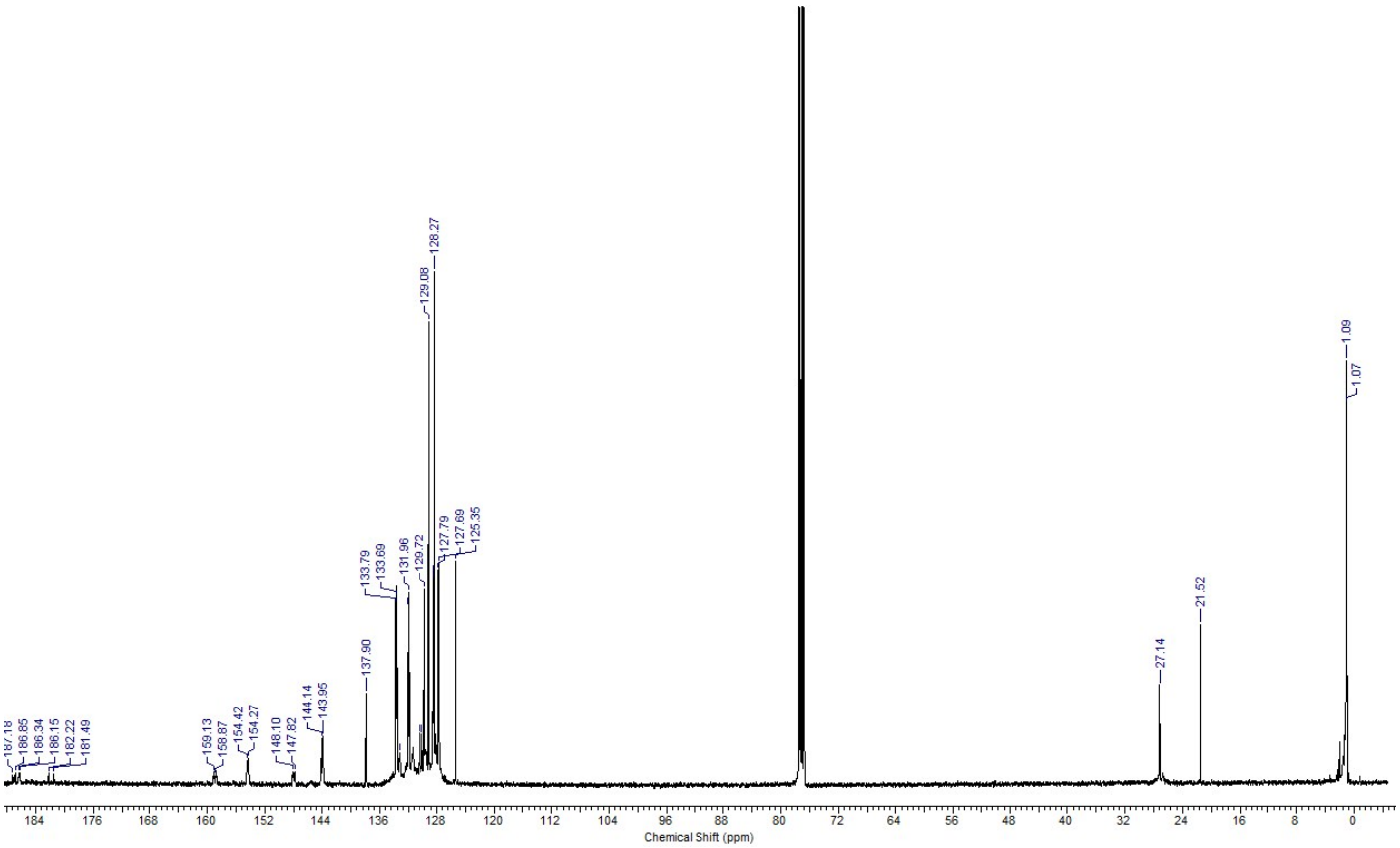

Figure S4. ^{13}C-NMR spectrum (100 MHz, $CDCl_3$) of **2**

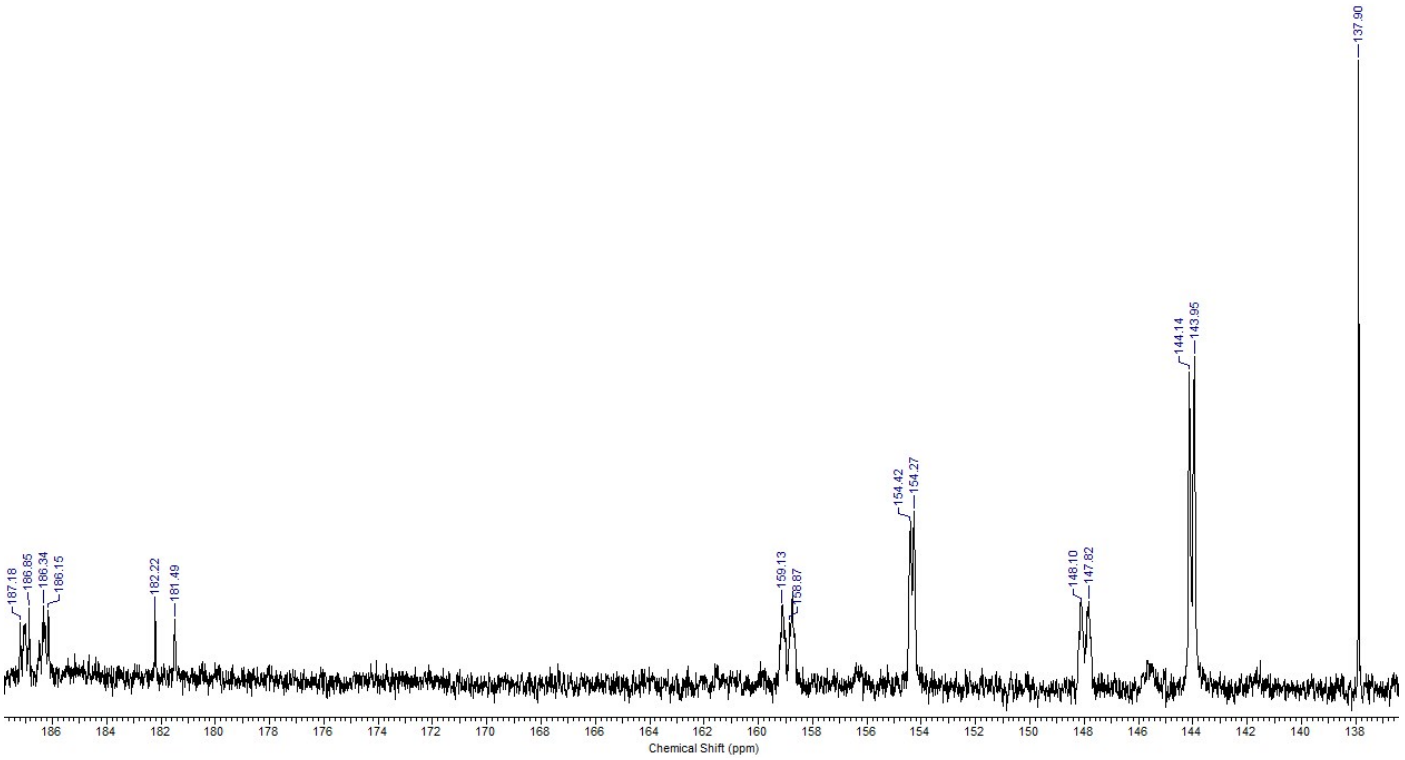

Figure S5. $^{13}C\{^1H\}$-NMR spectrum (carbonyl/aromatic region) of **2**

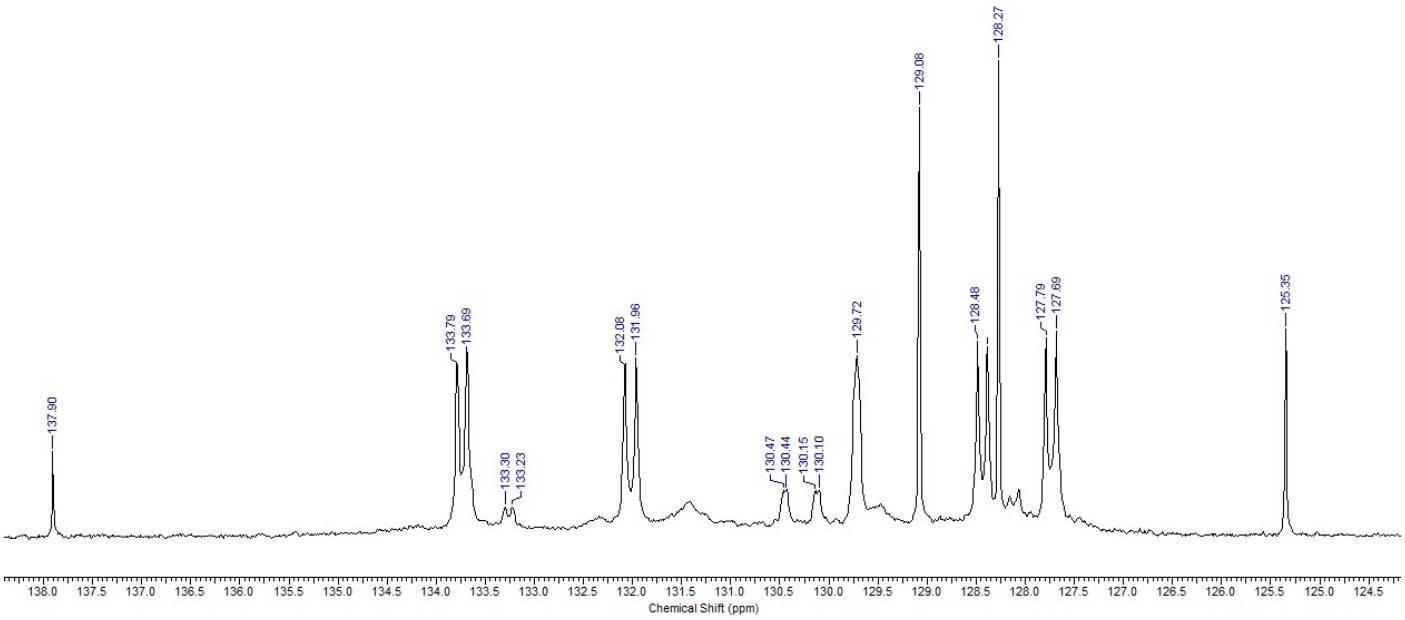

Figure S6. $^{13}C\{^{1}H\}$-NMR spectrum (aromatic region - continued) of **2**

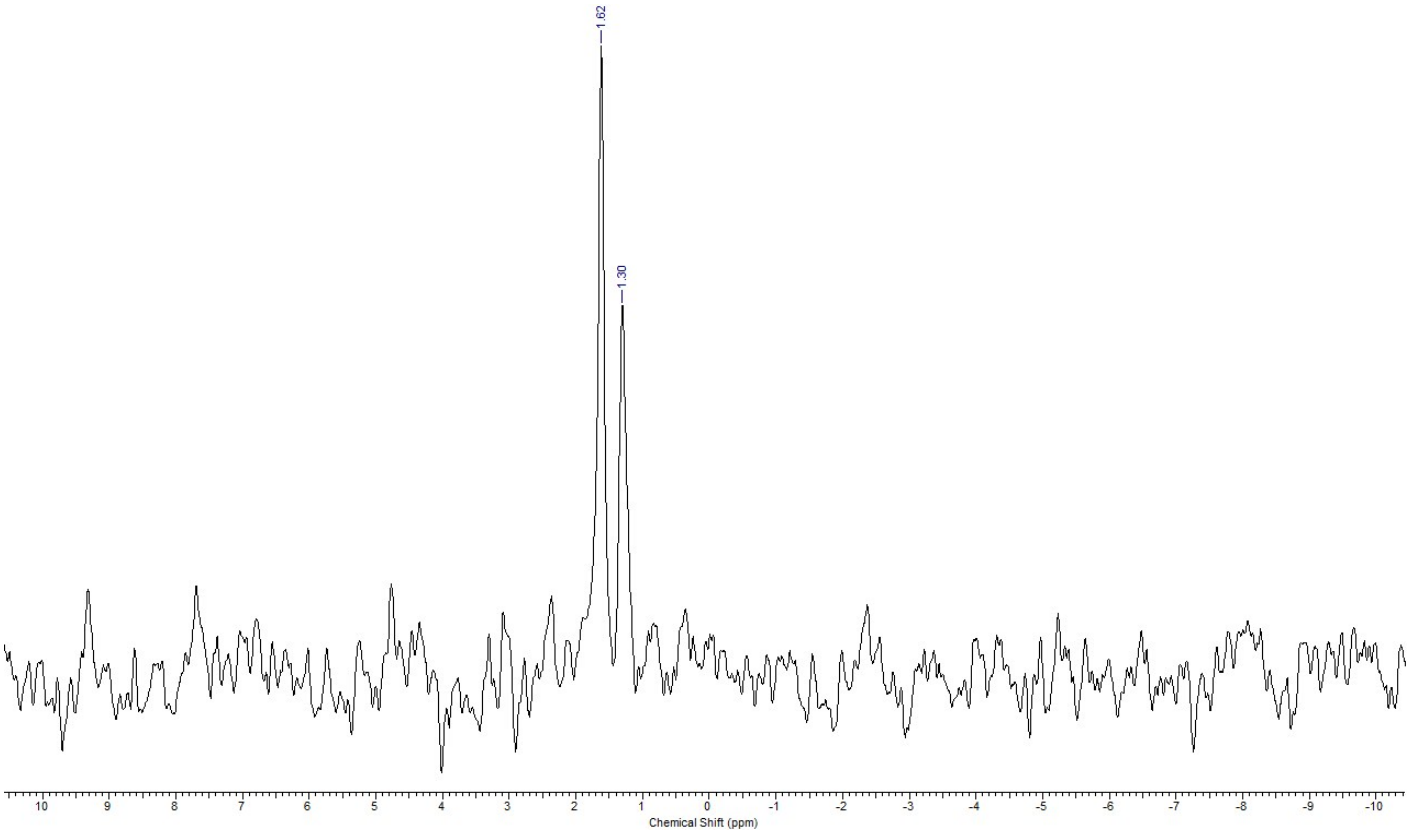

Figure S7. $^{29}Si\{^{1}H\}$-NMR spectrum (79 MHz, $CDCl_3$) of **2**

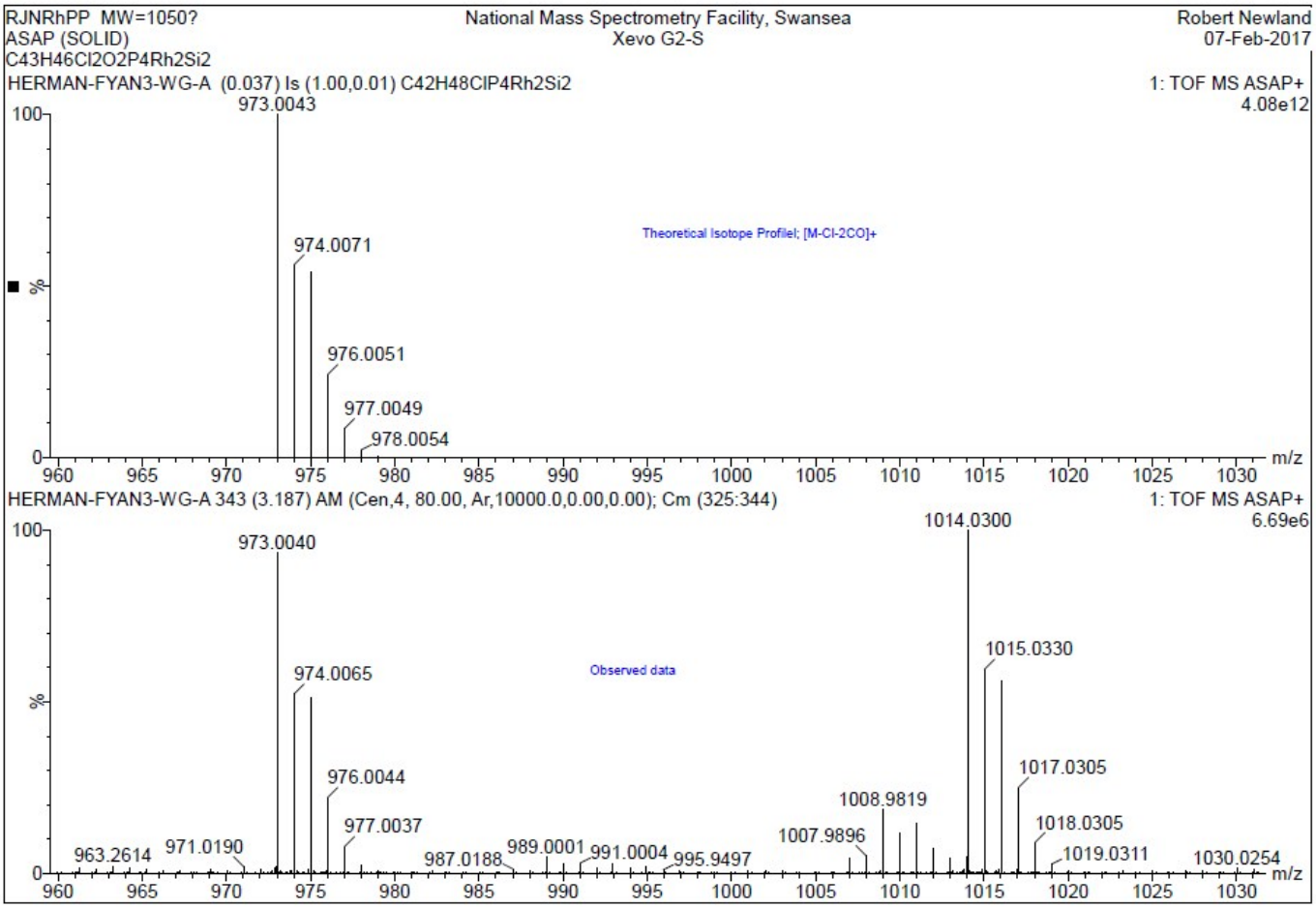

Figure S8. Accurate mass (ASAP/QTof) of **2**

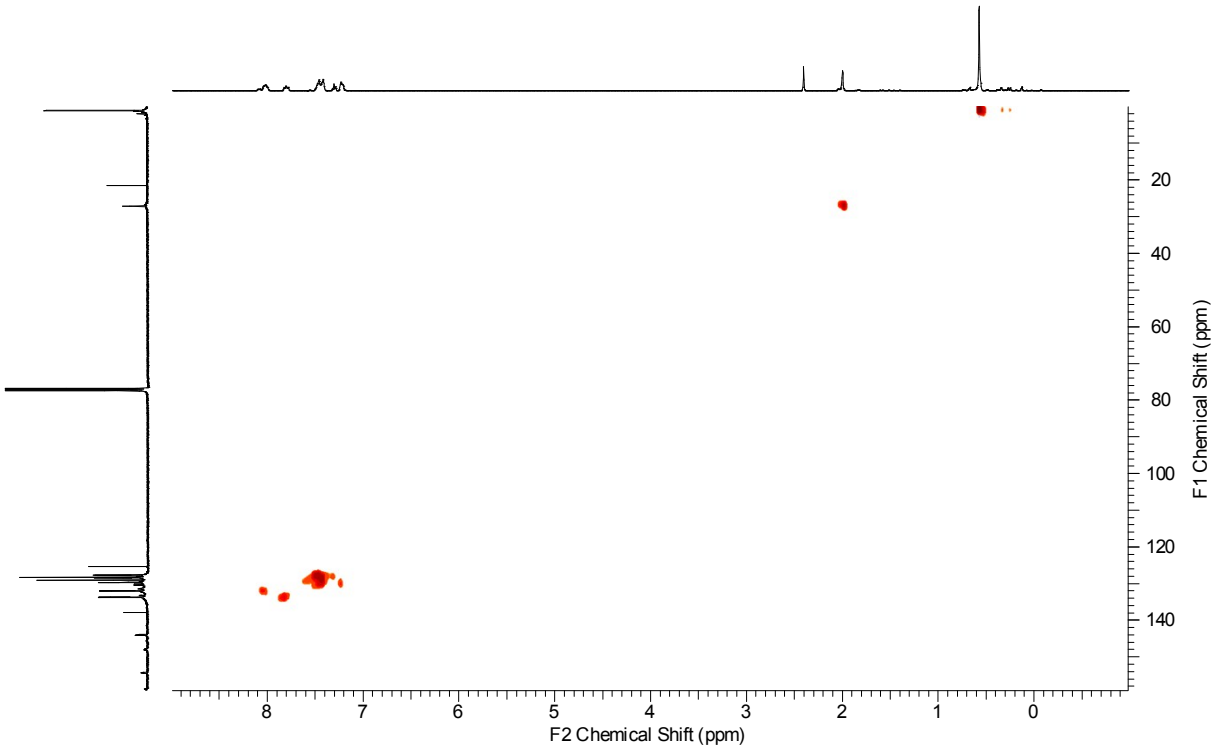

Figure S9. ^{1}H-^{13}C HSQC NMR (400 MHz) of **2**.

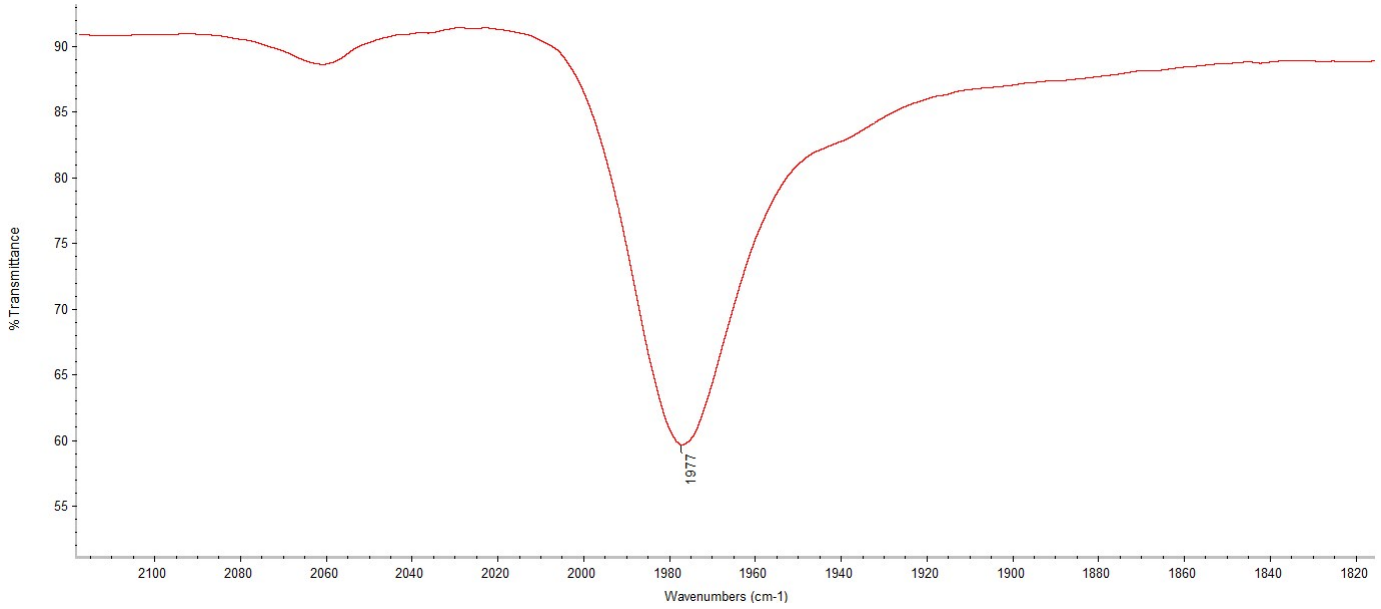

Figure S10. FTIR spectrum (ATR) of **2**.

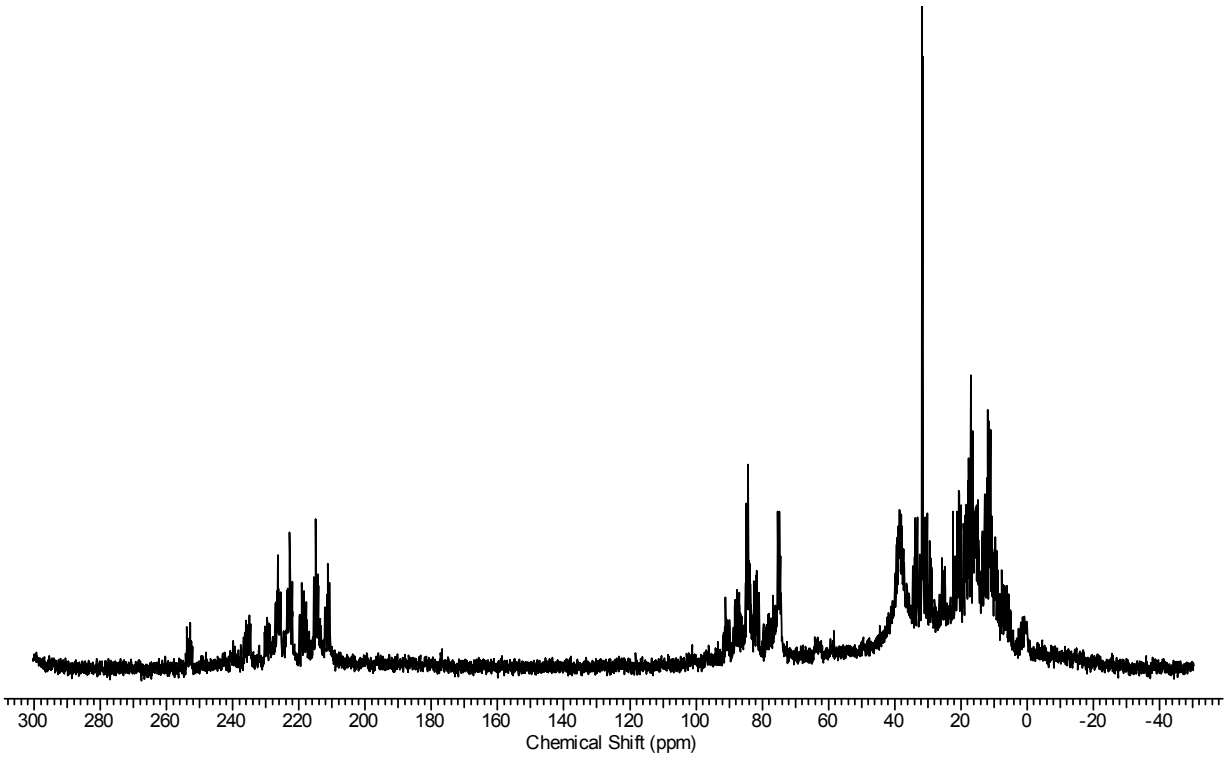

Figure S11. $^{31}P\{^{1}H\}$-NMR spectrum (162 MHz, $CDCl_3$) of **2** after 15h at 75°C

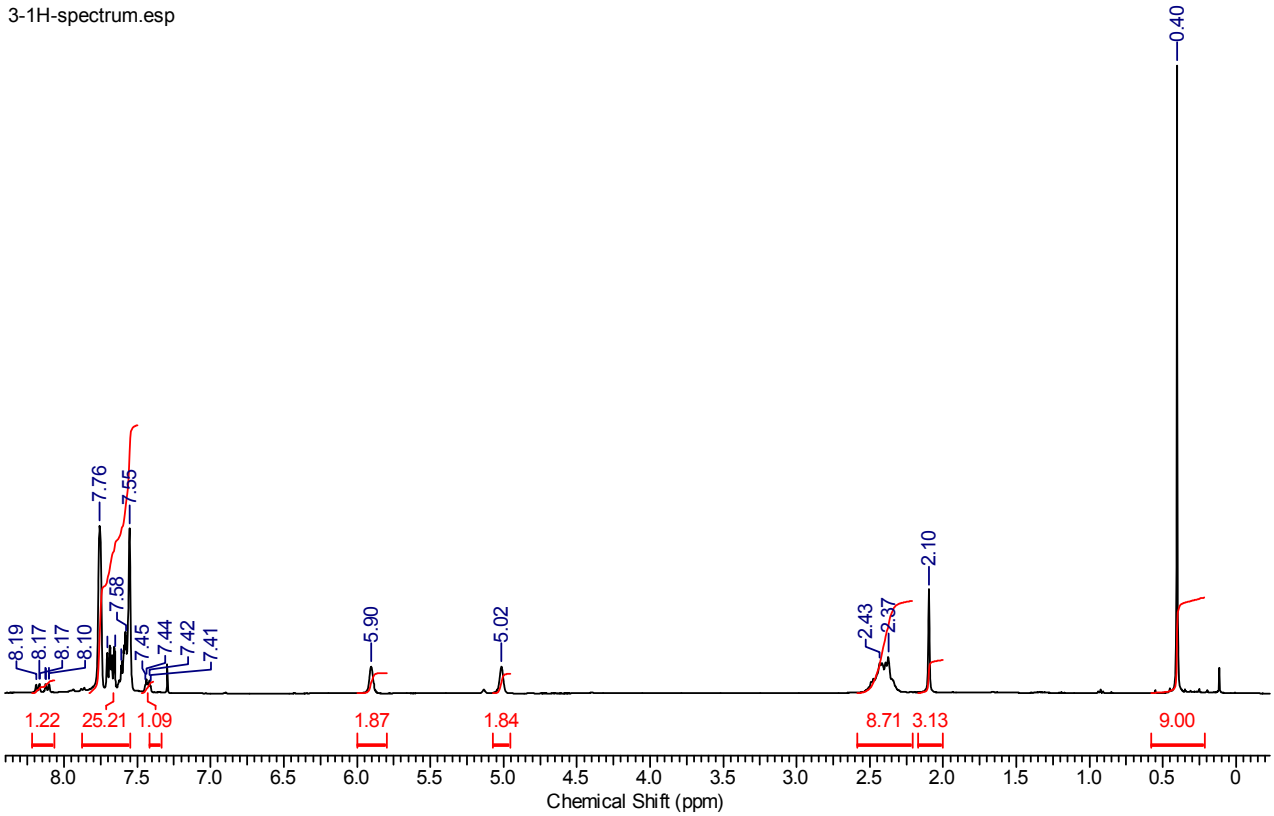

Figure S12. ^{1}H-NMR spectrum (400 MHz, $CDCl_3$) of **3**

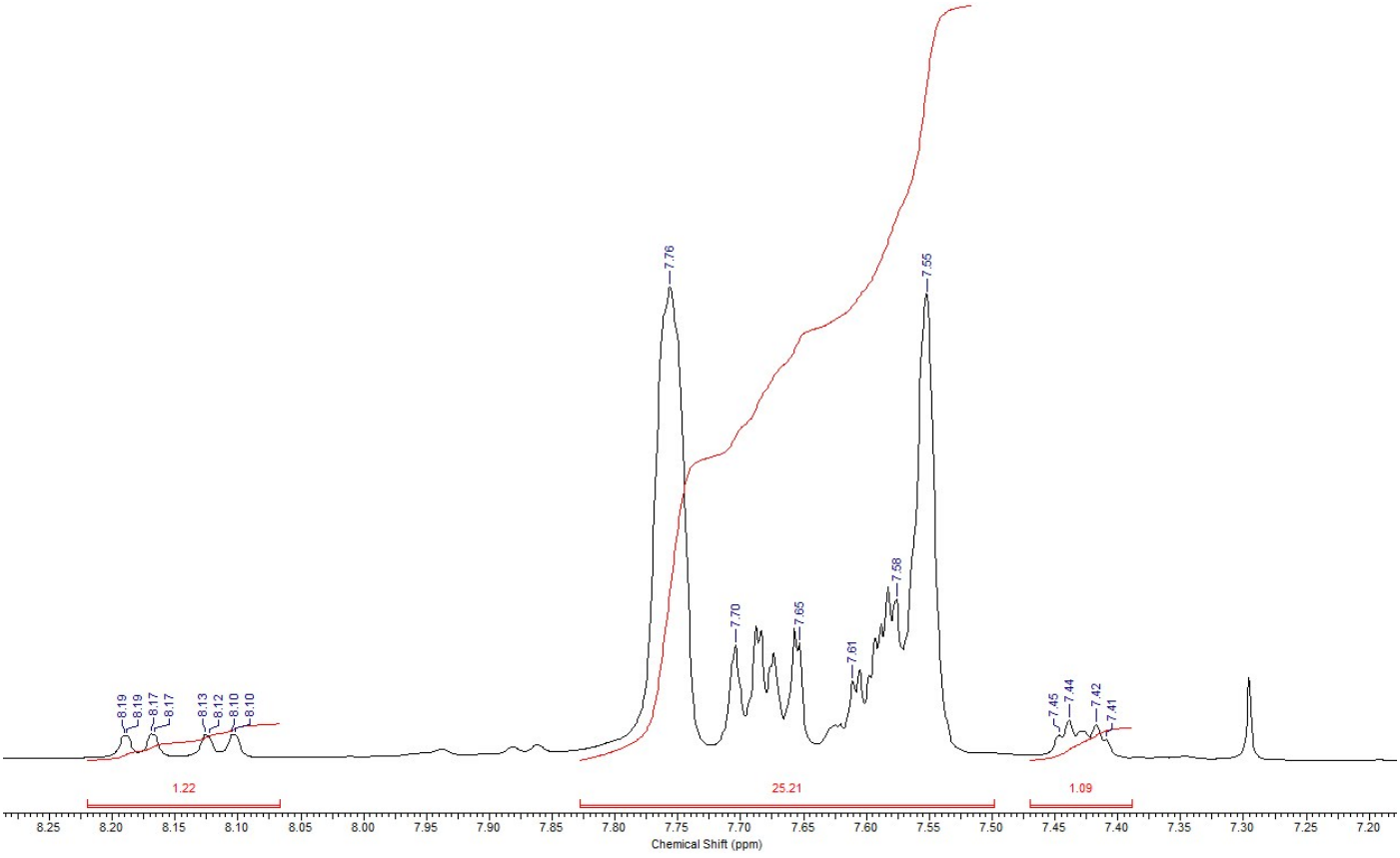

Figure S13. ^{1}H-NMR spectrum (aromatic region) of **3**

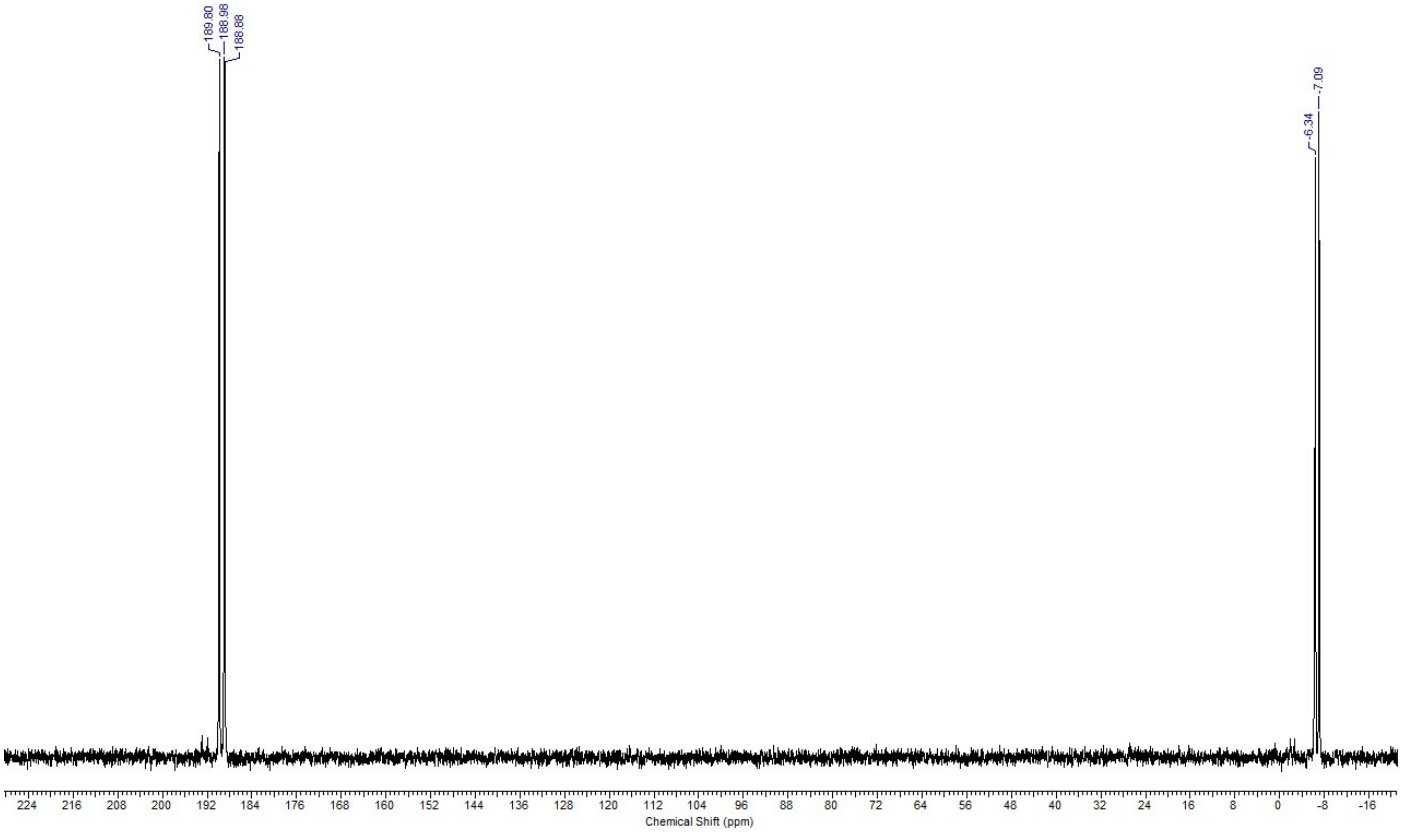

Figure S14. $^{31}P\{^{1}H\}$-NMR spectrum (162 MHz, $CDCl_3$) of **3**

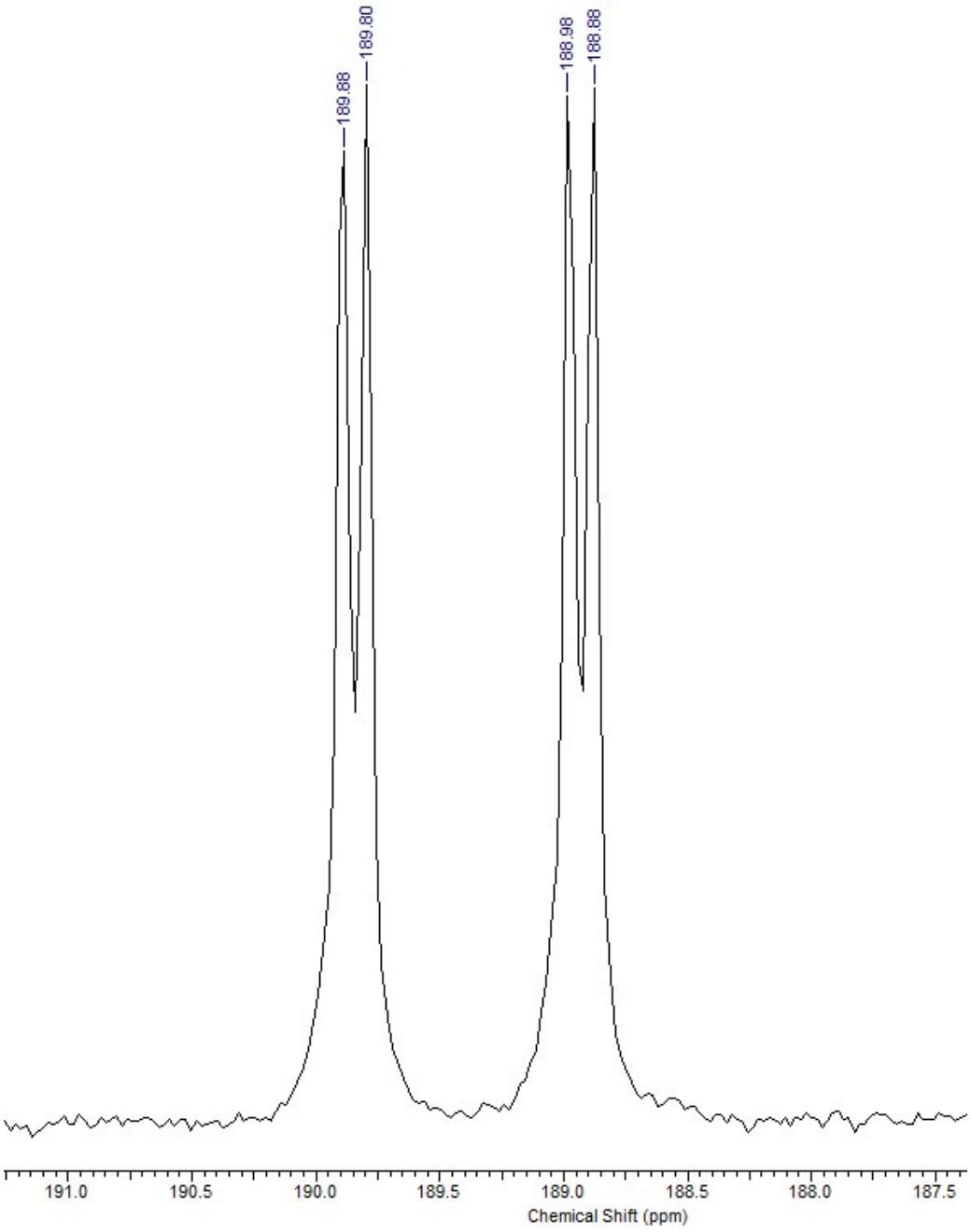

Figure S15A. $^{31}P\{^{1}H\}$-NMR spectrum (162 MHz, $CDCl_3$): phosphinine region of **3**

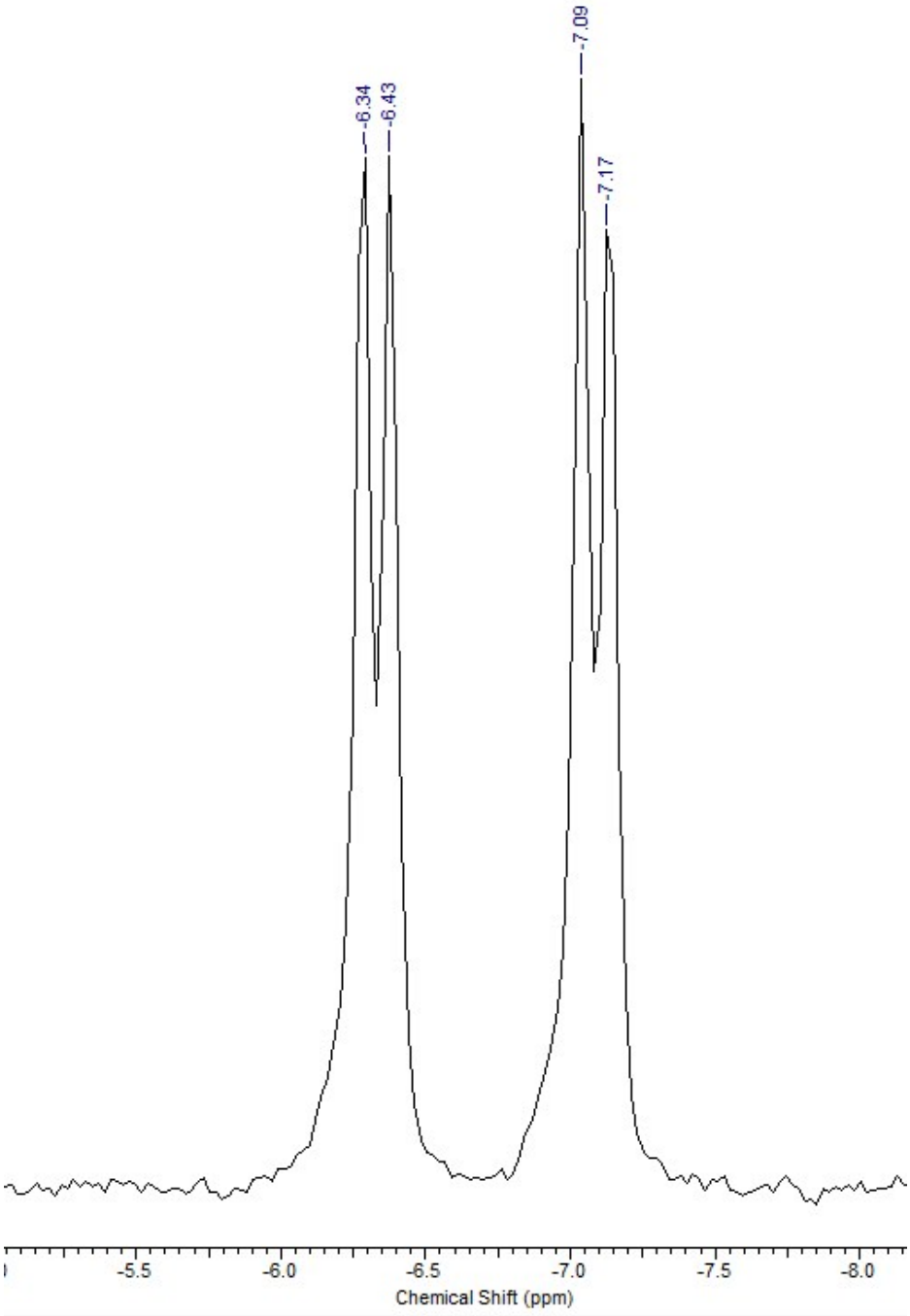

Figure S15B. $^{31}P\{^{1}H\}$-NMR spectrum (162 MHz, $CDCl_3$): phosphine region of **3**

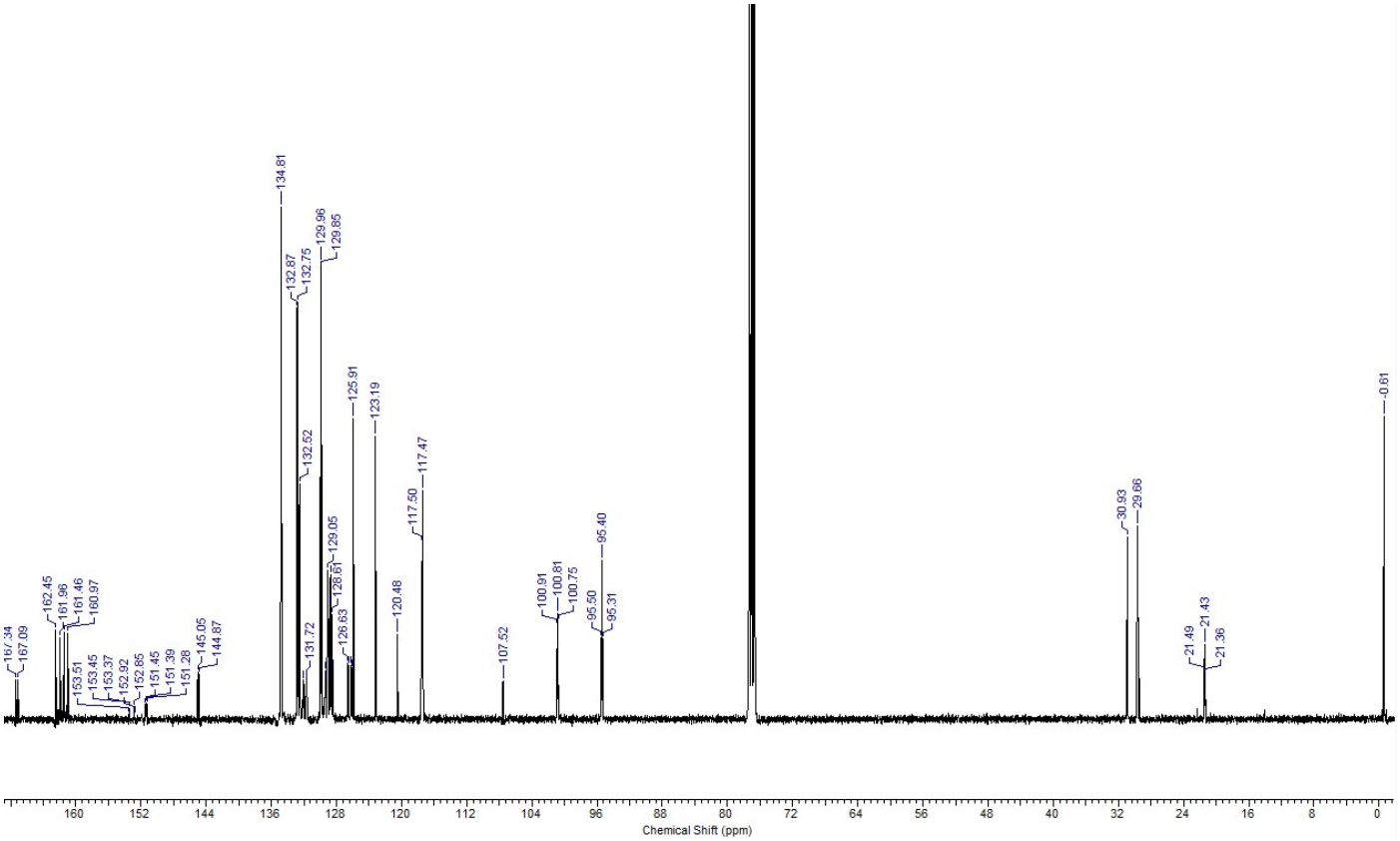

Figure S16. $^{13}C\{^{1}H\}$-NMR spectrum (100 MHz, $CDCl_3$) of **3**

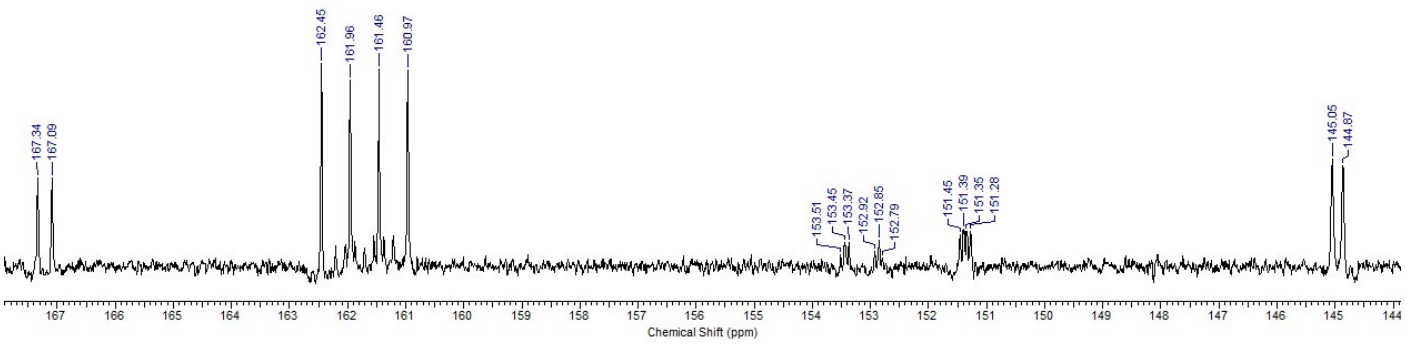

Figure S17A. $^{13}C\{^{1}H\}$-NMR (aromatic region) of **3**

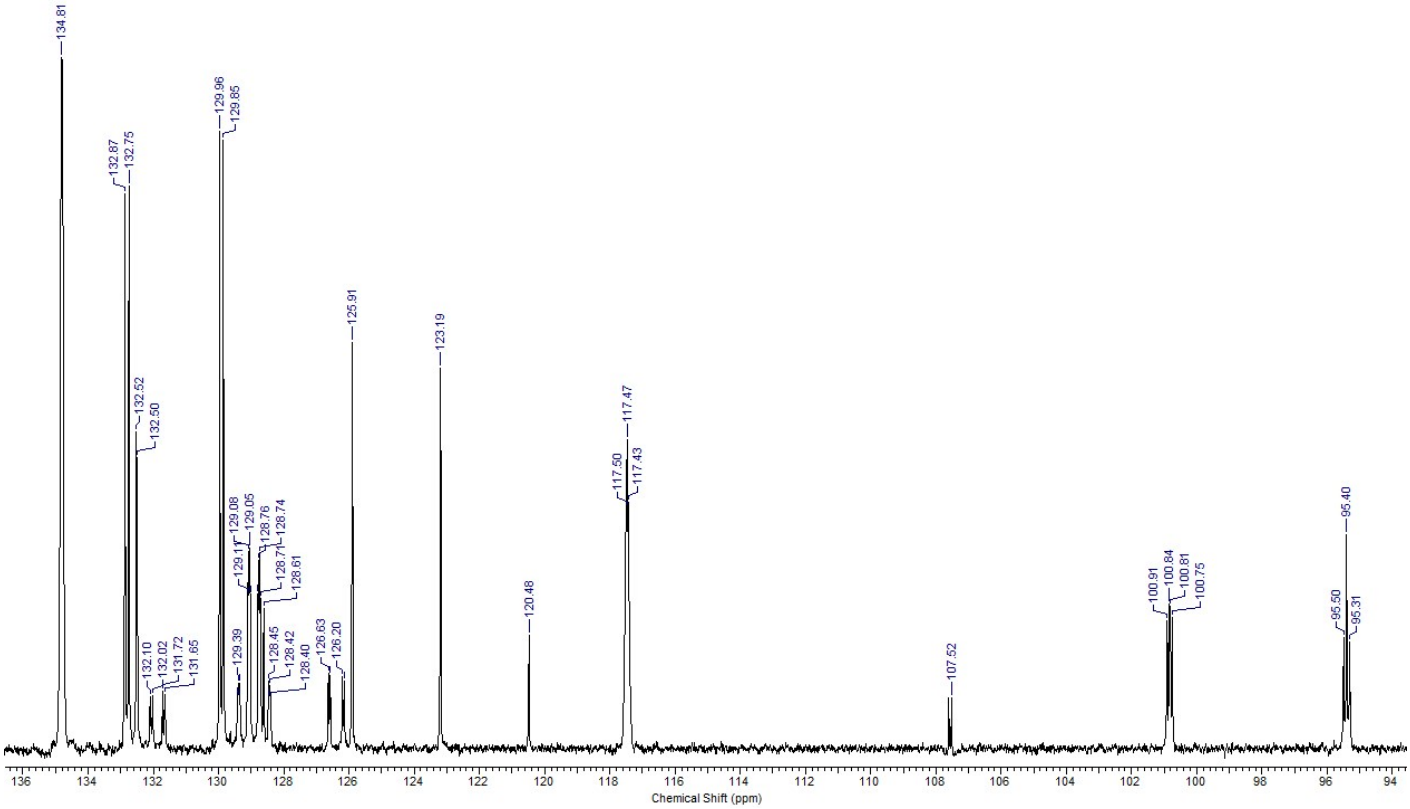

Figure S17B. $^{13}C\{^{1}H\}$-NMR (aromatic region to alkene region) of **3**

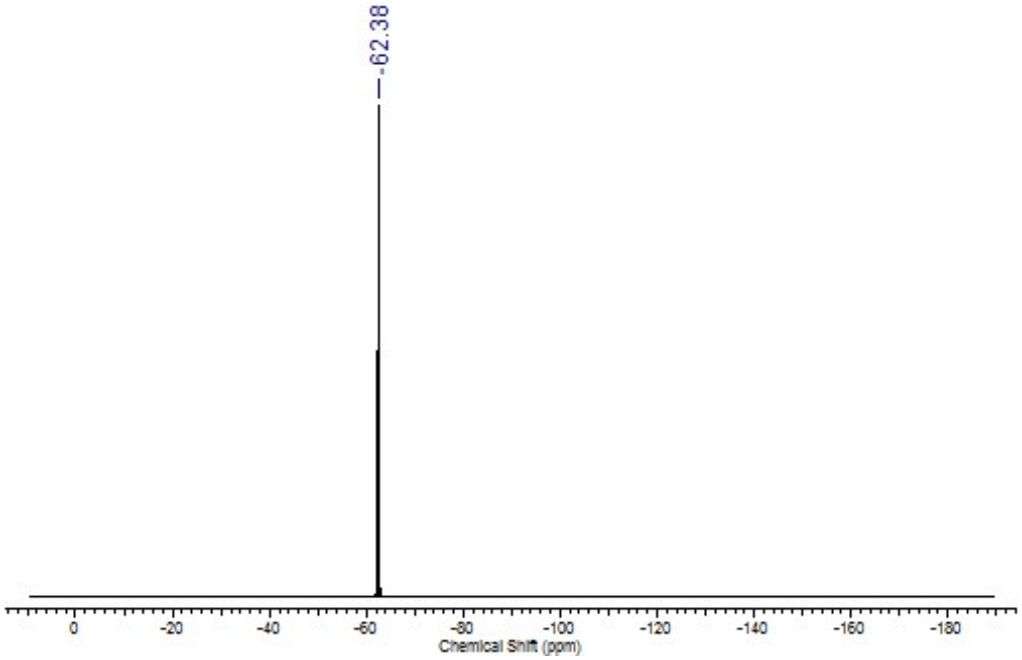

Figure S18. ^{19}F-NMR spectrum (376 MHz, $CDCl_3$) of **3**

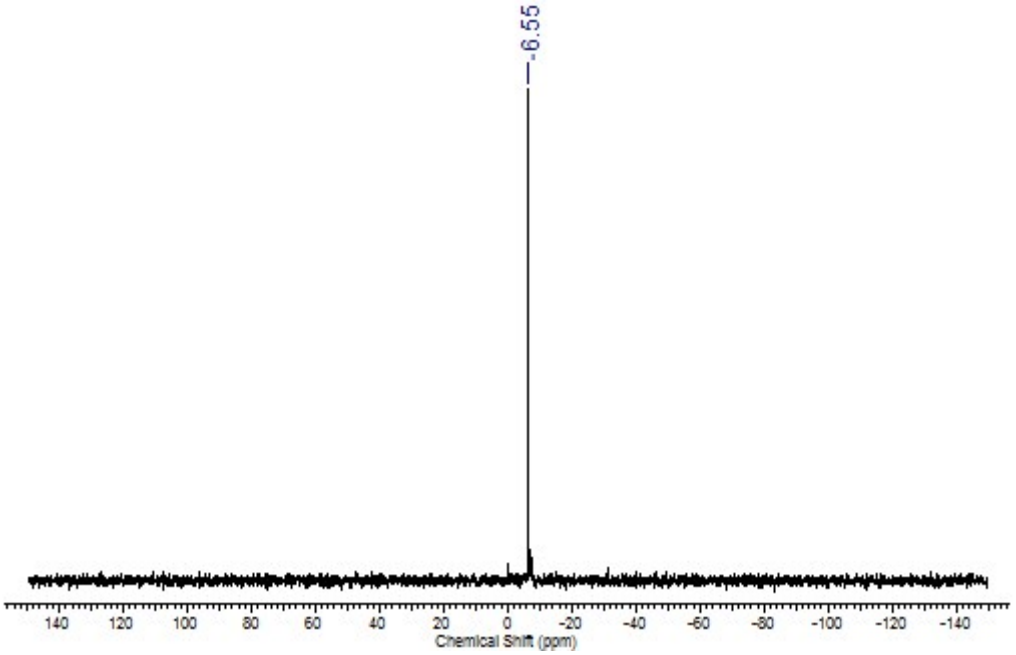

Figure S19. ^{11}B-NMR spectrum (128 MHz, $CDCl_3$) of **3**

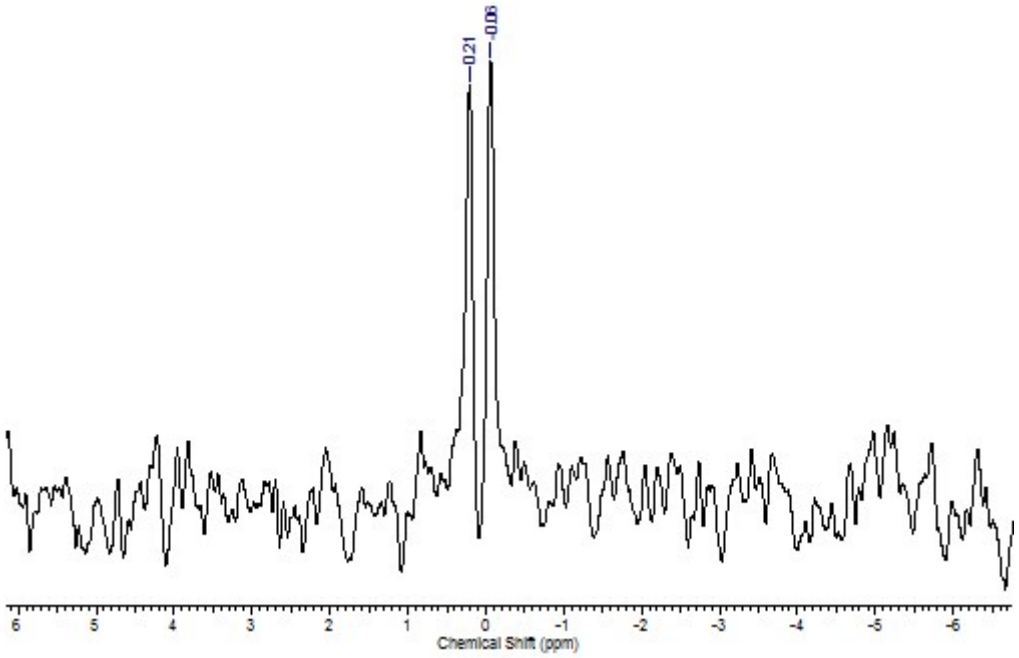

Figure S20. ^{29}Si{^{1}H}-NMR spectrum (79 MHz, $CDCl_3$) of **3**

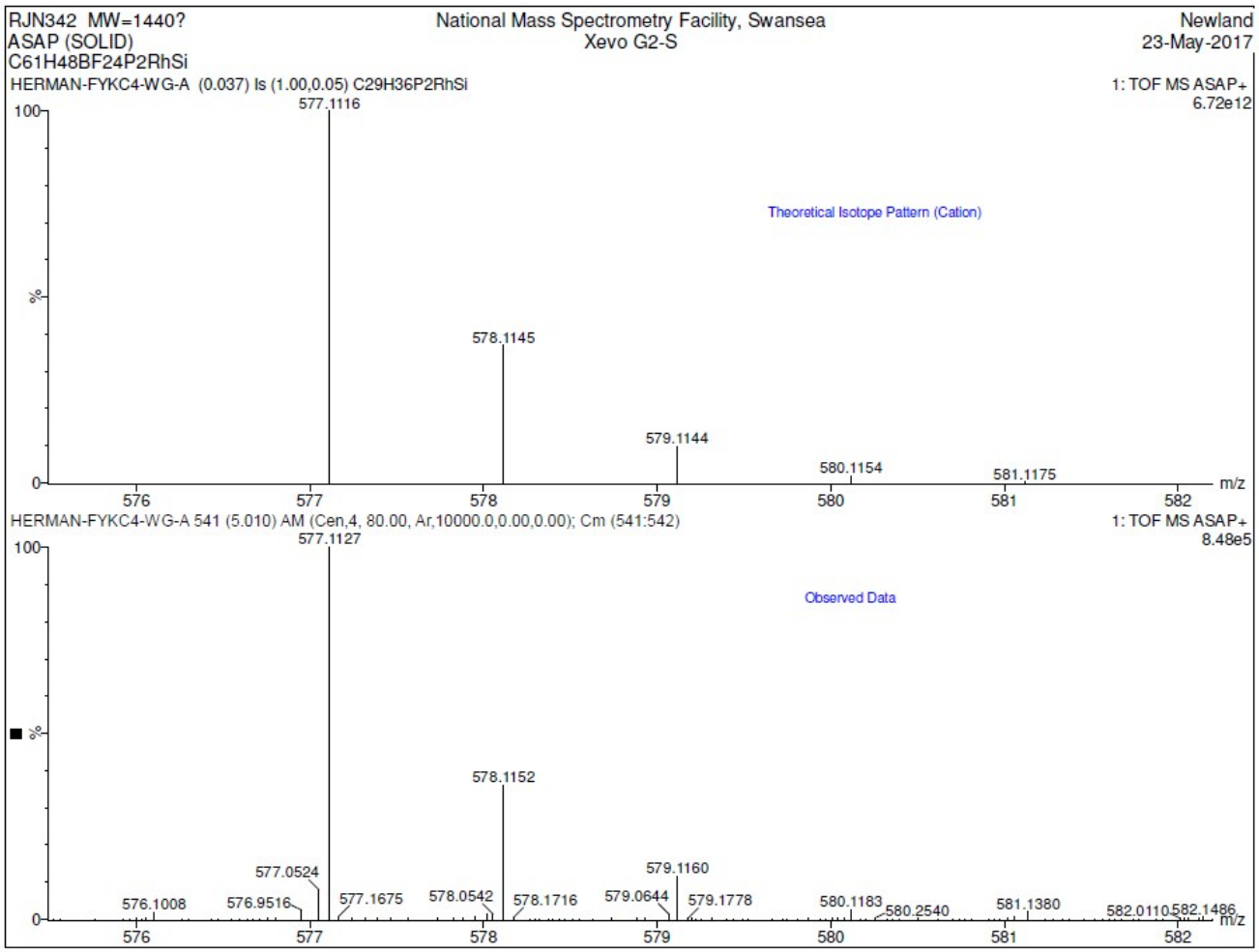

Figure S21. Accurate mass (ASAP/QTof) of **3**

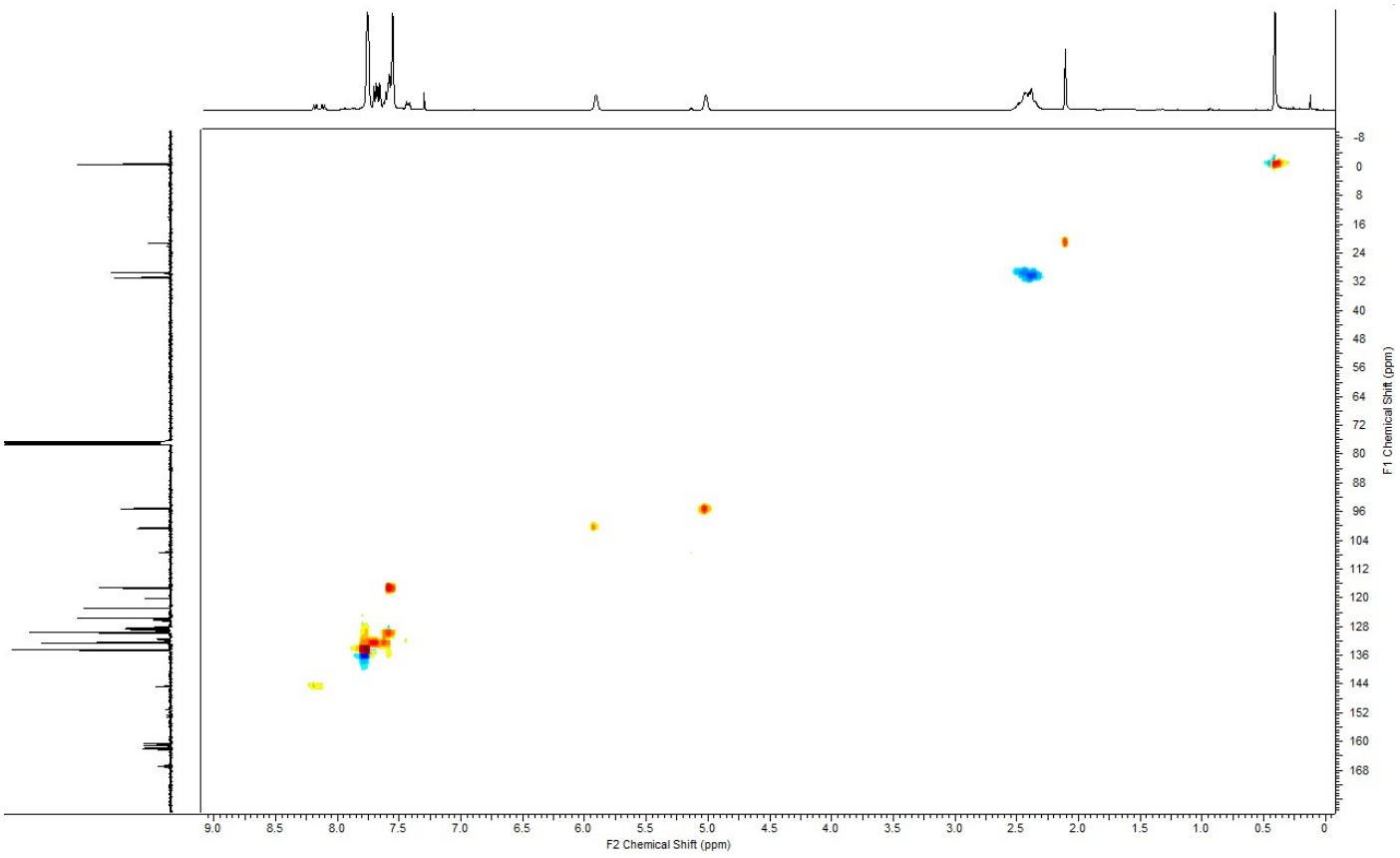

Figure S22. ^{1}H-^{13}C HSQC (400 MHz) spectrum of **3**

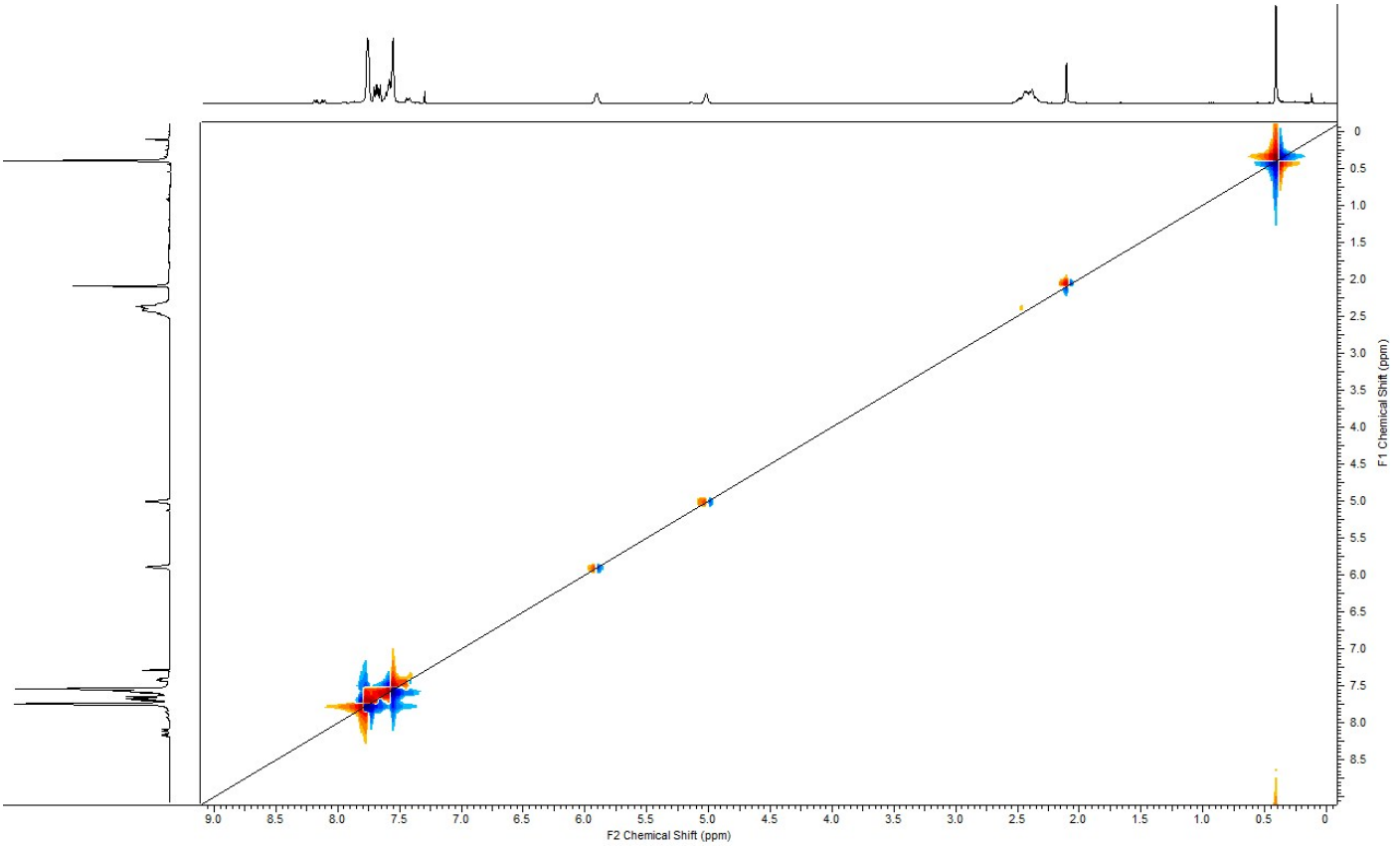

Figure S23. ^{1}H-^{1}H NOESY spectrum (400 MHz) of **3**

Crystallographic details

Single crystals of the samples were covered in inert oil and placed under the cold stream of a Bruker X8 APEXII four-circle diffractometer cooled to 100 K (**2**) or an Oxford Diffraction four-circle Supernova diffractometer cooled to 120 K (**3**). Exposures were collected using Mo Kα radiation (λ = 0.71073). Indexing, data collection and absorption correction were performed using the APEXII[8] or CrysAlisPro suite of programs. Structures were solved using direct methods (SHELXT)[9] and refined by full-matrix least-squares (SHELXL)[9] interfaced with the programme OLEX2[10] (Table S2).

Compound **2** co-crystallised with a benzene solvate molecule and the Cl / CO ligands were disordered over two positions that refined to give occupancy factors of 0.62/0.38 (Cl1A, O1A and C43A /Cl1B, O1B and C43B) and 0.58/0.42 (Cl2A, O2A and C44A/Cl2B, O2B and C44B). Compound **3** had a disordered $SiMe_3$ group and CF_3 group that were both modelled over two positions.

Table S1. Bond lengths (Å) and angles (°) for **2** and **3**

2	P(1)-C(1)	1.734(4)	P(1)-C(1)-C(2)	121.4(2)
	C(1)-C(2)	1.411(5)	C(1)-C(2)-C(3)	121.0(3)
	C(2)-C(3)	1.402(5)	C(2)-C(3)-C(4)	125.6(3)
	C(3)-C(4)	1.386(5)	C(3)-C(4)-C(5)	126.1(3)
	C(4)-C(5)	1.394(5)	C(4)-C(5)-P(1)	118.0(3)
	C(5)-P(1)	1.725(3)	C(5)-P(1)-C(1)	107.6(2)
	C(1)-P(2)	1.844(3)	P(1)-C(1)-P(2)	114.9(2)
	P(3)-C(22)	1.732(3)	P(3)-C(22)-C(23)	121.3(2)
	C(22)-C(23)	1.414(5)	C(22)-C(23)-C(24)	121.6(3)
	C(23)-C(24)	1.388(5)	C(23)-C(24)-C(25)	125.2(4)
	C(24)-C(25)	1.390(5)	C(24)-C(25)-C(26)	125.8(3)
	C(25)-C(26)	1.397(5)	(C(25)-C(26)-P(3)	118.6(3)
	C(26)-P(3)	1.721(3)	C(26)-P(3)-C(22)	107.2(2)
	C(22)-P(4)	1.837(3)	P(3)-C(22)-P(4)	115.5(2)
	P(1)-Rh(1)	2.2845(9)		
	P(2)-Rh(2)	2.3228(10)		
	P(3)-Rh(2)	2.2928(9)		
	P(4)-Rh(1)	2.3188(10)		
	Rh(1)-C(43A)	1.816(13)		
	Rh(1)-C(43B)	1.72(2)		
	Rh(2)-C(44A)	1.785(12)		
	Rh(2)-C(44B)	1.834(17)		
	C(43A)-(O1A)	1.13(2)		
	C(43B)-(O1B)	1.19(4)		
	C(44A)-(O2A)	1.183(18)		
	C(44B)-(O2B)	1.10(3)		
	Rh(1)-Cl(1A)	2.396(3)		
	Rh(1)-Cl(1B)	2.422(4)		
	Rh(2)-Cl(2A)	2.391(3)		
	Rh(2)-Cl(2B)	2.398(4)		
3	P(1)-C(1)	1.732(3)	P(1)-C(1)-C(2)	125.1(2)
	C(1)-C(2)	1.397(4)	C(1)-C(2)-C(3)	118.0(3)
	C(2)-C(3)	1.397(5)	C(2)-C(3)-C(4)	125.7(3)
	C(3)-C(4)	1.385(5)	C(3)-C(4)-C(5)	128.6(3)
	C(4)-C(5)	1.409(4)	C(4)-C(5)-P(1)	115.7(2)
	C(5)-P(1)	1.723(3)	C(5)-P(1)-C(1)	106.9(2)
	C(1)-P(2)	1.801(3)	P(1)-C(1)-P(2)	97.3(1)
	P(1)-Rh(1)	2.2932(8)	P(1)-Rh(1)-P(2)	70.64(3)
	P(2)-Rh(1)	2.2941(7)		

Table S2. Crystallographic data for compounds **2** and **3**

Identification code	**2**	**3**
Empirical formula	$C_{50}H_{54}Cl_2O_2P_4Rh_2Si_2$	$C_{61}H_{48}BF_{24}P_2RhSi$
Formula weight	1143.71	1440.74
Temperature/K	100(1)	120(1)
Crystal system	Orthorhombic	Triclinic
Space group	$P2_12_12_1$	P-1
a/Å	13.6107(5)	13.2396(4)
b/Å	19.3024(5)	14.6179(4)
c/Å	19.5658(7)	18.0412(5)
α/°	90	98.298(2)
β/°	90	102.651(2)
γ/°	90	110.657(3)
Volume/Å^3	5140.3(3)	3092.50(16)
Z	4	2
ρ_{calc}g/cm^3	1.478	1.547
μ/mm^{-1}	0.955	0.459
F(000)	2328.0	1448.0
Crystal size/mm^3	0.20 × 0.10 × 0.02	0.29 × 0.22 × 0.17
Radiation	MoKα (λ = 0.71073)	MoKα (λ = 0.71073)
2Θ range for data collection/°	5.128 to 56.64	5.758 to 59.498
Index ranges	-18 ≤ h ≤ 17, -25 ≤ k ≤ 25, -25 ≤ l ≤ 25	-17 ≤ h ≤ 18, -19 ≤ k ≤ 18, -24 ≤ l ≤ 24
Reflections collected	62167	69611
Independent reflections	12732 [R_{int} = 0.0496, R_{sigma} = 0.0464]	15721 [R_{int} = 0.0487, R_{sigma} = 0.0479]
Data/restraints/parameters	12732/18/623	15721/78/896
Goodness-of-fit on F^2	1.024	1.024
Final R indexes [I>=2σ (I)]	R_1 = 0.0280, wR_2 = 0.0504	R_1 = 0.0550, wR_2 = 0.1258
Final R indexes [all data]	R_1 = 0.0350, wR_2 = 0.0523	R_1 = 0.0695, wR_2 = 0.1340
Largest diff. peak/hole / e Å^{-3}	0.43/-0.38	1.46/-0.96
Flack parameter	-0.015(10)	
CCDC deposition number	1822415	1822416

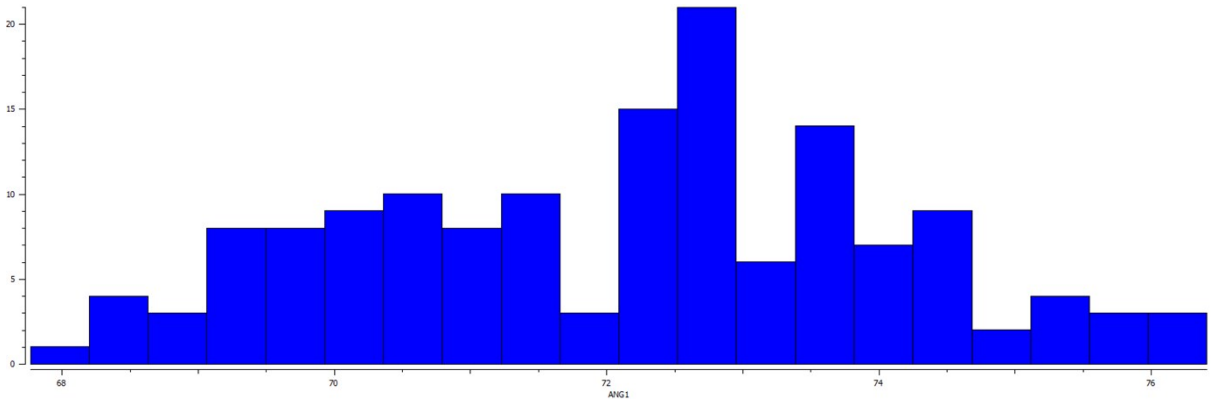

Figure S24. Histogram of Rh(κ_2-PEP) bite angles of entries found in the CSD (E = C, N, O).

Experimental Procedure

A dry NMR tube was charged with substrate (0.43 mmol, 1 equiv), **3** (0.1-3 mol%), catecholborane (56.7 mg, 0.47 mmol, 1.1 equiv), 1,3,5-trimethoxybenzene (~15 mg, internal standard) and C_6D_6 (0.6 cm^3) before being sealed under nitrogen with a Young's tap and shaken thoroughly. For the majority of substrates, the reaction was followed by running the required number (30-150) of 60 second NMR experiments (4 scans, d1 > 10 seconds, RG = 32) at 25°C (spectrometer temperature) consecutively using the multizg command in Topspin and integrating product signals against the 3H or 9H singlets of trimethoxybenzene. For substrates that required heating, after mixing the NMR tube was clamped in a pre-heated oil bath until the desired time period had passed. At which point, the tube was rapidly cooled in an ice bath before being analysed using ^{1}H-NMR spectroscopy. For the screening reactions where pre-formed complexes were not used, the ligand and Rh precursor were pre-mixed (see **Table 1** in paper for details) in ~0.1 ml of solvent for 10 minutes before starting the reaction.

Note: For best results, due to the sensitivity of the reagent, catecholborane was freshly distilled (under a static vacuum) and stored in the glovebox freezer at -25°C.

Crude Product NMR Spectra

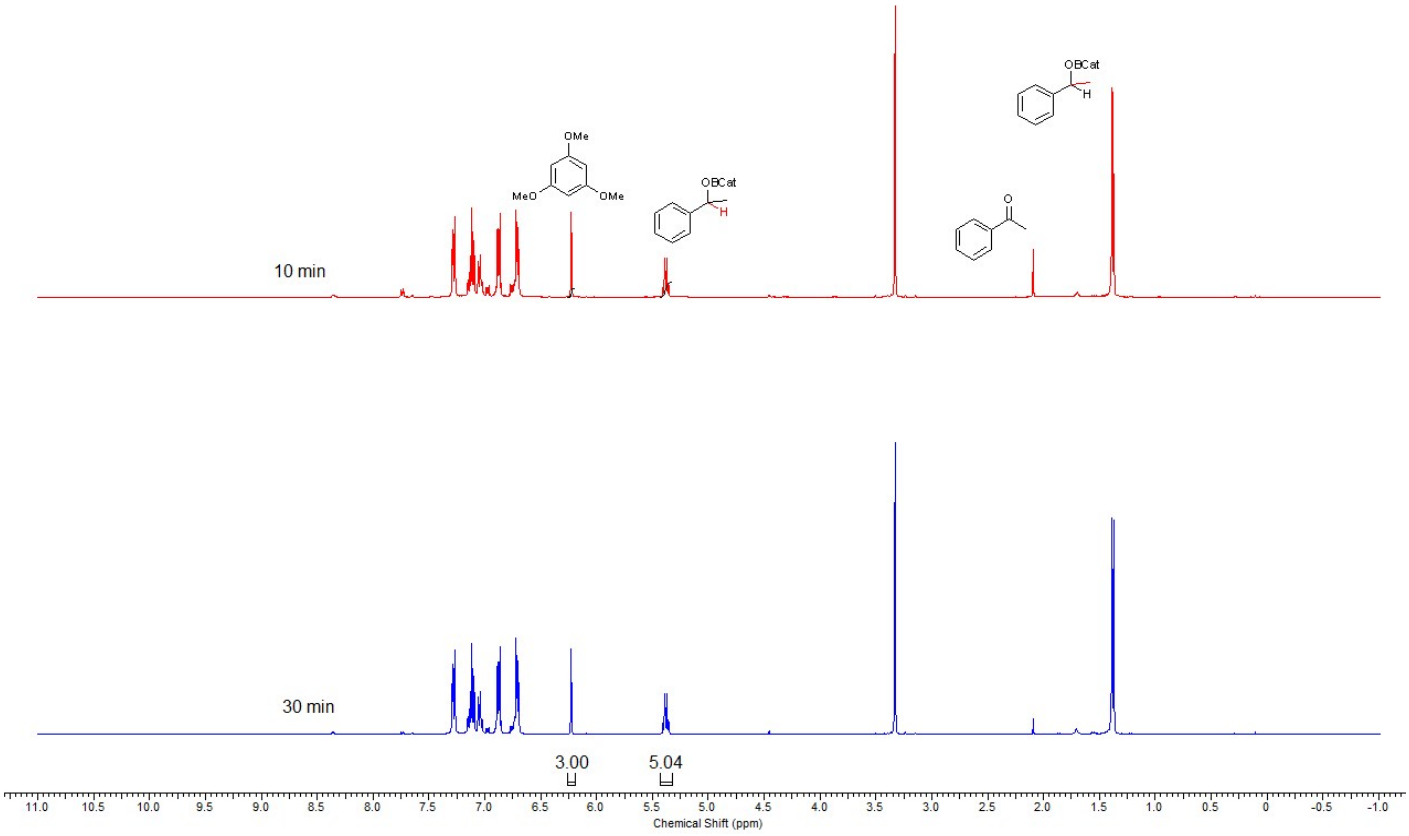

Figure S25. Hydroboration of acetophenone (400 MHz, C_6D_6), 25°C, 30 minutes, 0.1 mol% **3** (data matches that in the literature).[11]

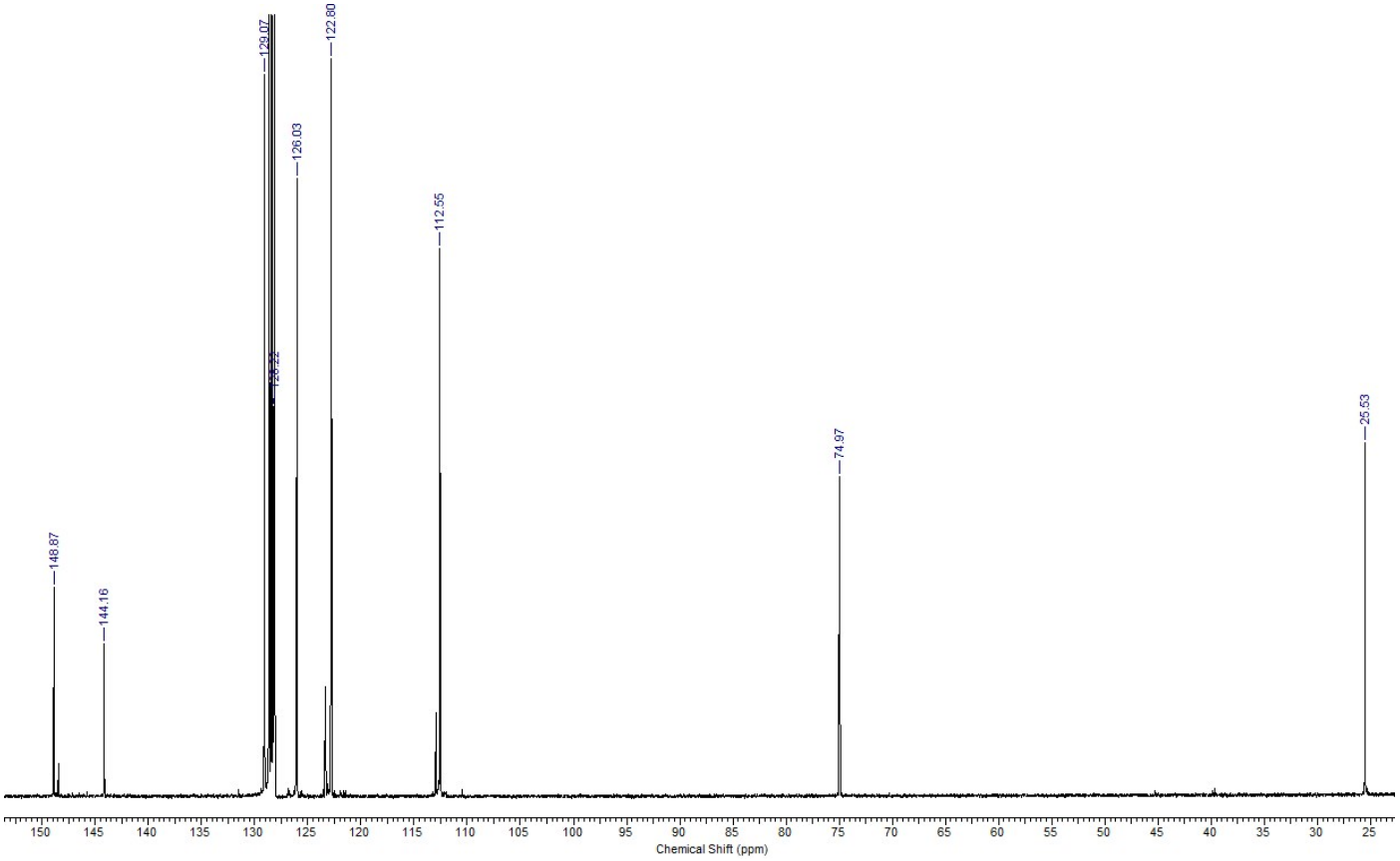

Figure S25B. Hydroboration of acetophenone (100 MHz, C_6D_6), $^{13}C\{^1H\}$ NMR spectrum of product (data matches that in the literature).[11]

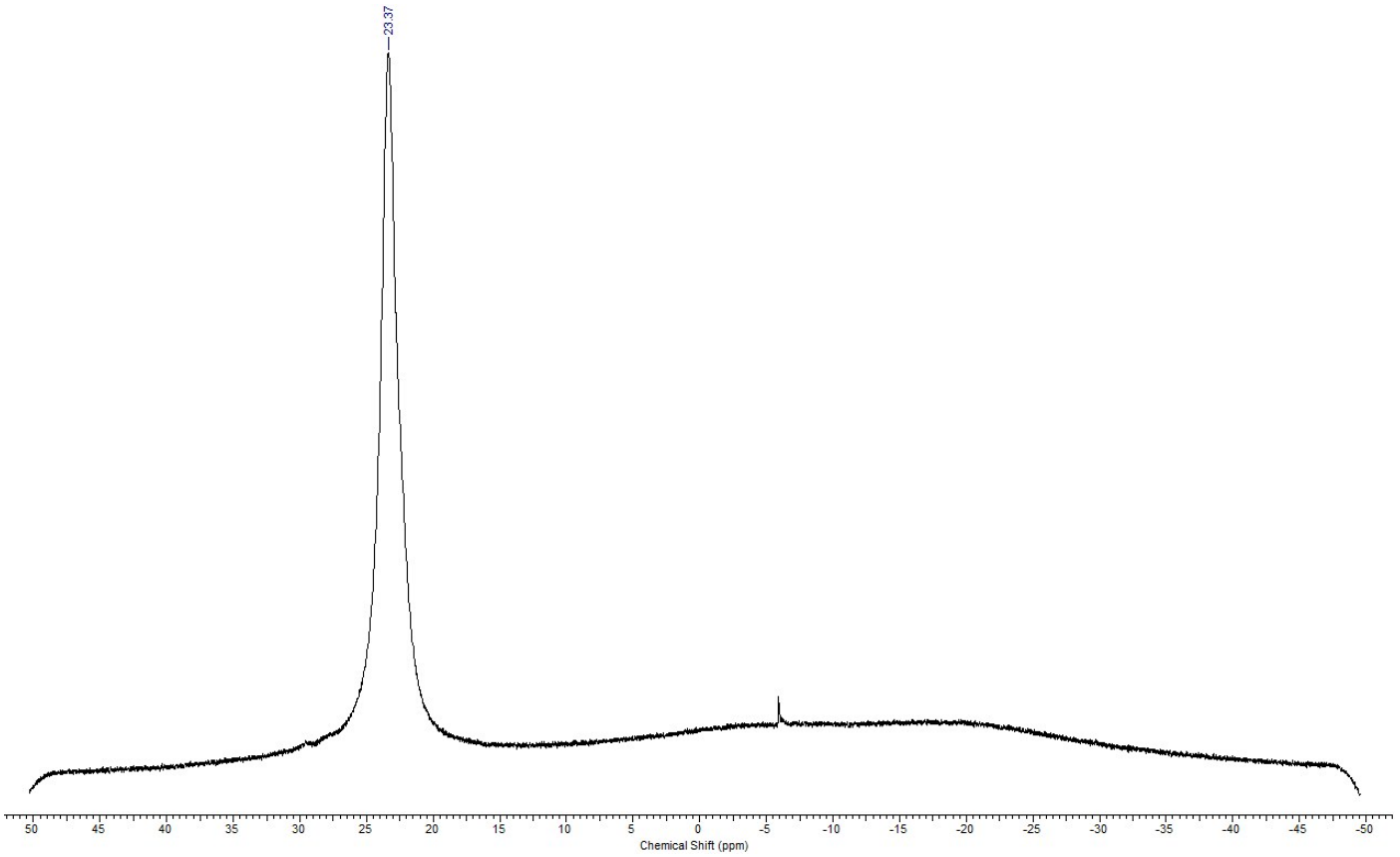

Figure S25C. Hydroboration of acetophenone (128 MHz, C_6D_6), ^{11}B NMR spectrum of product (data matches that in the literature).[11]

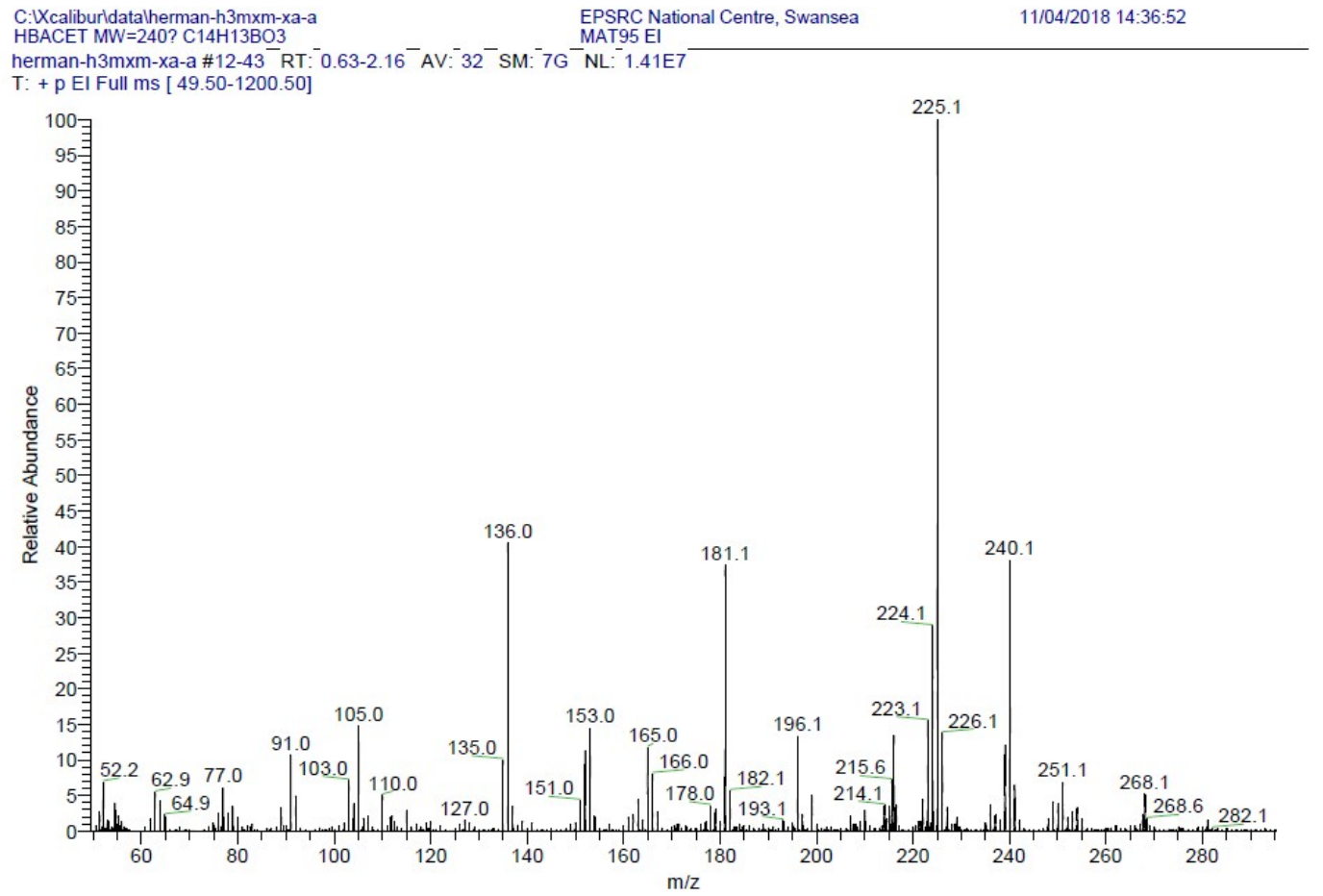

Figure S25D. Hydroboration of acetophenone, MS (EI) of product in PhMe solution

EI: *m/z*: ([M]$^+$) 240.1, ([M-CH_3]$^+$) 225.1

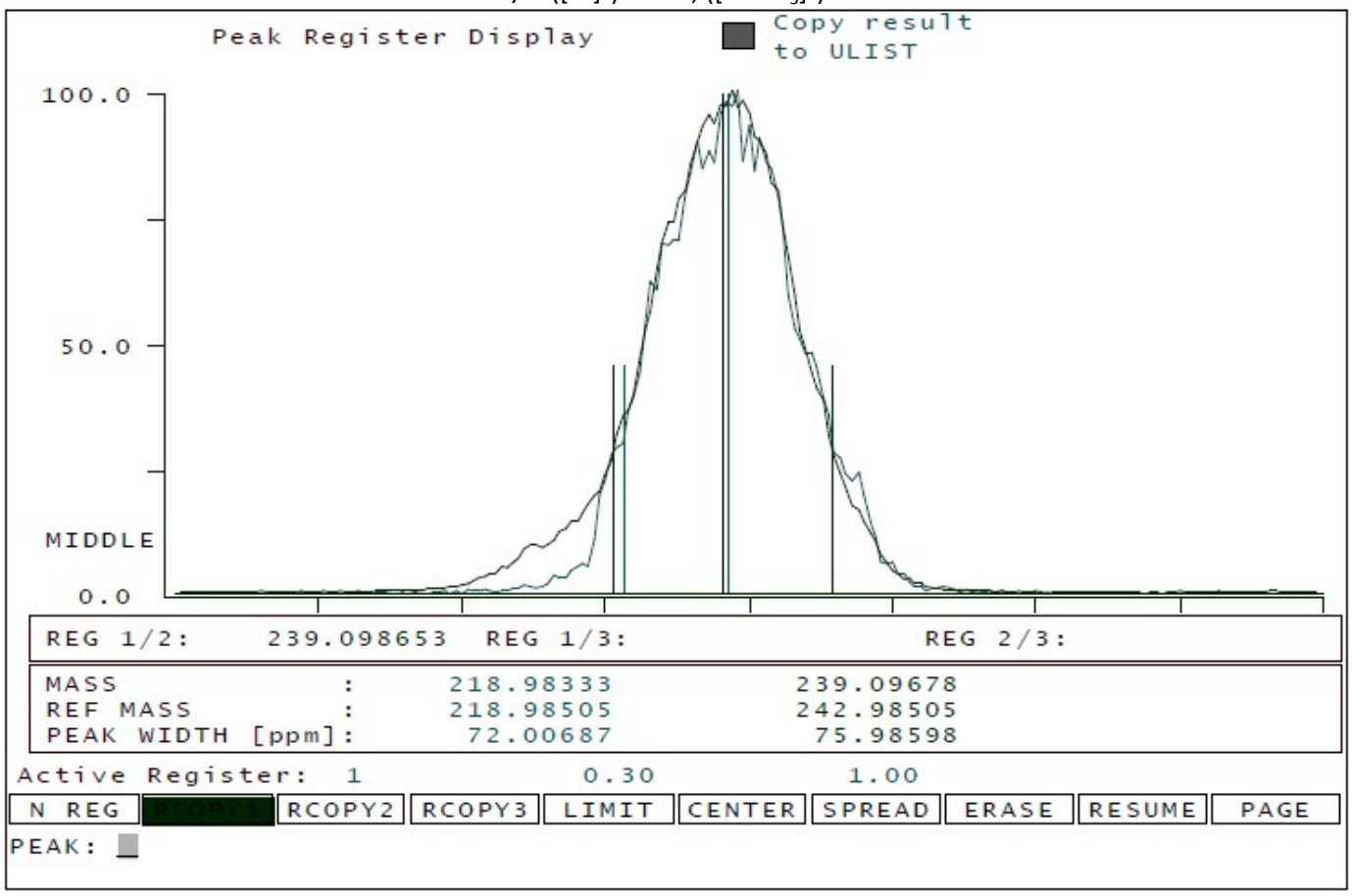

Figure S25E. Hydroboration of acetophenone, HRMS of product in PhMe solution.

HRMS (ASAP/Qtof): *m/z*: ([M(^{10}B)]$^+$) Calcd. for $C_{14}H_{13}BO_3$: 239.0987 ; Found : 239.0989.

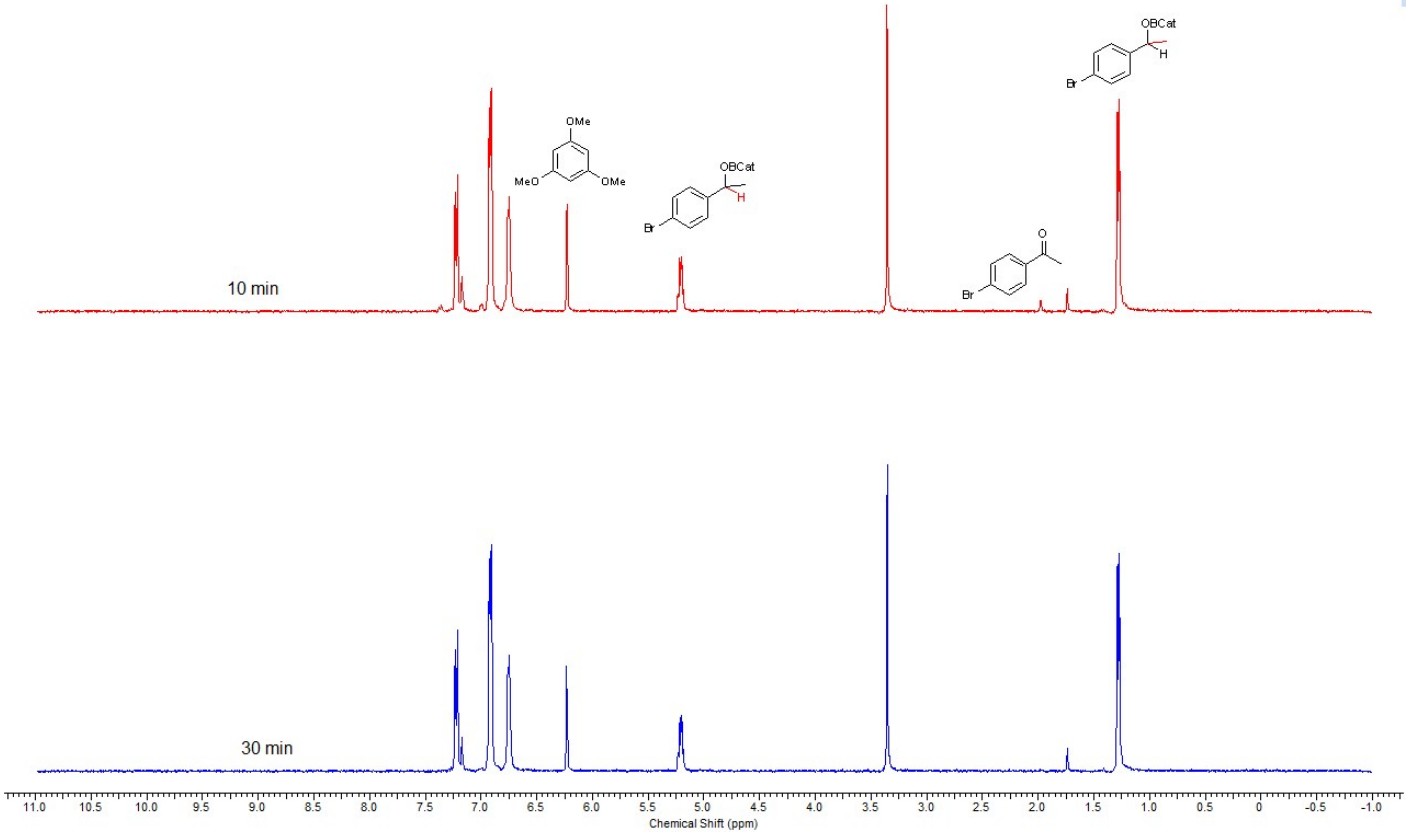

Figure S26A. Hydroboration of 4'-bromoacetophenone (400 MHz, C_6D_6), 25°C, 30 minutes, 0.1 mol% **3**.
^{1}H-NMR (400 MHz, 25 °C, C_6D_6): δ = 7.22 (d, 2H, $^1J_{H\text{-}H}$ = 7.6 Hz, *o*-Ph), 7-6.6 (m, 6H, *m*-Ph & B*Cat*), 5.21 (q,1H, $^1J_{H\text{-}H}$ = 6.1 Hz, benzylic C-*H*), 1.28 (d, 3H, $^1J_{H\text{-}H}$ = 6.1 Hz, CH_3)

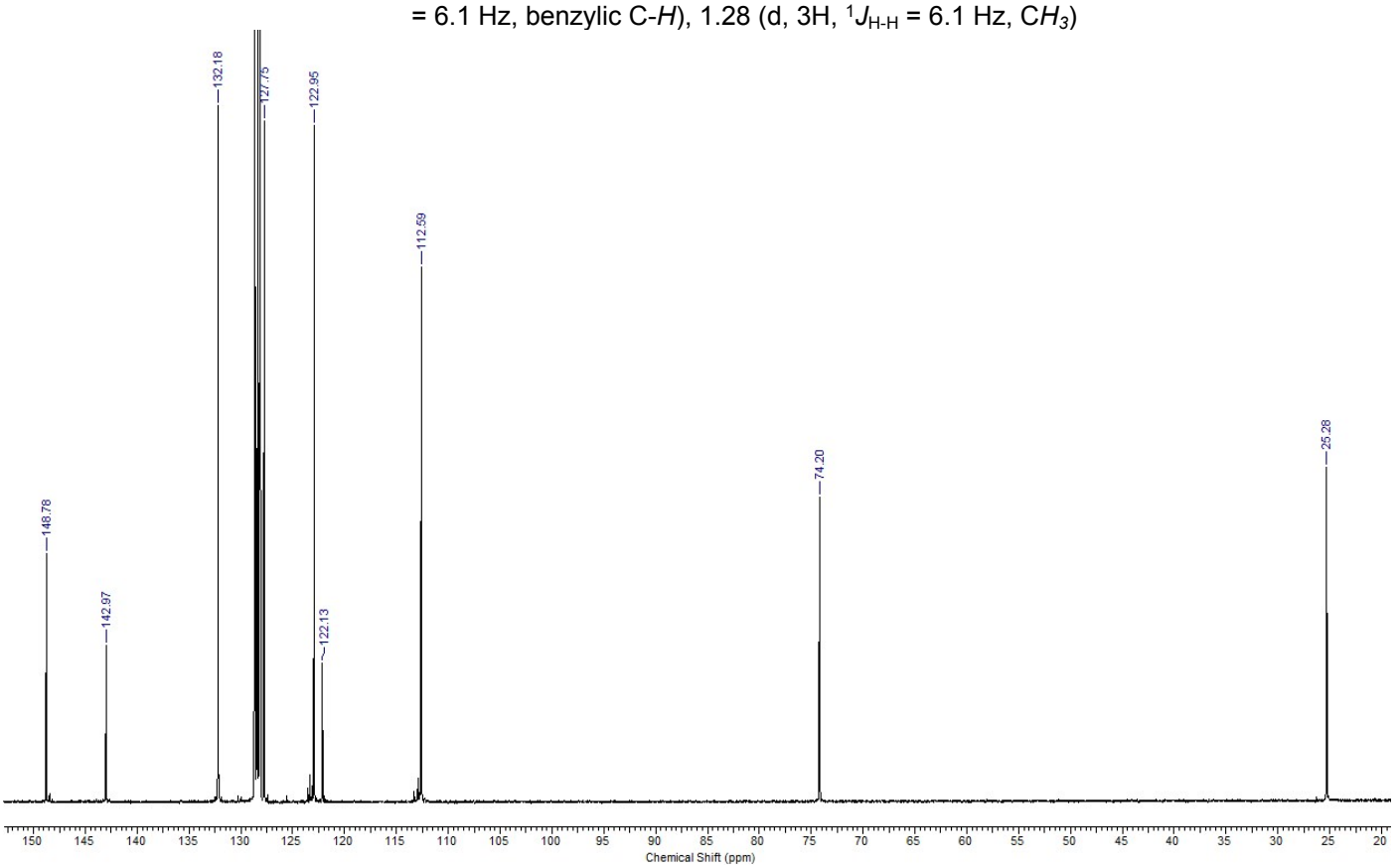

Figure S26B. Hydroboration of 4'-bromoacetophenone (100 MHz, C_6D_6), $^{13}C\{^1H\}$ NMR spectrum of product.
$^{13}C\{^1H\}$-NMR (100 MHz, 25 °C, C_6D_6): δ = 148.8 (s, 2x B*Cat* quaternary C), 143.0 (s, *C*-Br), 132.2 (s, 2x C(Br)-CH-C*H*), 127.8 (s, 2x C(Br)-*C*H), 123.0 (s, 2x B*Cat* *C*H), 122.1 (s, *C*(CH{OB-}CH_3)), 112.6 (s, 2x B*Cat* *C*H), 74.2 (s, C-*C*H{OB-}CH_3)), 25.3 (s, *C*H_3).

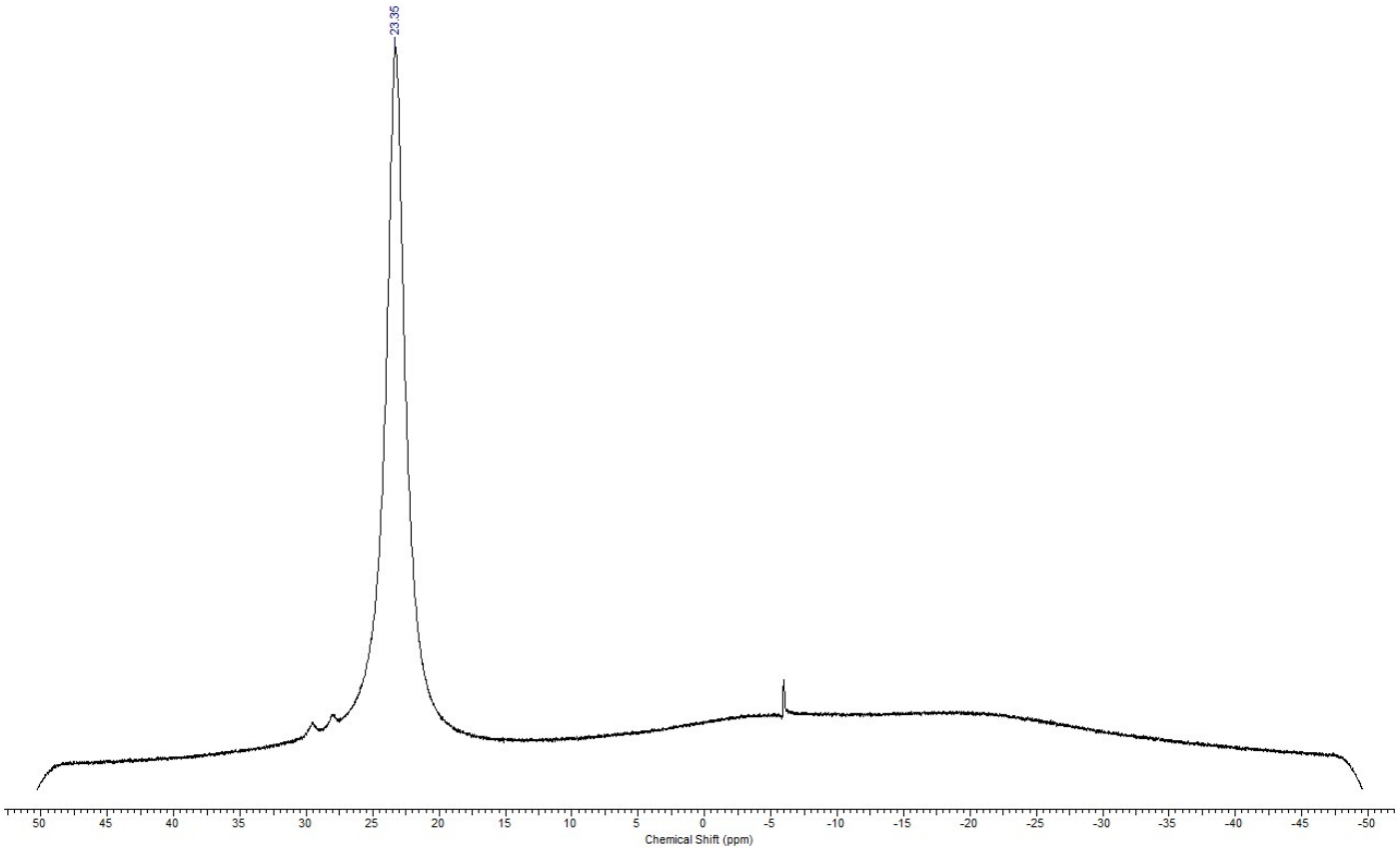

Figure S26C. Hydroboration of 4'-bromoacetophenone (128 MHz, C_6D_6), ^{11}B NMR spectrum of product

$^{11}B\{^1H\}$-NMR (128 MHz, 25°C, $CDCl_3$): δ = 23.4 (s, *B*Cat)

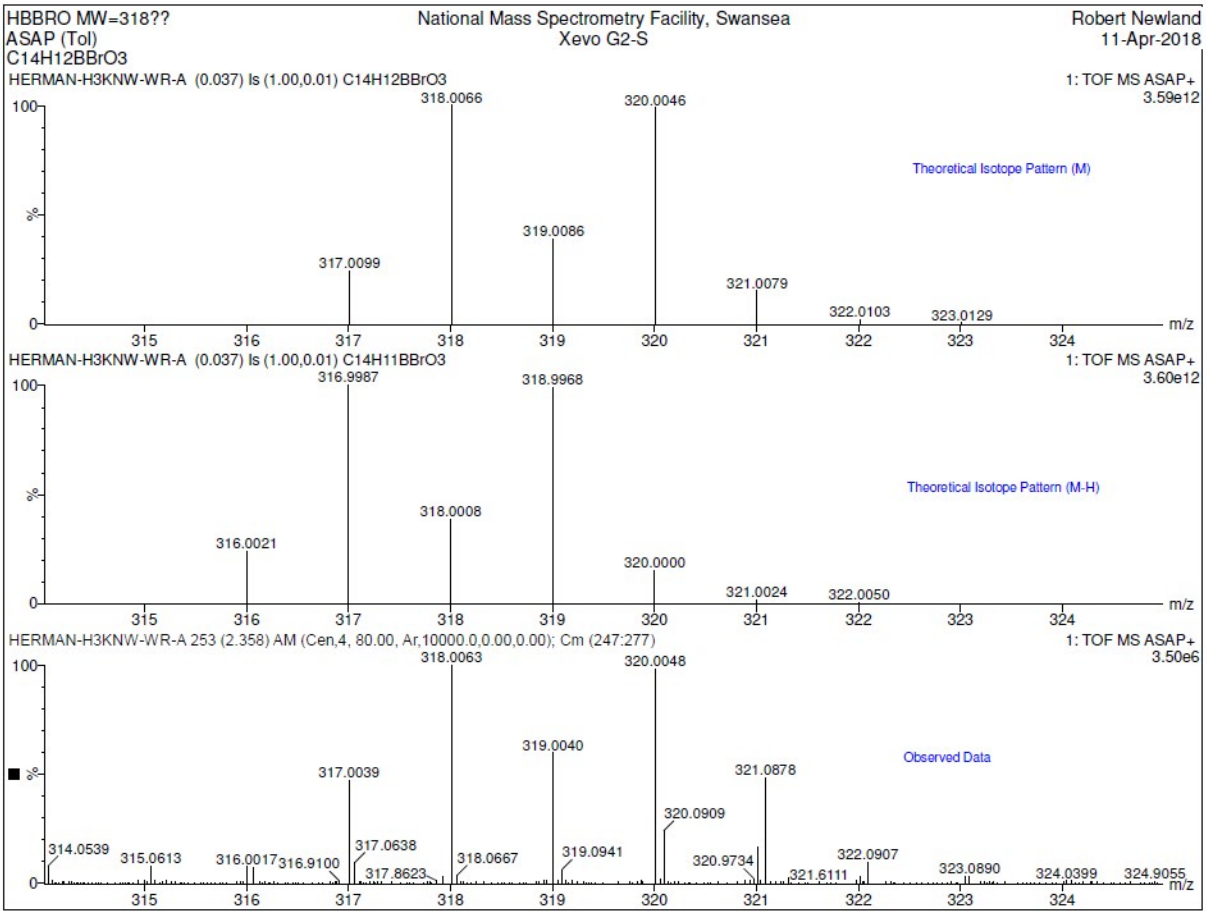

Figure S26D. Hydroboration of 4'-bromoacetophenone, HRMS of product in PhMe solution

HRMS (ASAP/Qtof) *m/z*: ([M(^{79}Br)]$^+$) Calcd. for $C_{14}H_{12}BBrO_3$: 318.0066 ; Found : 318.0063; ([M(^{81}Br)]$^+$) Calcd. for $C_{14}H_{12}BBrO_3$: 320.0046; Found : 320.0048.

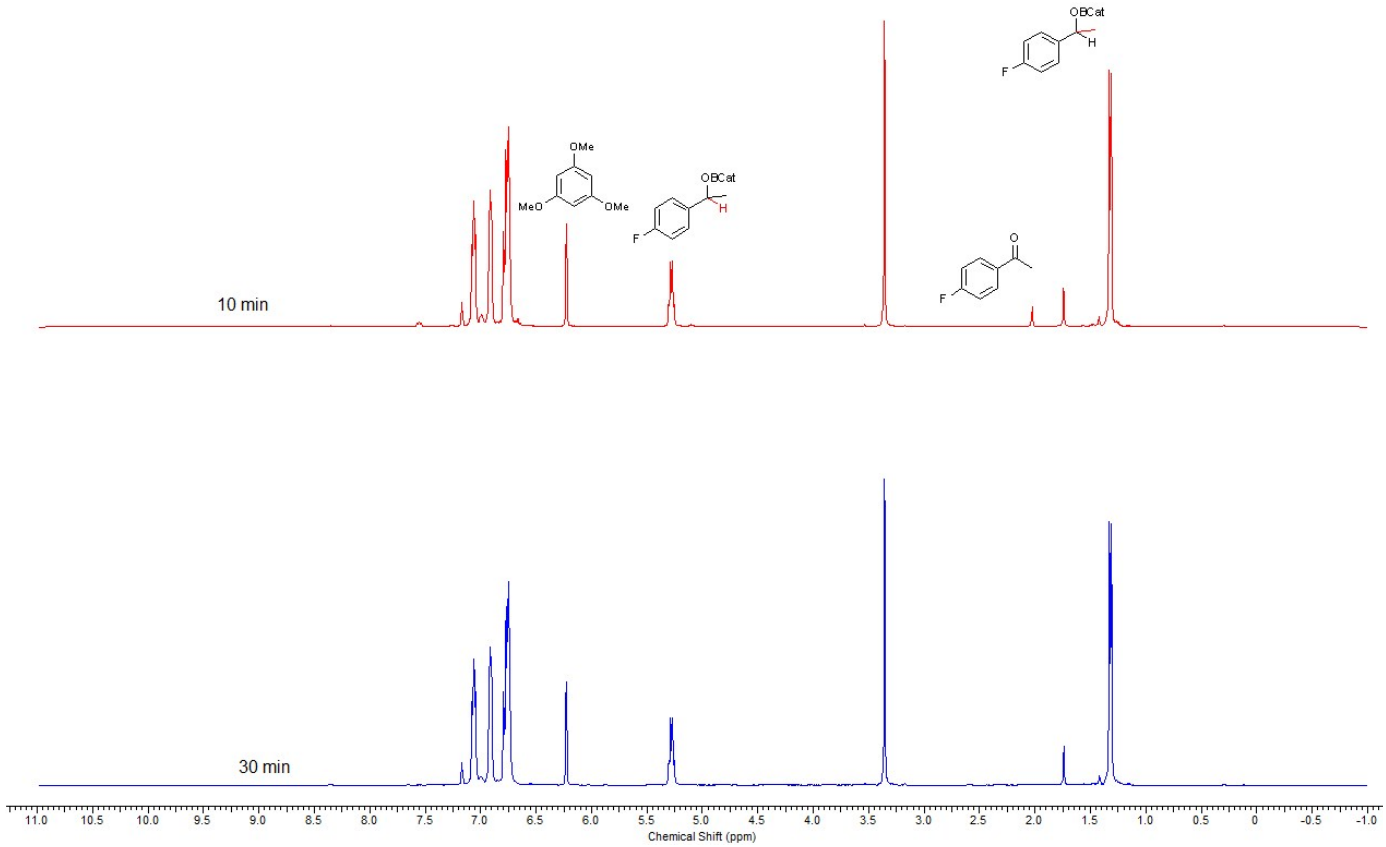

Figure S27A. Hydroboration of 4'-fluoroacetophenone (400 MHz, C_6D_6), 25°C, 30 minutes, 0.1 mol% **3**. **^{1}H-NMR (400 MHz, 25 °C, C_6D_6):** δ = 7.05 (t, 2H, $^1J_{H\text{-}H}$ = 6.1 Hz, *o*-Ph), 6.95-6.65 (m, 6H, *m*-Ph & B*Cat*), 5.27 (q,1H, $^1J_{H\text{-}H}$ = 6.1 Hz, benzylic C-*H*), 1.31 (d, 3H, $^1J_{H\text{-}H}$ = 6.4 Hz, CH_3).

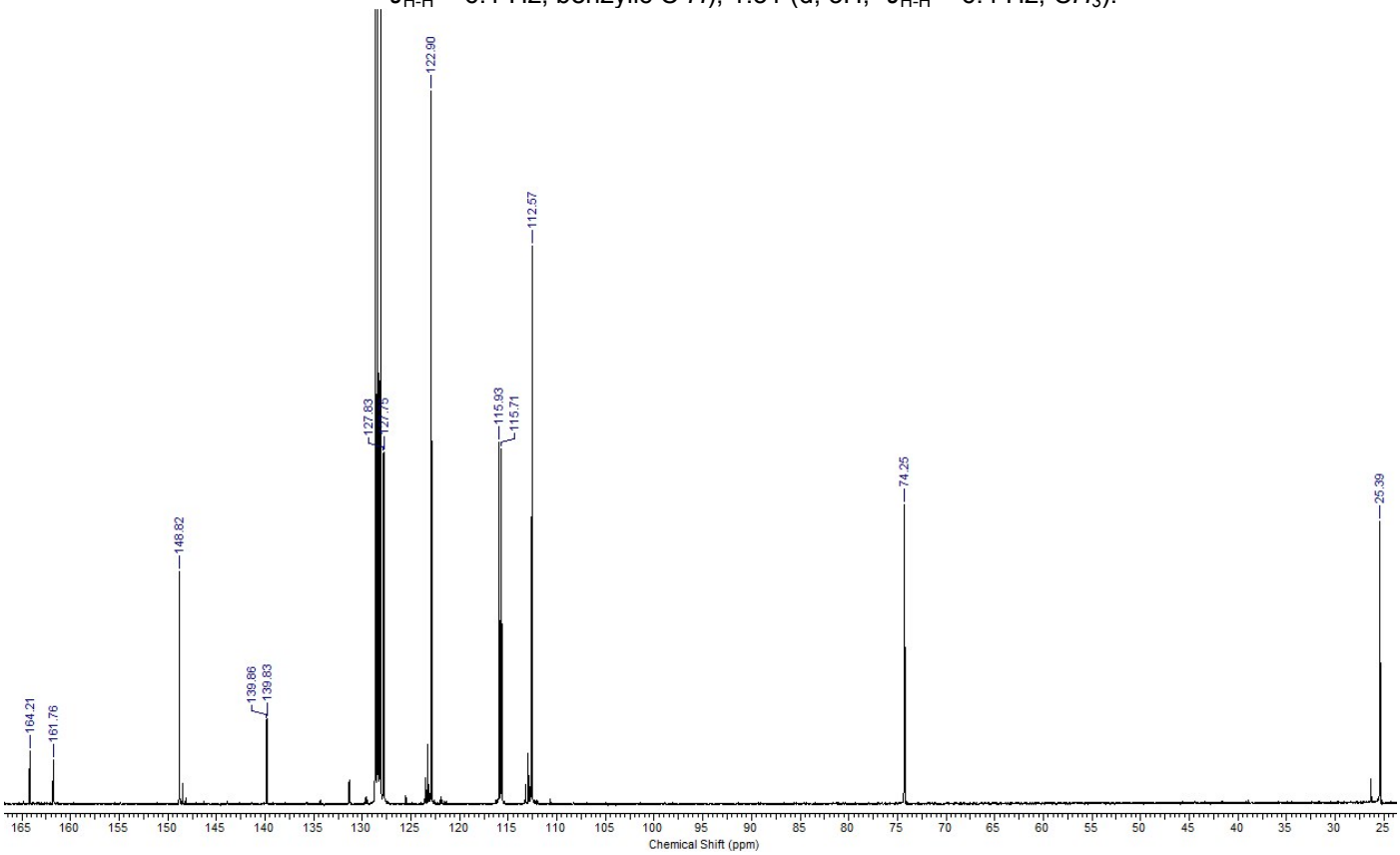

Figure S27B. Hydroboration of 4'-fluoroacetophenone (100 MHz, C_6D_6), $^{13}C\{^1H\}$ NMR spectrum of product **$^{13}C\{^1H\}$-NMR (100 MHz, 25 °C, C_6D_6):** δ = 163.0 (d, $^1J_{C\text{-}F}$ = 246.1 Hz, *C*-F), 148.8 (s, 2x B*Cat* quaternary C), 139.9 (d,$^4J_{C\text{-}F}$ = 3.2 Hz, *C*(CH{OB-}CH_3)), 127.8 (d, $^3J_{C\text{-}F}$ = 8.0 Hz, 2x C(F)-CH-C*H*), 122.9 (s, 2x B*Cat* *C*H), 115.8 (d, $^2J_{C\text{-}F}$ = 21.6 Hz, 2x C(F)-*C*H-), 112.6 (s, 2x B*Cat* *C*H), 74.3 (s, C-*C*H{OB-}CH_3)), 25.4 (s, *C*H_3)

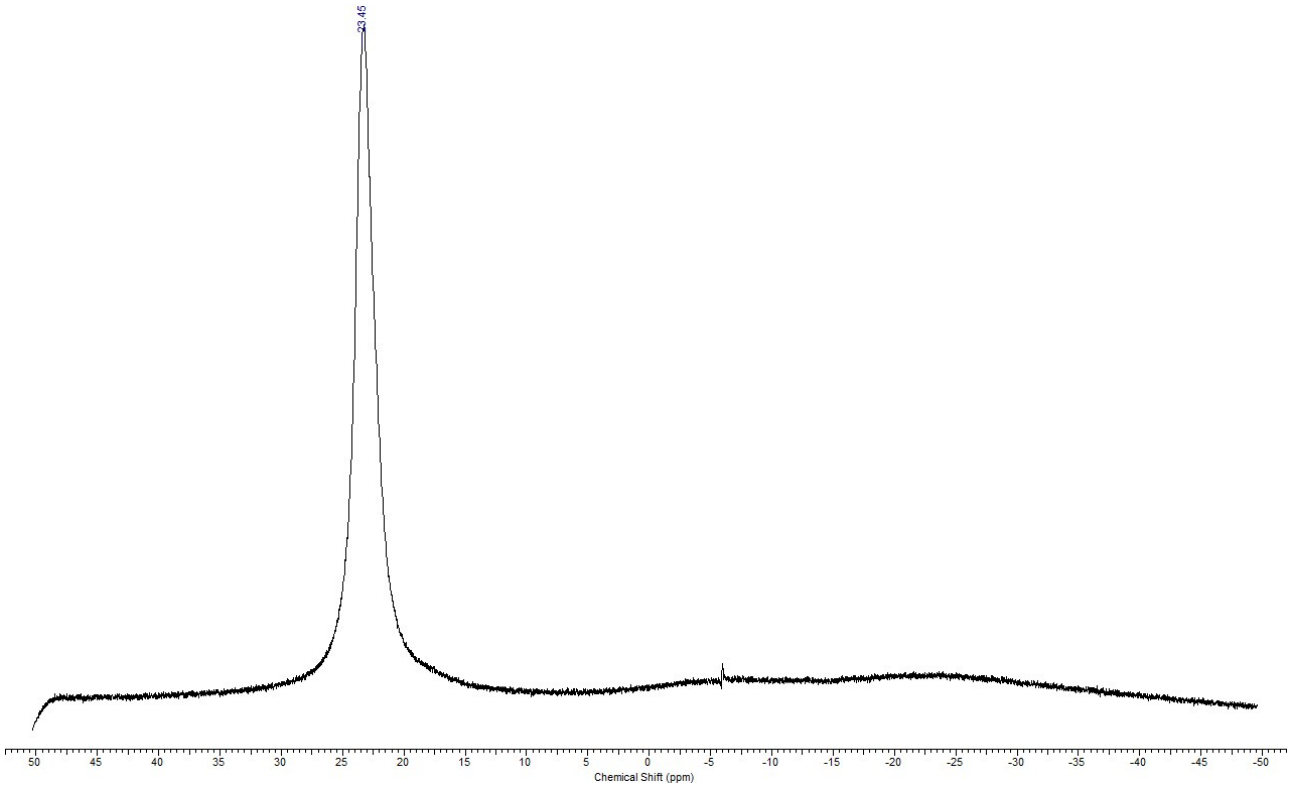

Figure S27C. Hydroboration of 4'-fluoroacetophenone (128 MHz, C_6D_6), ^{11}B NMR spectrum of product

$^{11}B\{^1H\}$-NMR (128 MHz, 25°C, $CDCl_3$): δ = 23.5 (s, *B*Cat)

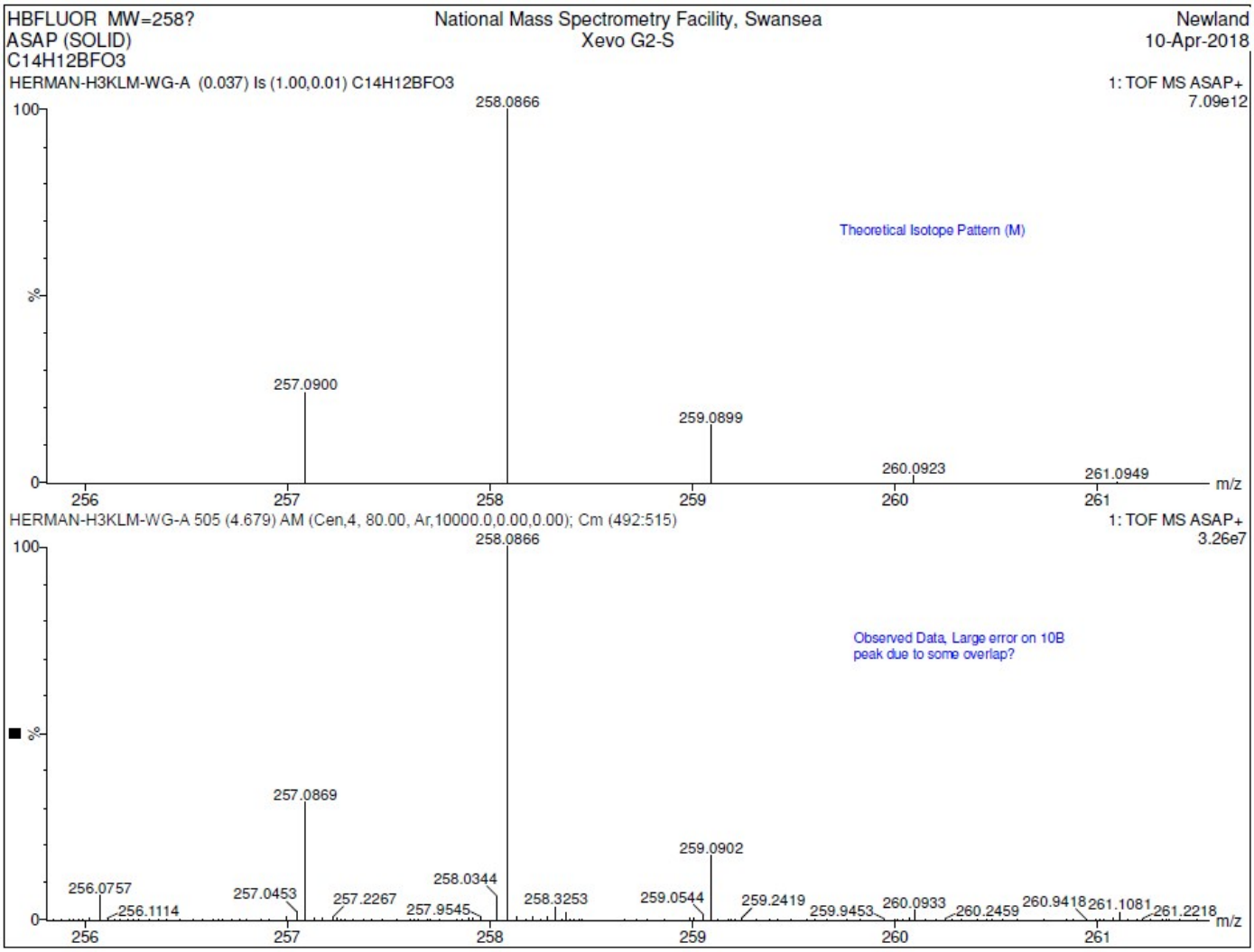

Figure S27D. Hydroboration of 4'-fluoroacetophenone, HRMS of product in PhMe solution.

HRMS (ASAP/Qtof) *m/z*: ([M]$^+$) Calcd. for $C_{14}H_{12}BFO_3$: 258.0866; Found : 286.0866.

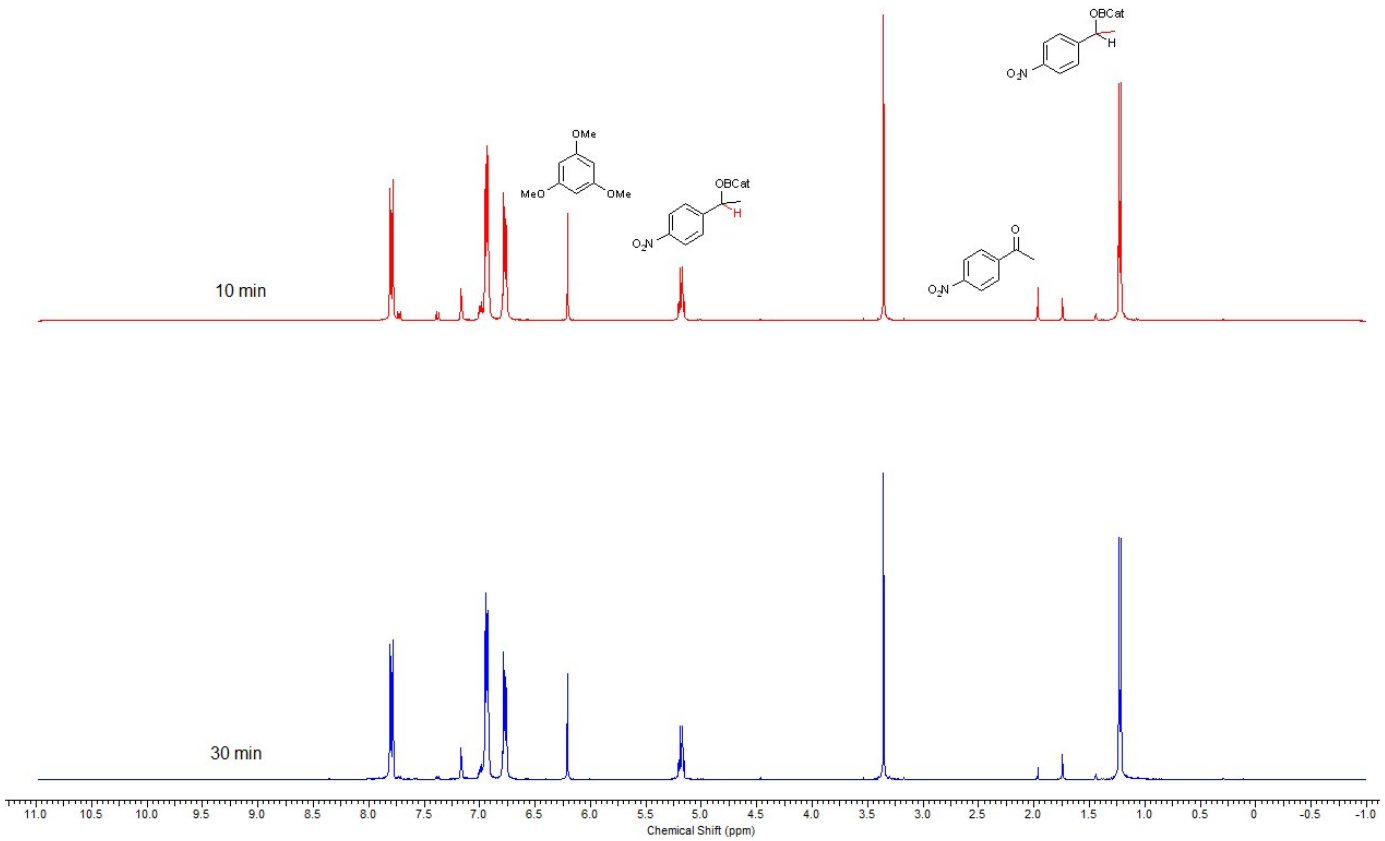

Figure S28A. Hydroboration of 4'-nitroacetophenone (400 MHz, C_6D_6), 25°C, 30 minutes, 0.1 mol% **3** (data matches that in the literature).[11]

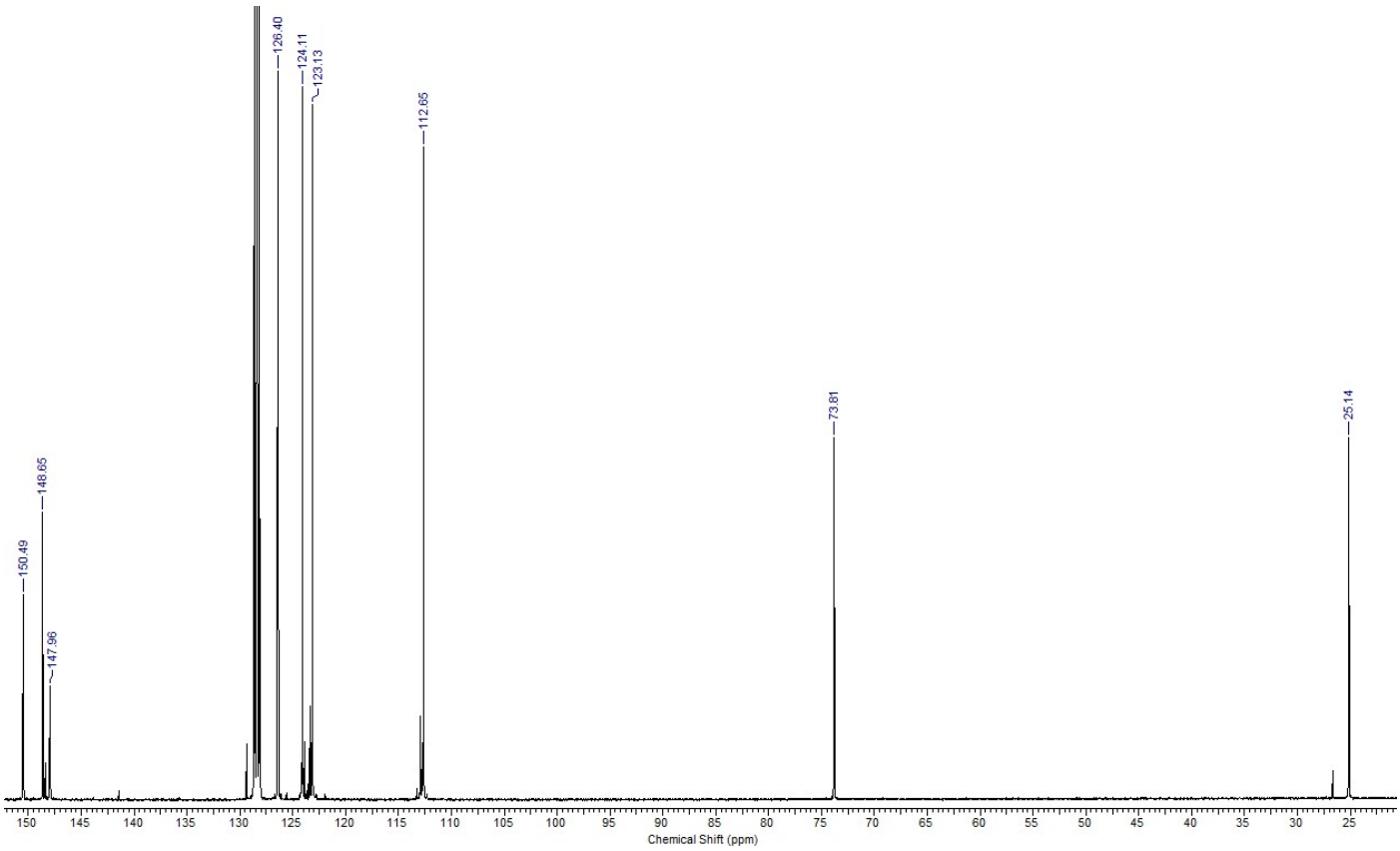

Figure S28B. Hydroboration of 4'-nitroacetophenone (100 MHz, C_6D_6), $^{13}C\{^1H\}$ NMR spectrum of product (data matches that in the literature).[11]

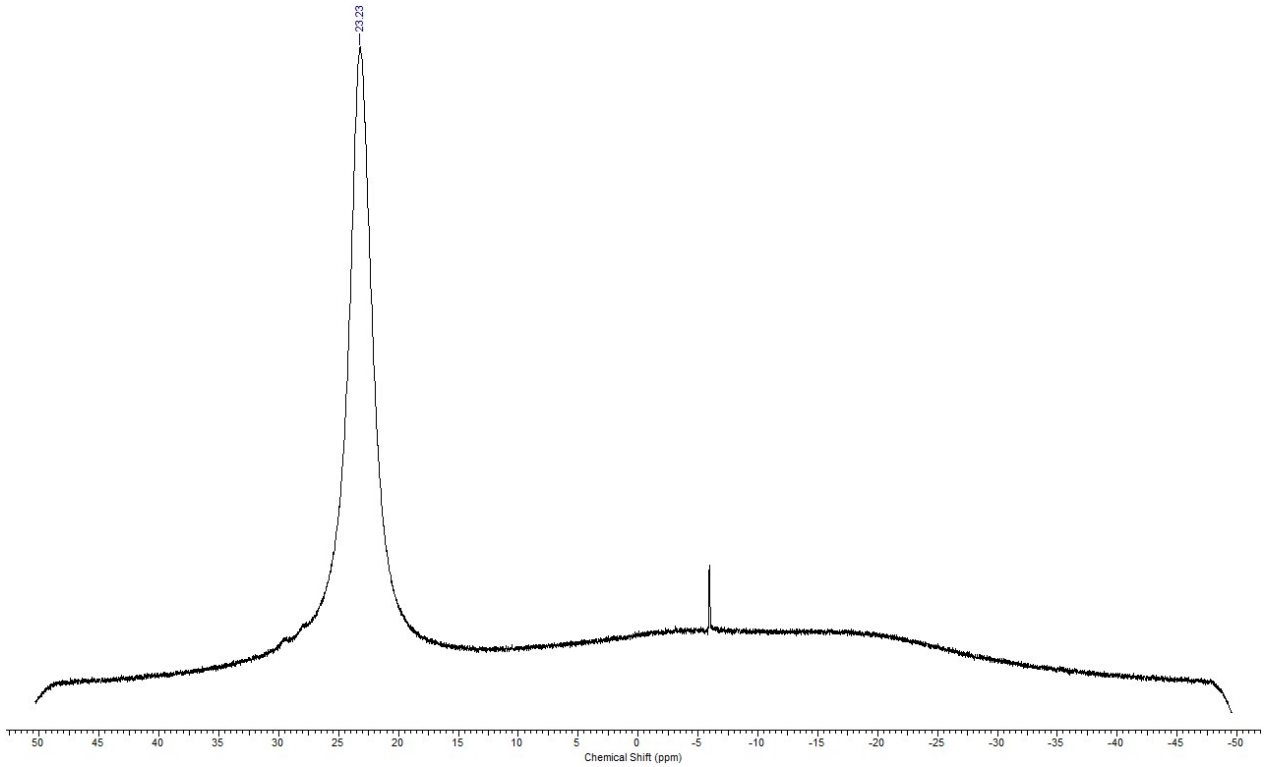

Figure S28C. Hydroboration of 4'-nitroacetophenone (128 MHz, C_6D_6), ^{11}B NMR spectrum of product (data matches that in literature)[11]

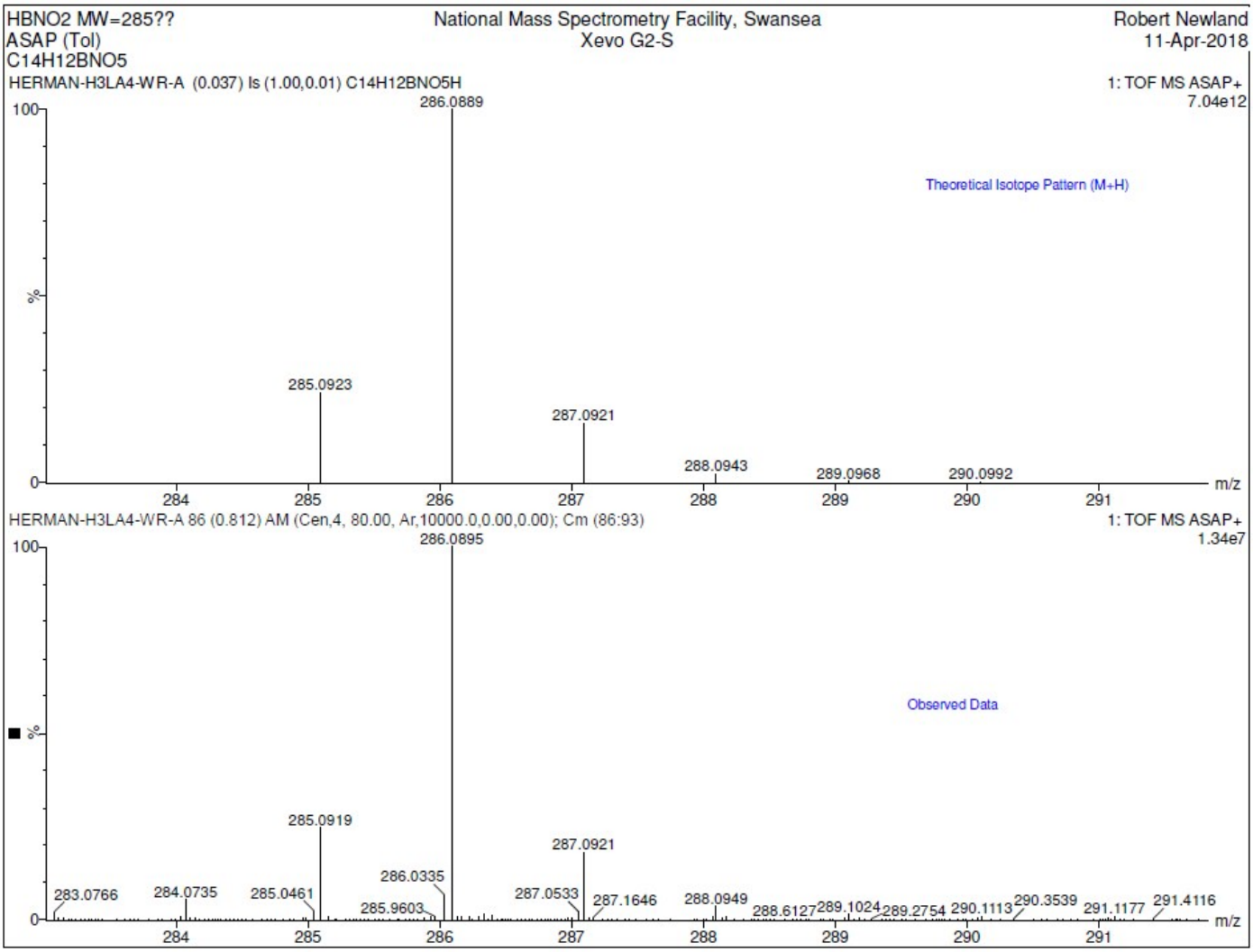

Figure S28D. Hydroboration of 4'-nitroacetophenone, HRMS of product in PhMe solution
HRMS (ASAP/Qtof) *m/z*: ([M+H]$^+$) Calcd. for $C_{14}H_{13}BNO_5$: 286.0889; Found : 286.0895

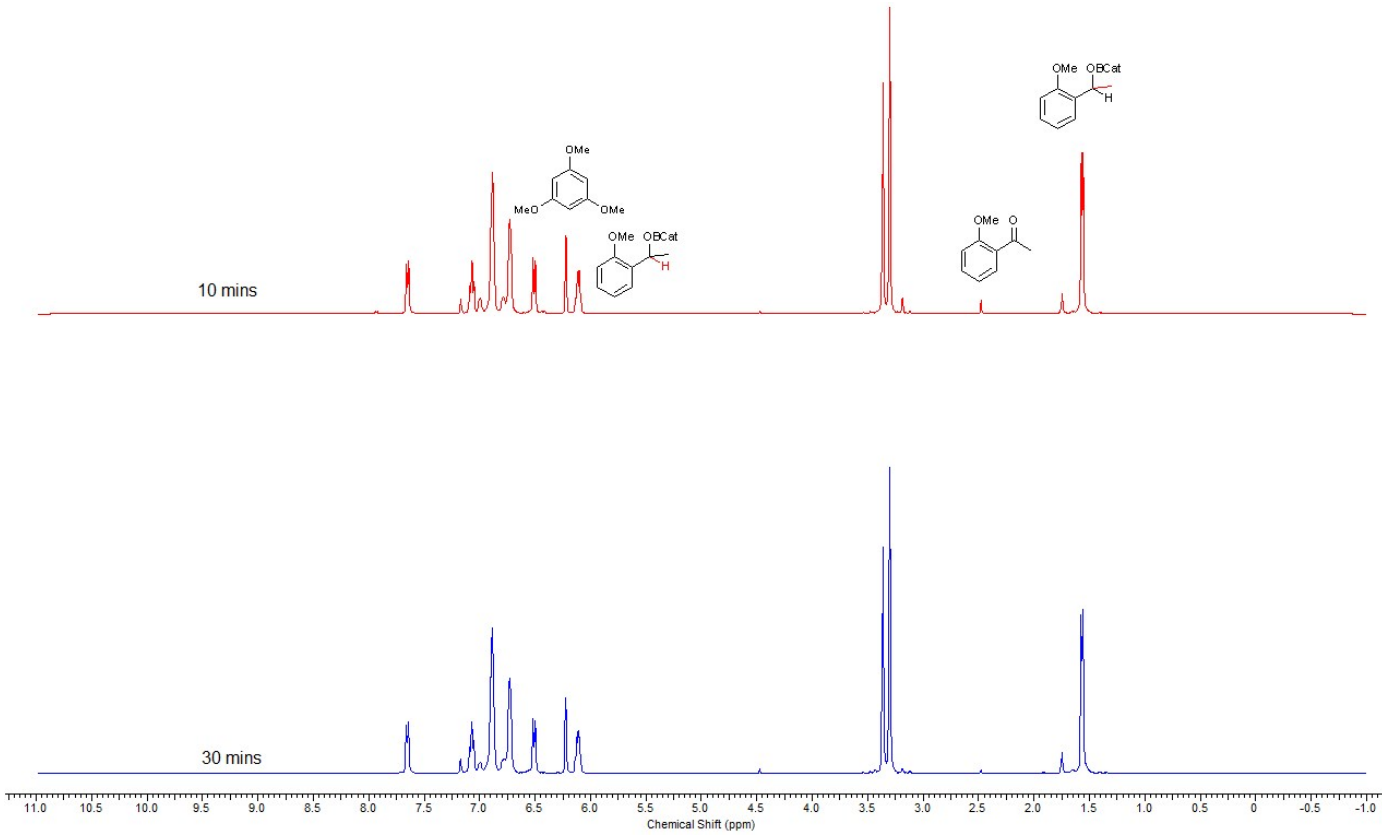

Figure S29. Hydroboration of 2'-methoxyacetophenone (400 MHz, C_6D_6), 25°C, 30 minutes, 0.1 mol% **3**
^{1}H-NMR (400 MHz, 25 °C, C_6D_6): δ = 7.65 (s, 1H, -C(OMe)-C*H*-), 7.07 (t, 1H, $^1J_{H\text{-}H}$ = 7.6 Hz, -C(OMe)-CH-C*H*-), 6.89 (bs, 3H, B*Cat* & -C(OMe)-CH-CH-C*H*-), 6.73 (bs, 2H, B*Cat*), 6.51 (d, 1H, $^1J_{H\text{-}H}$ = 7.9 Hz, C(CH{OBCat}CH_3)-C*H*-), 6.12 (q,1H, $^1J_{H\text{-}H}$ = 6.1 Hz, benzylic C-*H*), 1.57 (d, 3H, $^1J_{H\text{-}H}$ = 6.1 Hz, CH_3)

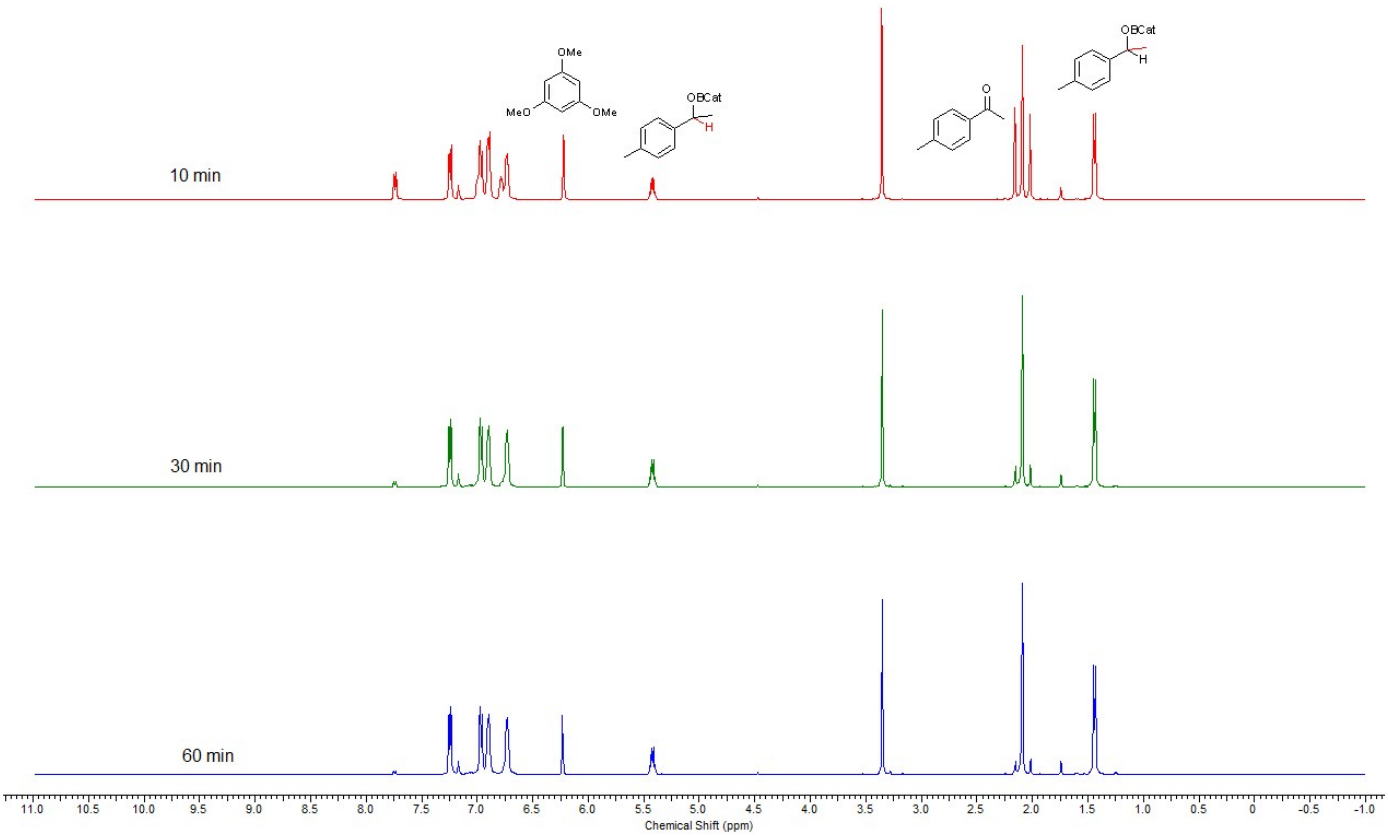

Figure S30A. Hydroboration of 4'-methylacetophenone (400 MHz, C_6D_6), 25°C, 60 minutes, 0.1 mol% **3**
^{1}H-NMR (400 MHz, 25 °C, C_6D_6): δ = 7.24 (d, 2H, $^1J_{H\text{-}H}$ = 7.6 Hz, *o*-Ph), 6.97 (d, 2H, $^1J_{H\text{-}H}$ = 7.6 Hz, *m*-Ph), 6.90 (bs, 2H, B*Cat*), 6.74 (d, 2H, $^1J_{H\text{-}H}$ = 3.2 Hz, B*Cat*), 5.42 (q,1H, $^1J_{H\text{-}H}$ = 6.4 Hz, benzylic C-*H*), 2.09 (s, 3H, Ph-CH_3), 1.44 (d, 3H, $^1J_{H\text{-}H}$ = 6.4 Hz, CH_3)

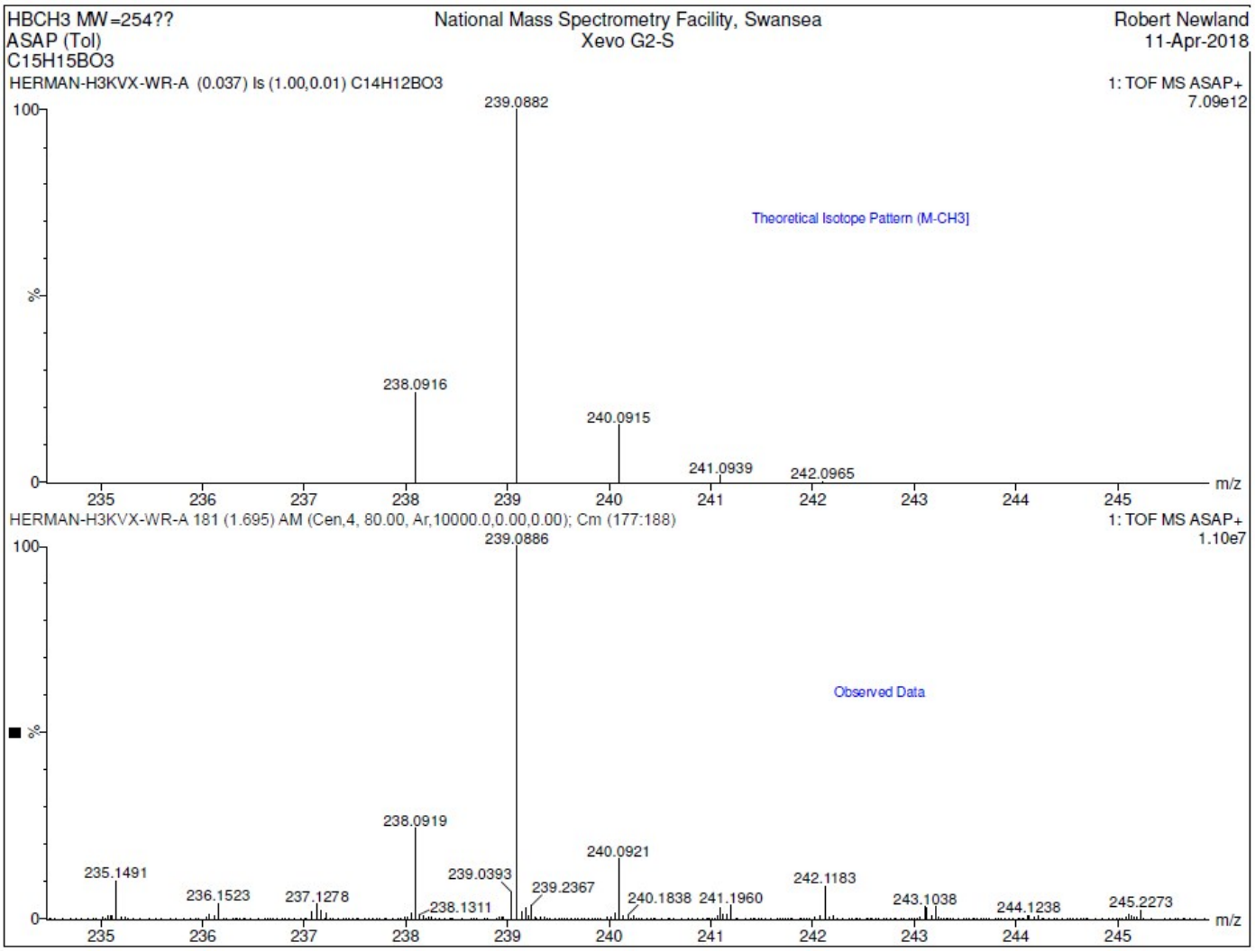

Figure S30B. Hydroboration of 4'-methylacetophenone, HRMS of product in PhMe solution
HRMS (ASAP/Qtof) *m/z*: ([M-CH_3]$^+$) Calcd. for $C_{14}H_{12}BO_3$: 239.0882; Found : 239.0886

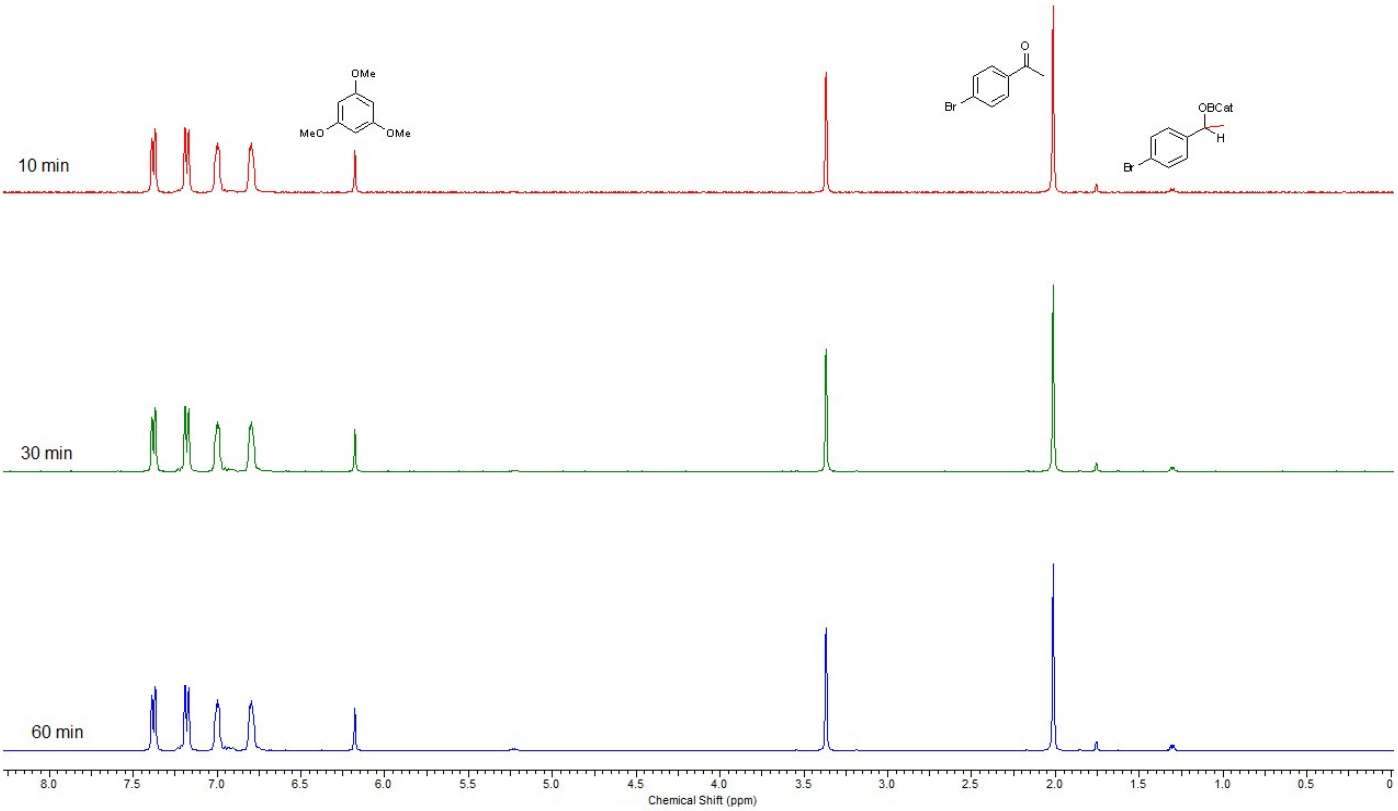

Figure S31. Hydroboration of 4'-bromoacetophenone, 25°C (400 MHz, C_6D_6), 60 minutes, no catalyst showing almost no conversion

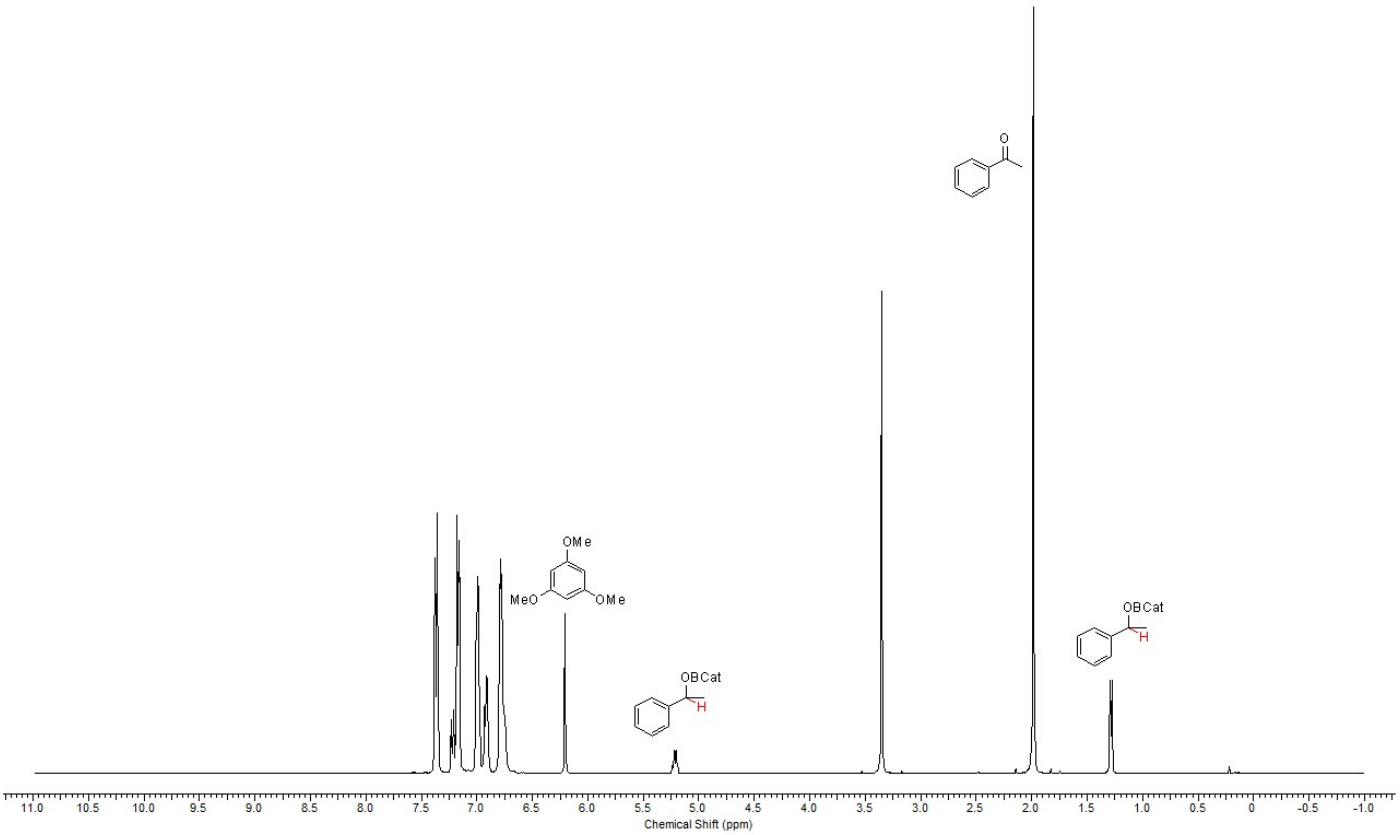

Figure S32. Hydroboration of 4'-bromoacetophenone (400 MHz, C_6D_6), 25°C, 30 minutes, 0.1 mol% **1**

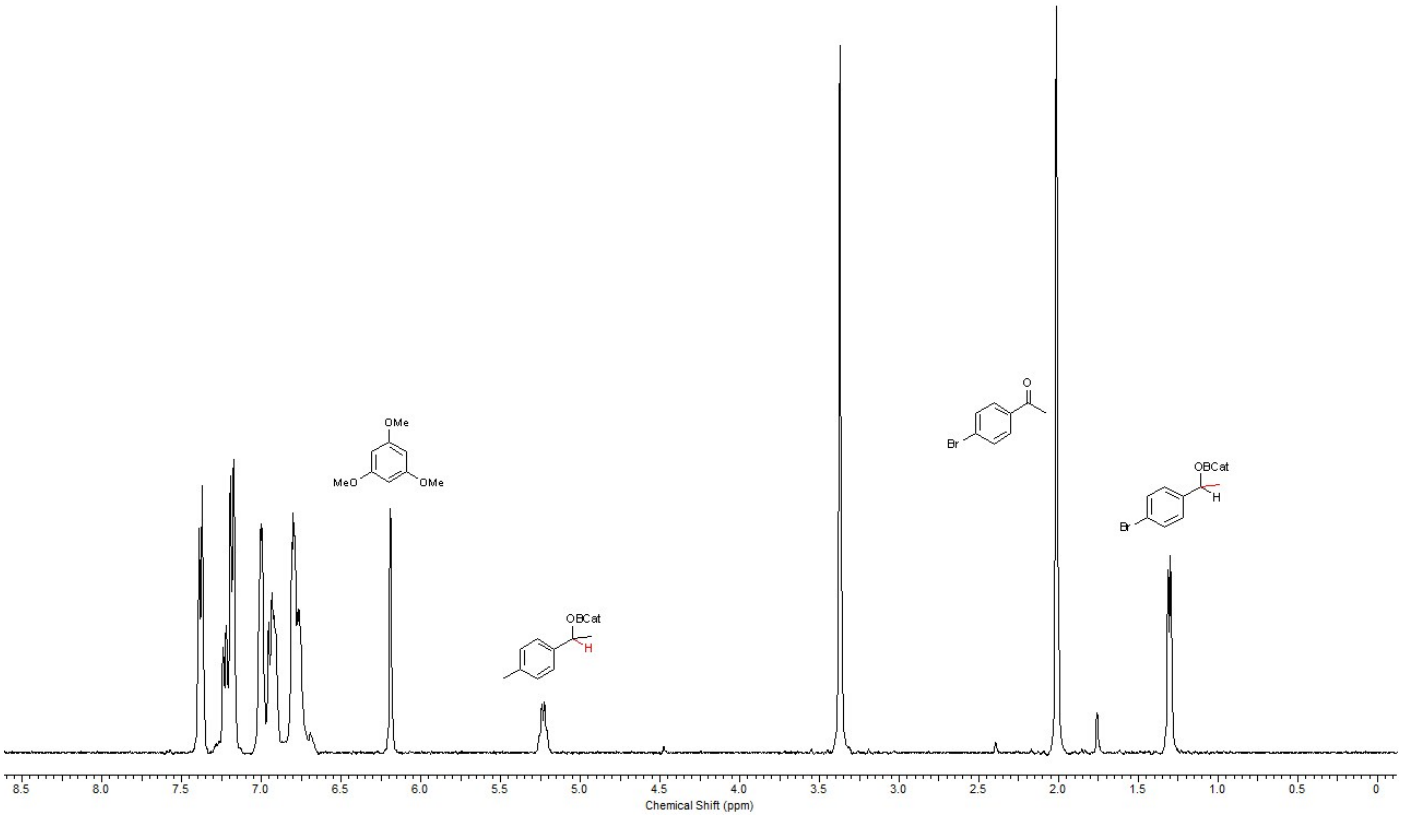

Figure S33. Hydroboration of 4'-bromoacetophenone (400 MHz, C_6D_6), 25°C, 30 minutes, 0.1 mol% **2**

Figure S34. Hydroboration of 4'-bromoacetophenone (400 MHz, C_6D_6), 25°C, 30 minutes, 0.1 mol% [$Rh(PPh_3)_3Cl$]

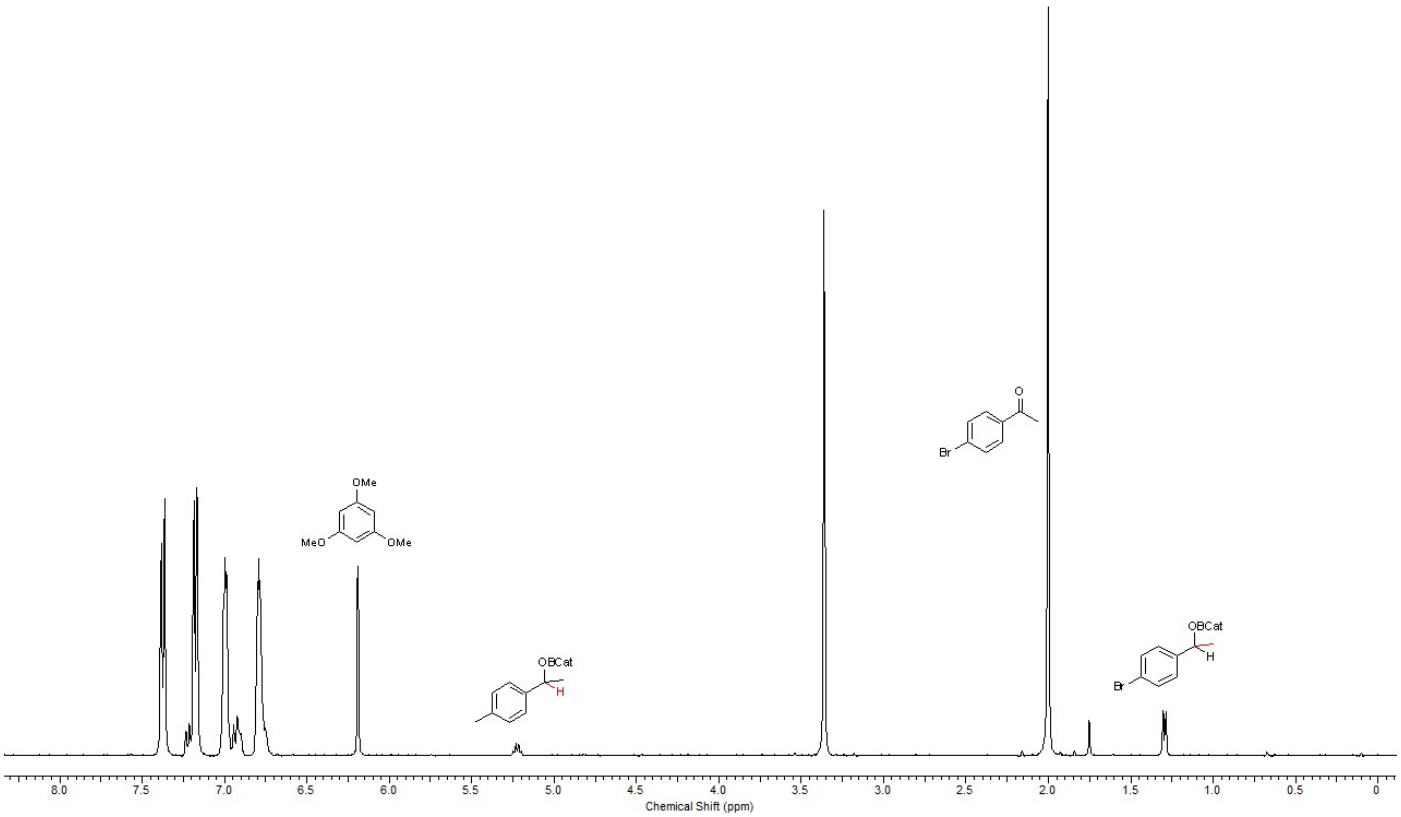

Figure S35. Hydroboration of 4'-bromoacetophenone (400 MHz, C_6D_6), 25°C, 30 minutes, 0.1 mol% **4**

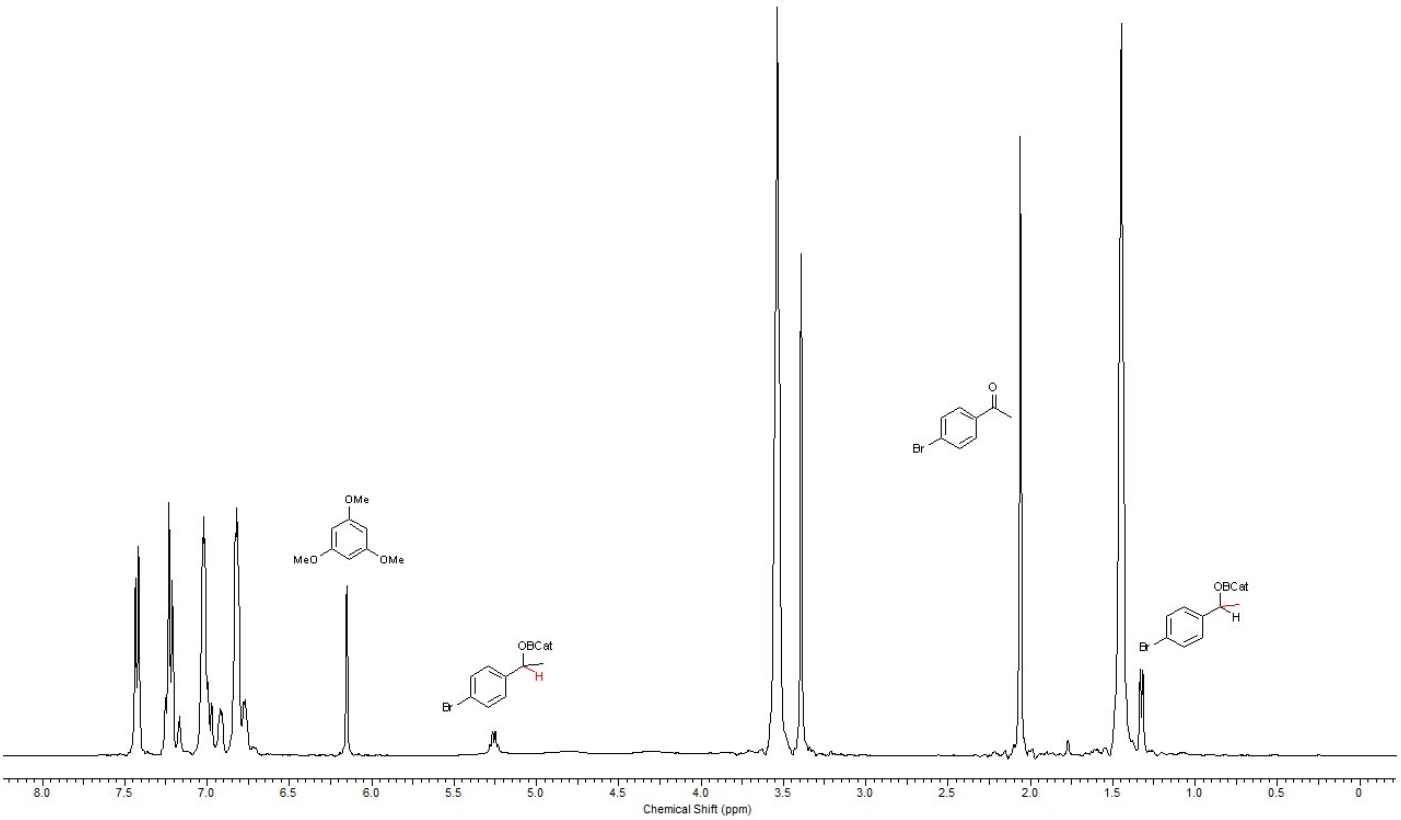

Figure S36. Hydroboration of 4'-bromoacetophenone (400 MHz, C_6D_6), 25°C, 30 minutes, 0.1 mol% $[Rh(COD)_2][BAr^F]$ premixed with 0.2 mol% PCy_3

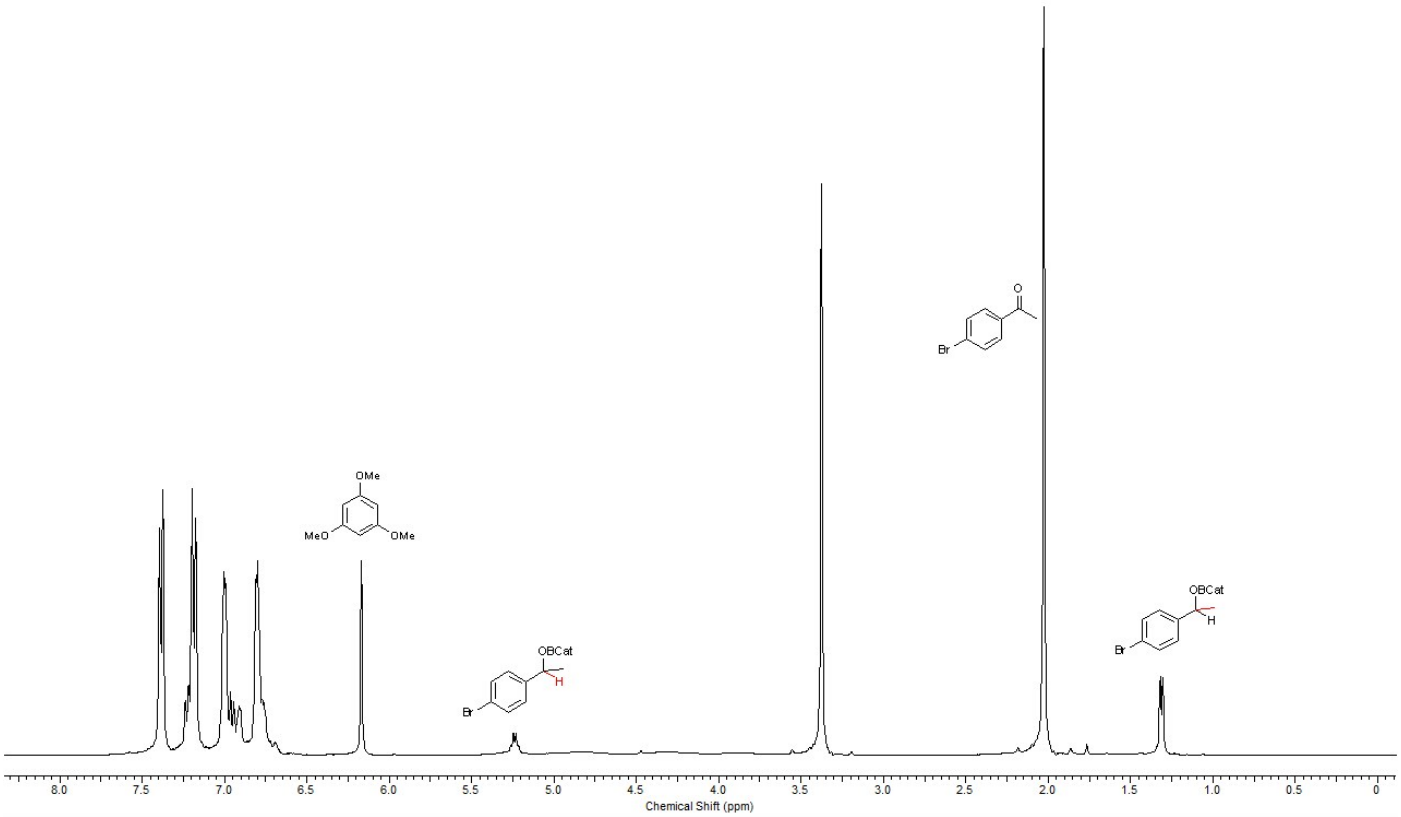

Figure S37. Hydroboration of 4'-bromoacetophenone (400 MHz, C_6D_6), 25°C, 30 minutes, 0.05 mol% [{Rh(COD)Cl}$_2$] premixed with 0.2 mol% PCy_3

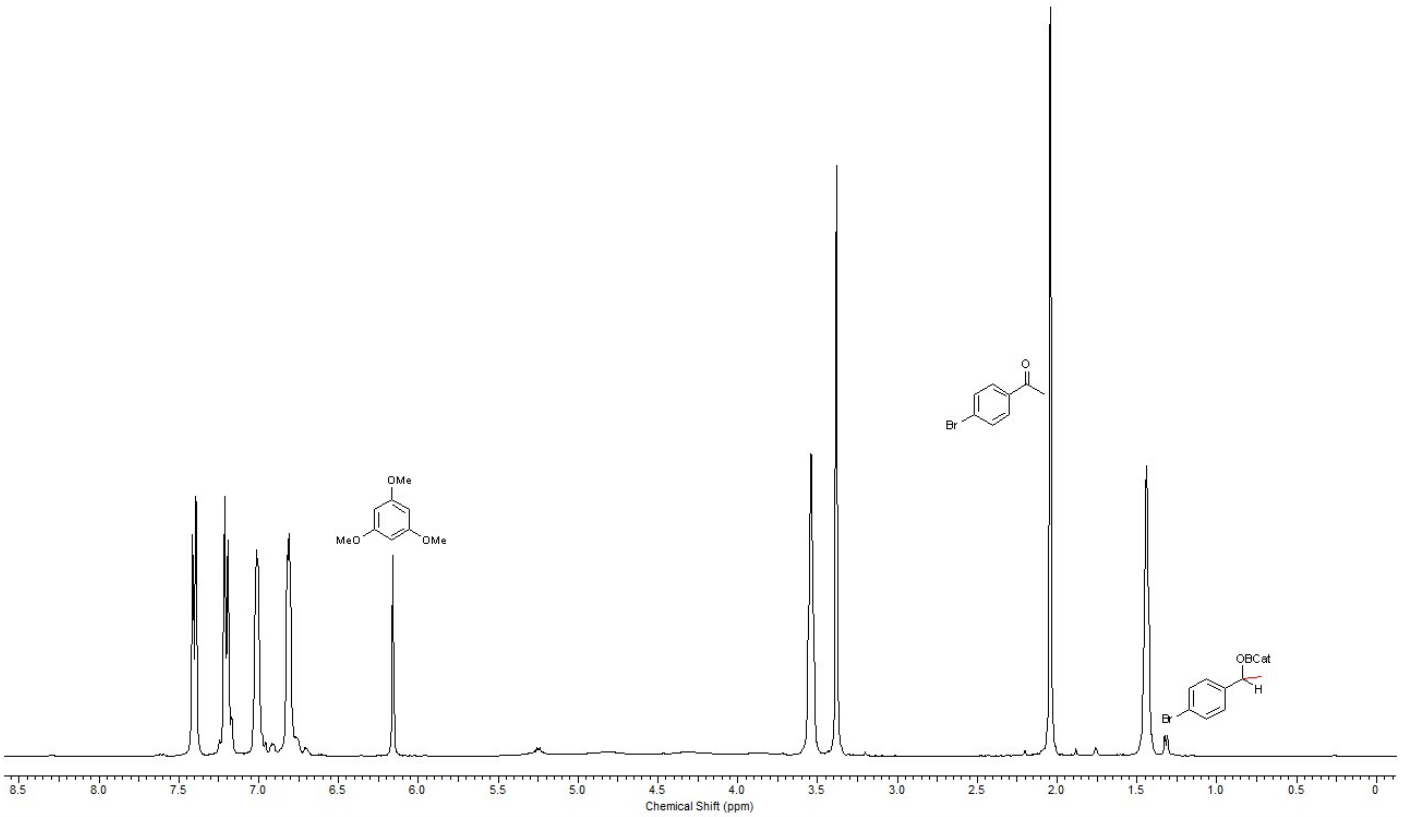

Figure S38. Hydroboration of 4'-bromoacetophenone (400 MHz, C_6D_6), 25°C, 30 minutes, 0.1 mol% [$Rh(COD)_2$][BAr^F] premixed with 0.2 mol% PPh_3

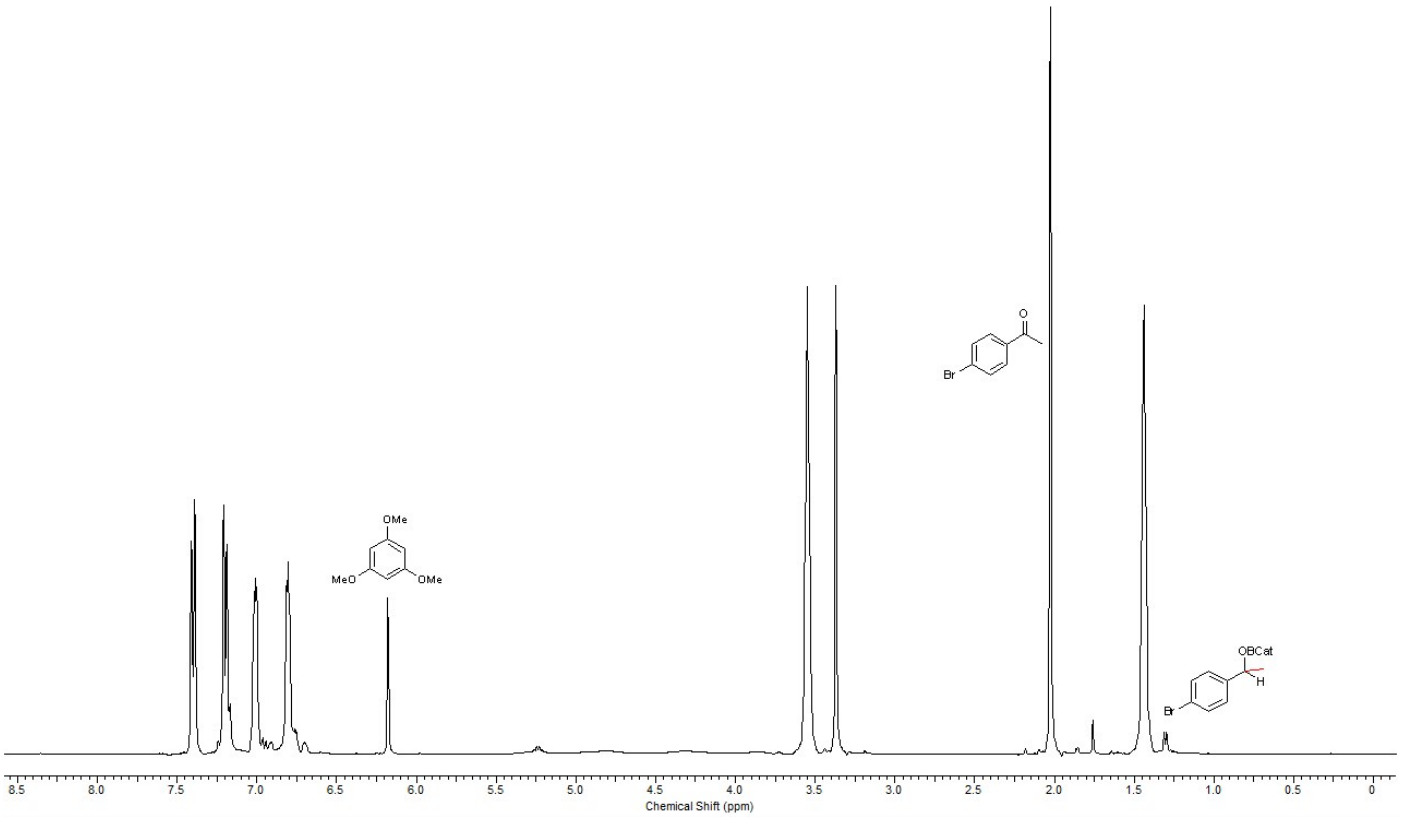

Figure S39. Hydroboration of 4'-bromoacetophenone (400 MHz, C_6D_6), 25°C, 30 minutes, 0.1 mol% $[Rh(COD)_2][BAr^F]$ premixed with 0.1 mol% dppm

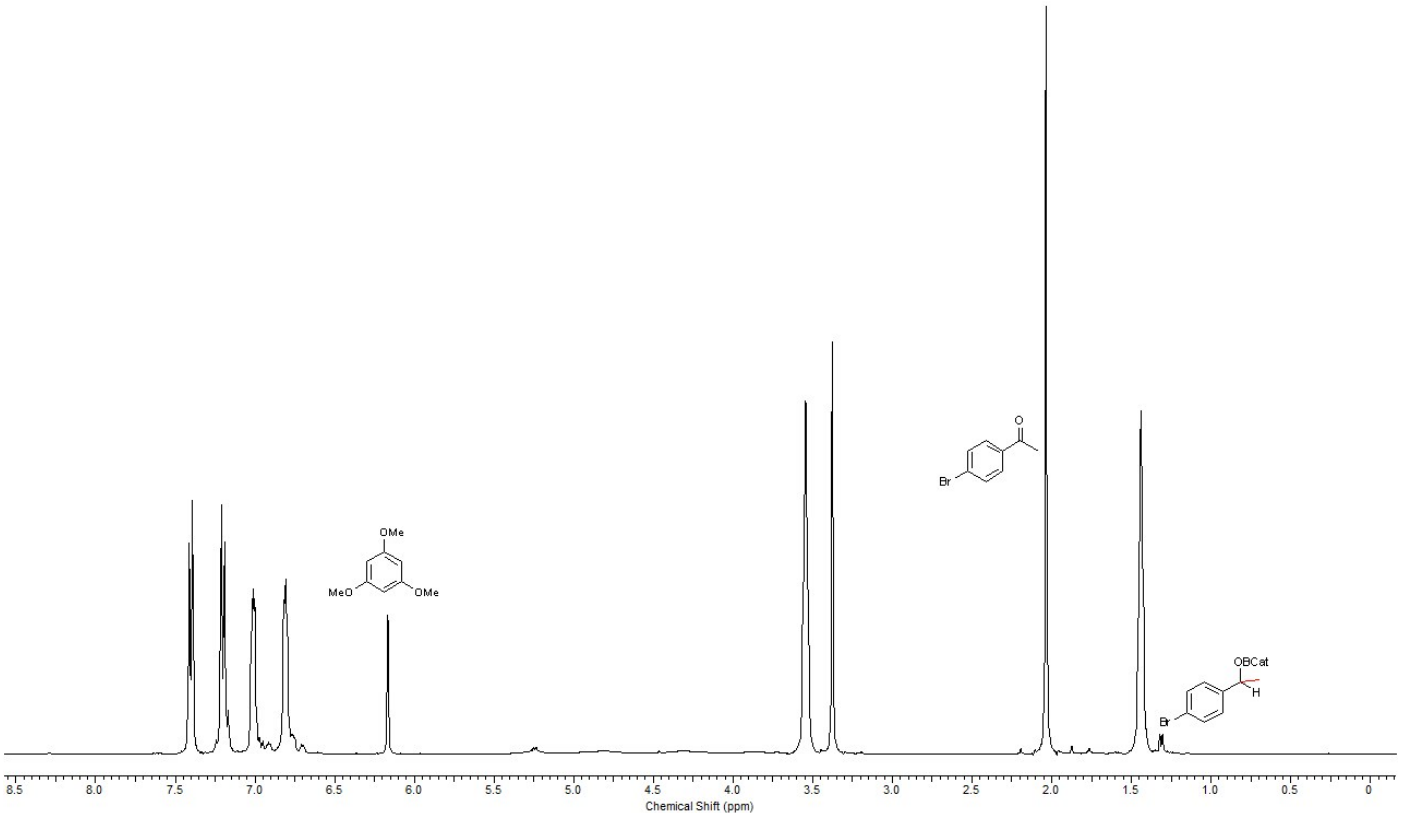

Figure S40. Hydroboration of 4'-bromoacetophenone (400 MHz, C_6D_6), 25°C, 30 minutes, 0.1 mol% $[Rh(COD)_2][BAr^F]$ premixed with 0.2 mol% $P(OPh)_3$

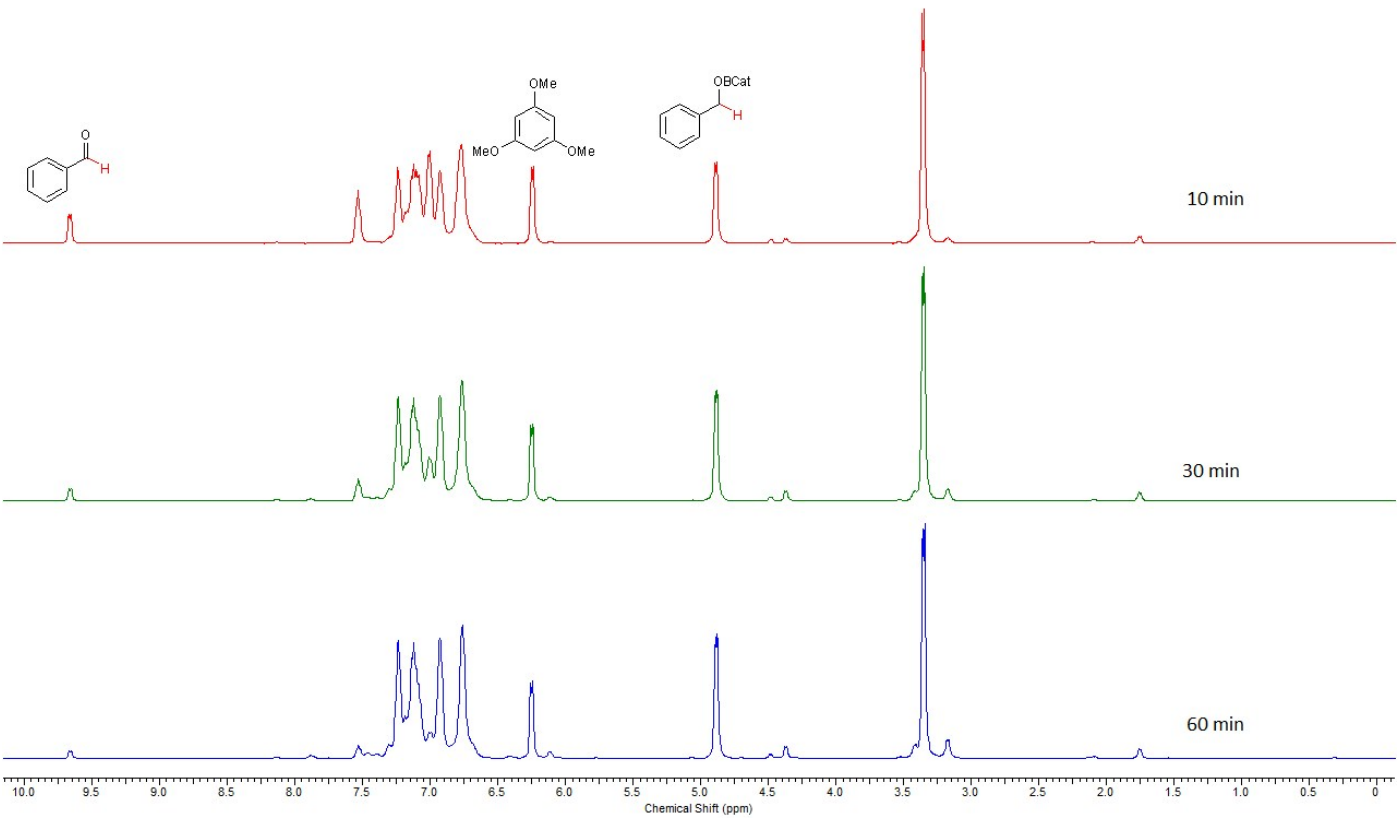

Figure S41-A. Hydroboration of benzaldehyde (400 MHz, C_6D_6), 25°C, 60 minutes, no catalyst, showing an appreciable rate of conversion over 60 mins.

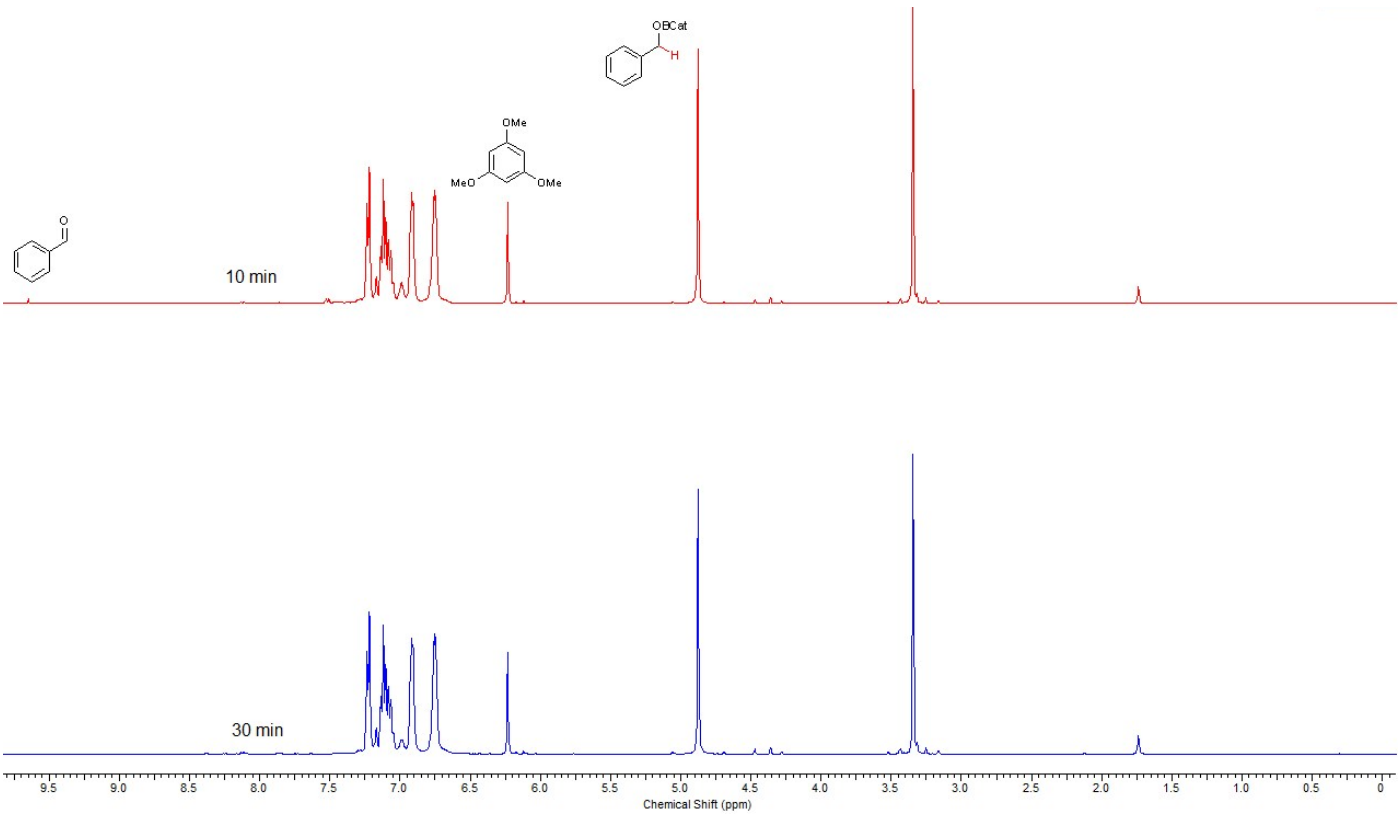

Figure S41-B. Rapid hydroboration of benzaldehyde (400 MHz, C_6D_6), 25°C, 30 minutes, 0.1 mol% **3**
^{1}H-NMR (400 MHz, 25 °C, C_6D_6): δ = 7.28-7.02 (m, 5H, *Ph-H*), 6.92 (bs, 2H, B*Cat*), 6.76 (d, 2H, $^1J_{H\text{-}H}$ = 3.3 Hz, B*Cat*), 4.88 (s,2H, benzylic CH_2)

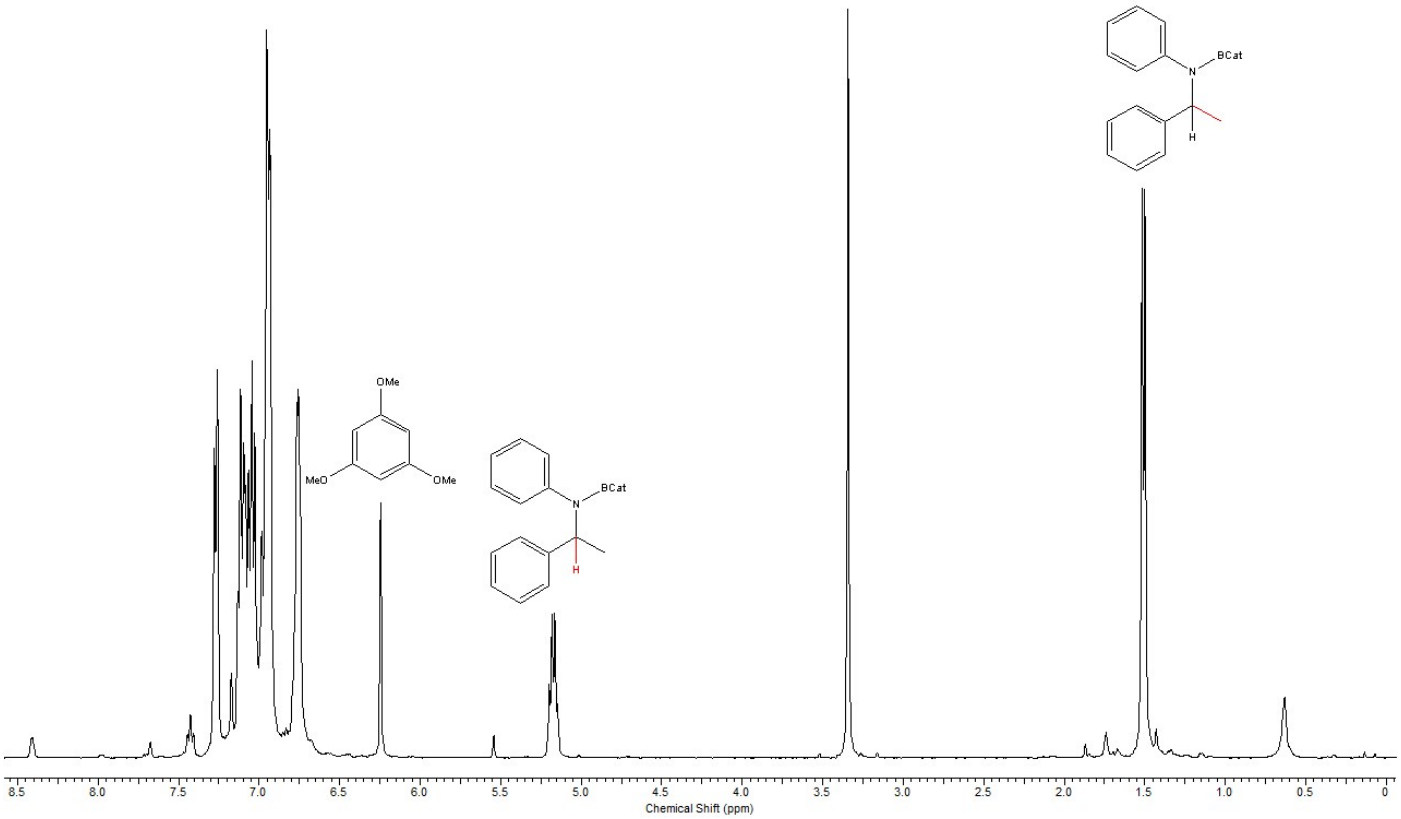

Figure S42. Hydroboration of Phenyl-(1-phenylethylidene)amine (400 MHz, C_6D_6), 50°C, 60 minutes, 1 mol% **3**

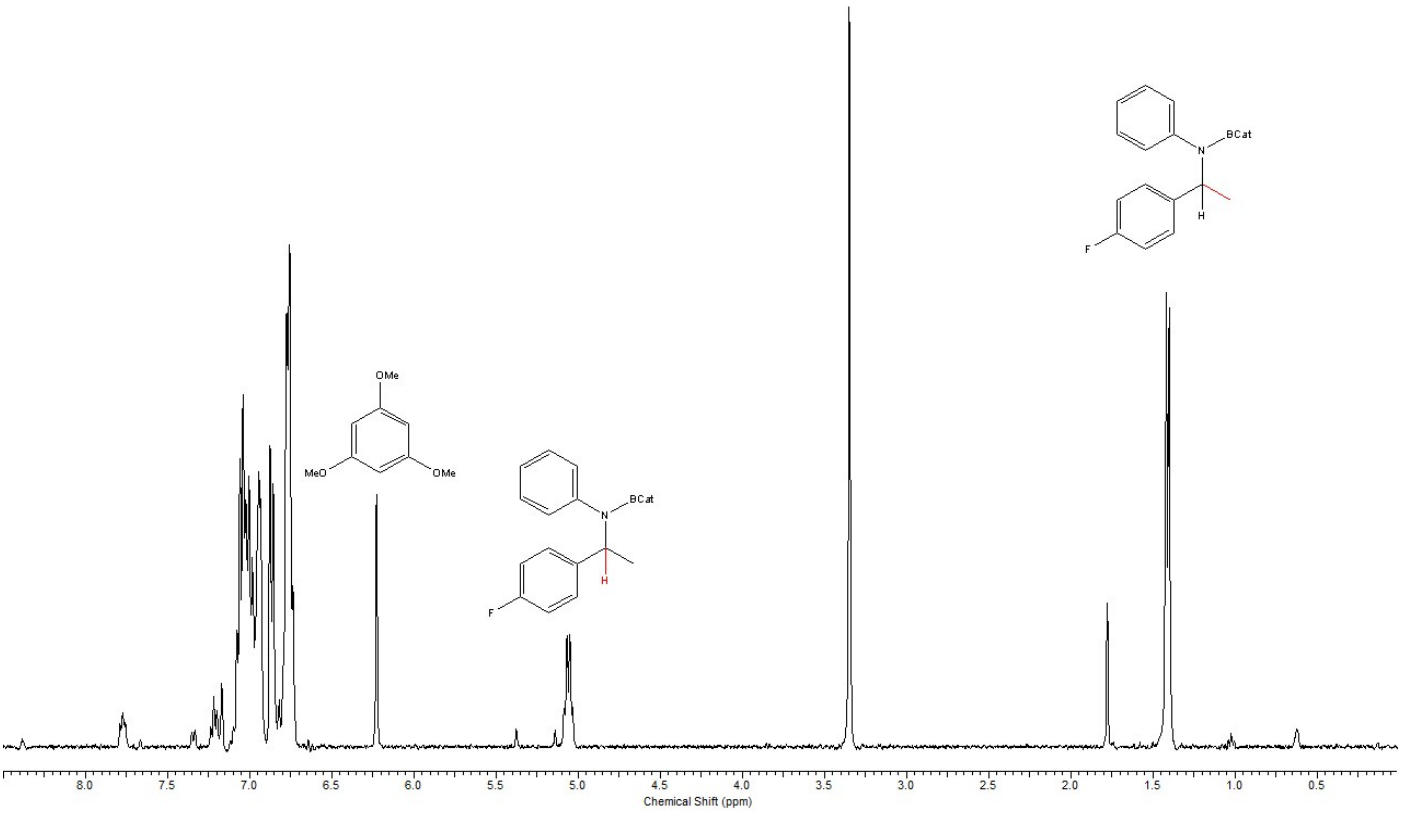

Figure S43. Hydroboration of Phenyl-(1-{4-fluorophenylethylidene)amine (400 MHz, C_6D_6), 50°C, 60 minutes, 1 mol% **3**

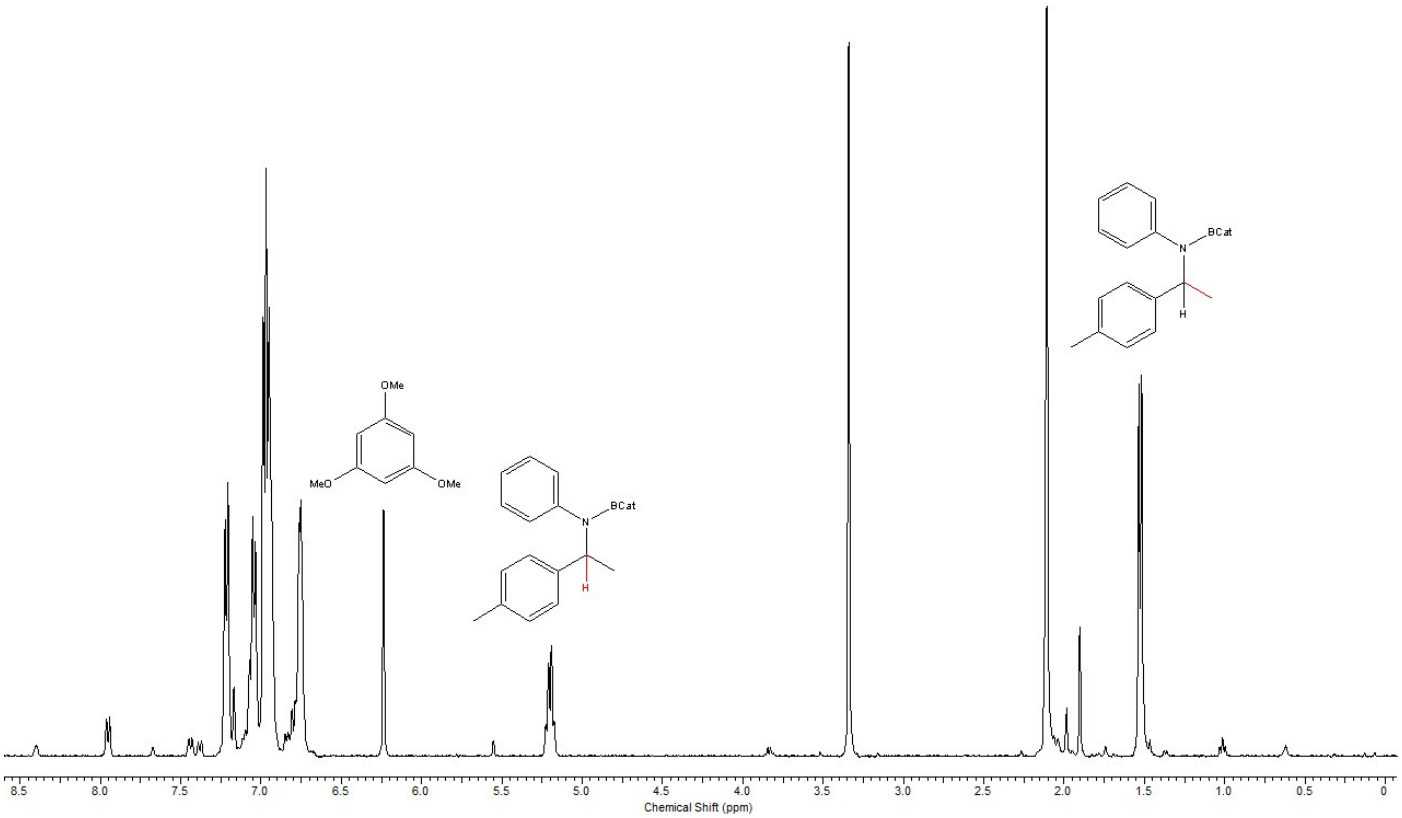

Figure S44. Hydroboration of Phenyl-(1-{4-methylphenyl6ethylidene)amine (400 MHz, C_6D_6), 50°C, 60 minutes, 1 mol% **3**

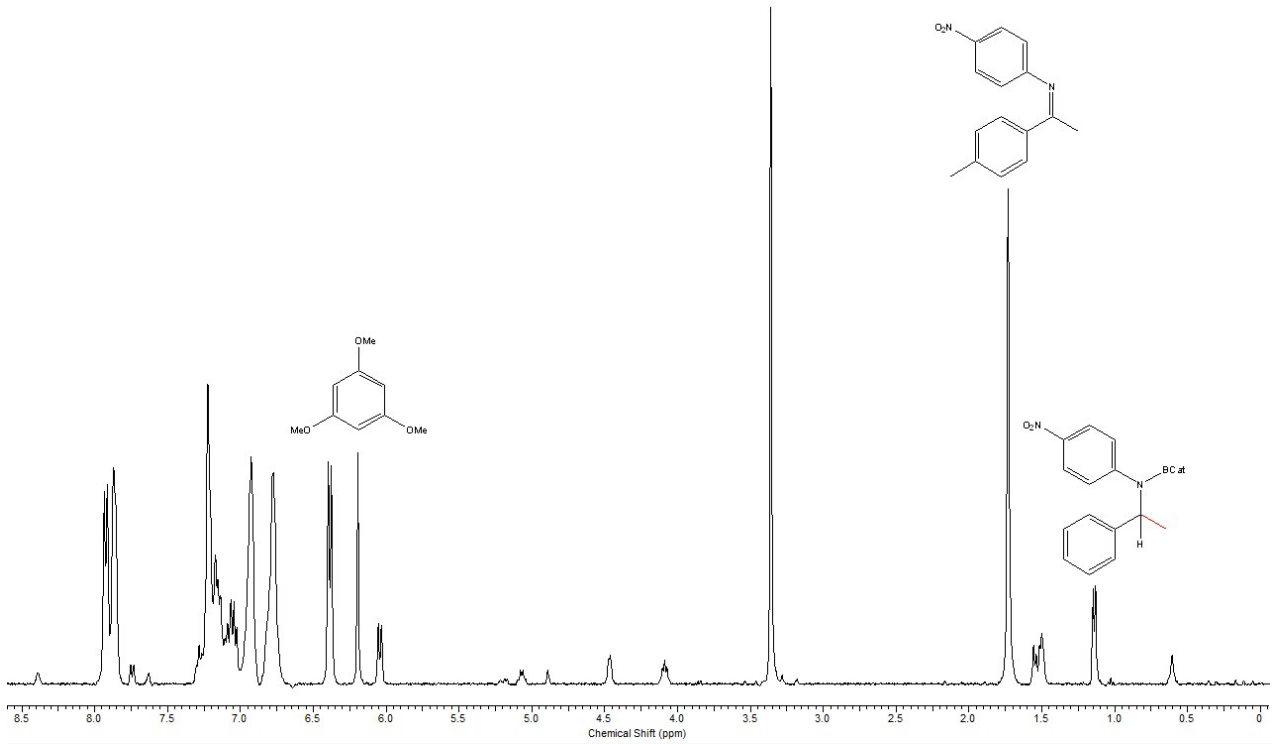

Figure S45. Hydroboration of 4-nitrophenyl-(1-phenylethylidene)amine (400 MHz, C_6D_6), 50°C, 60 minutes, 1 mol% **3**

Hydroboration of Heterocycles

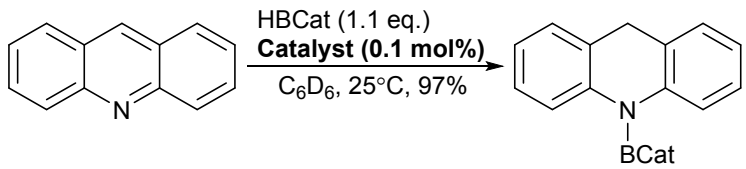

Scheme 1. Hydroboration of acridine

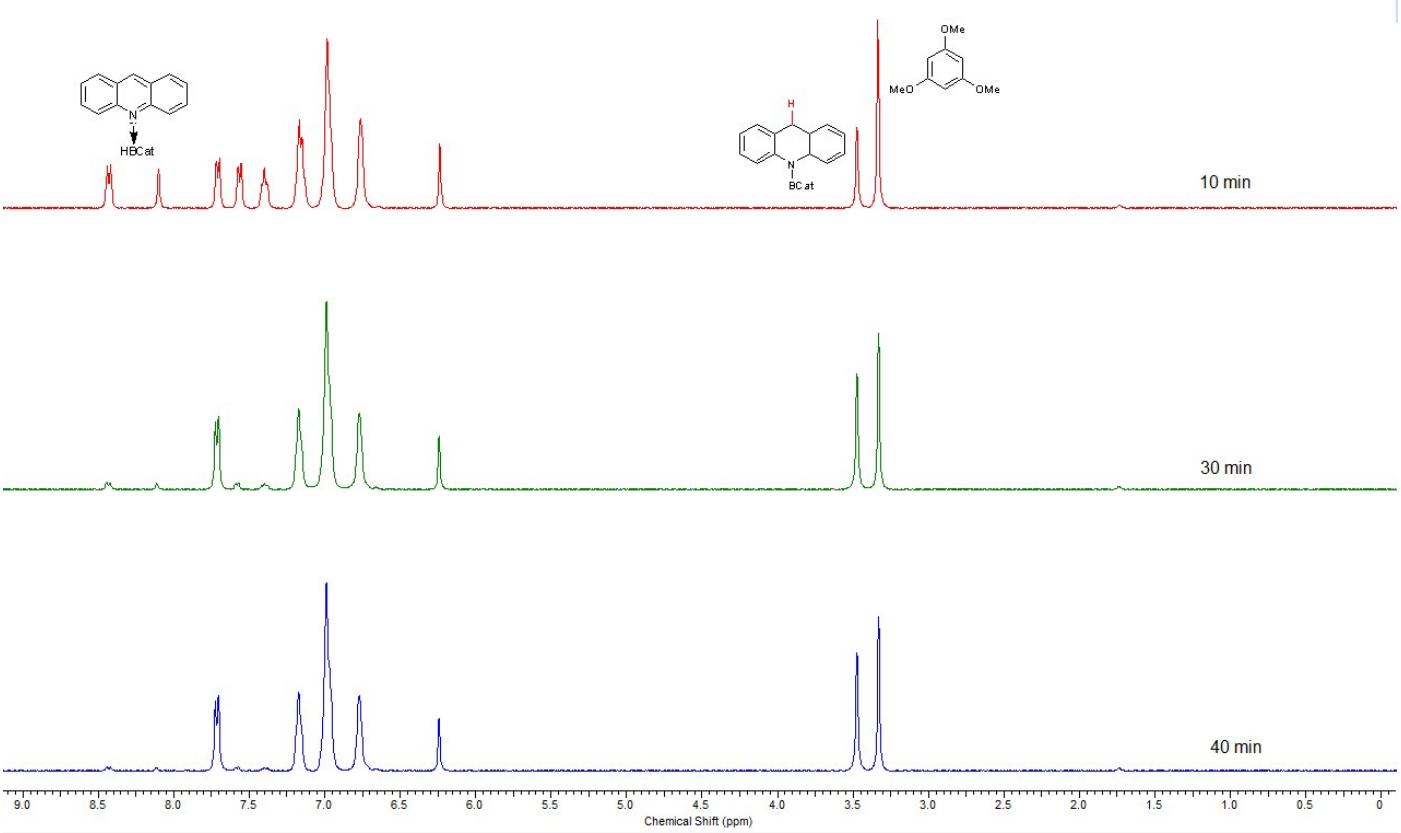

Figure S46. Hydroboration of acridine (400 MHz, C_6D_6), 25°C, 40 minutes, 0.1 mol% **3**

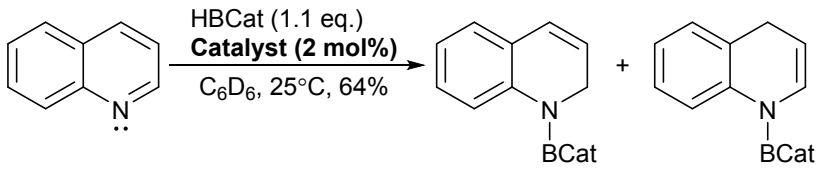

1,2: **58%** 1,4: **6%**

Scheme 2. Hydroboration of quinoline, 25°C, 2 hours, 2 mol% **3**

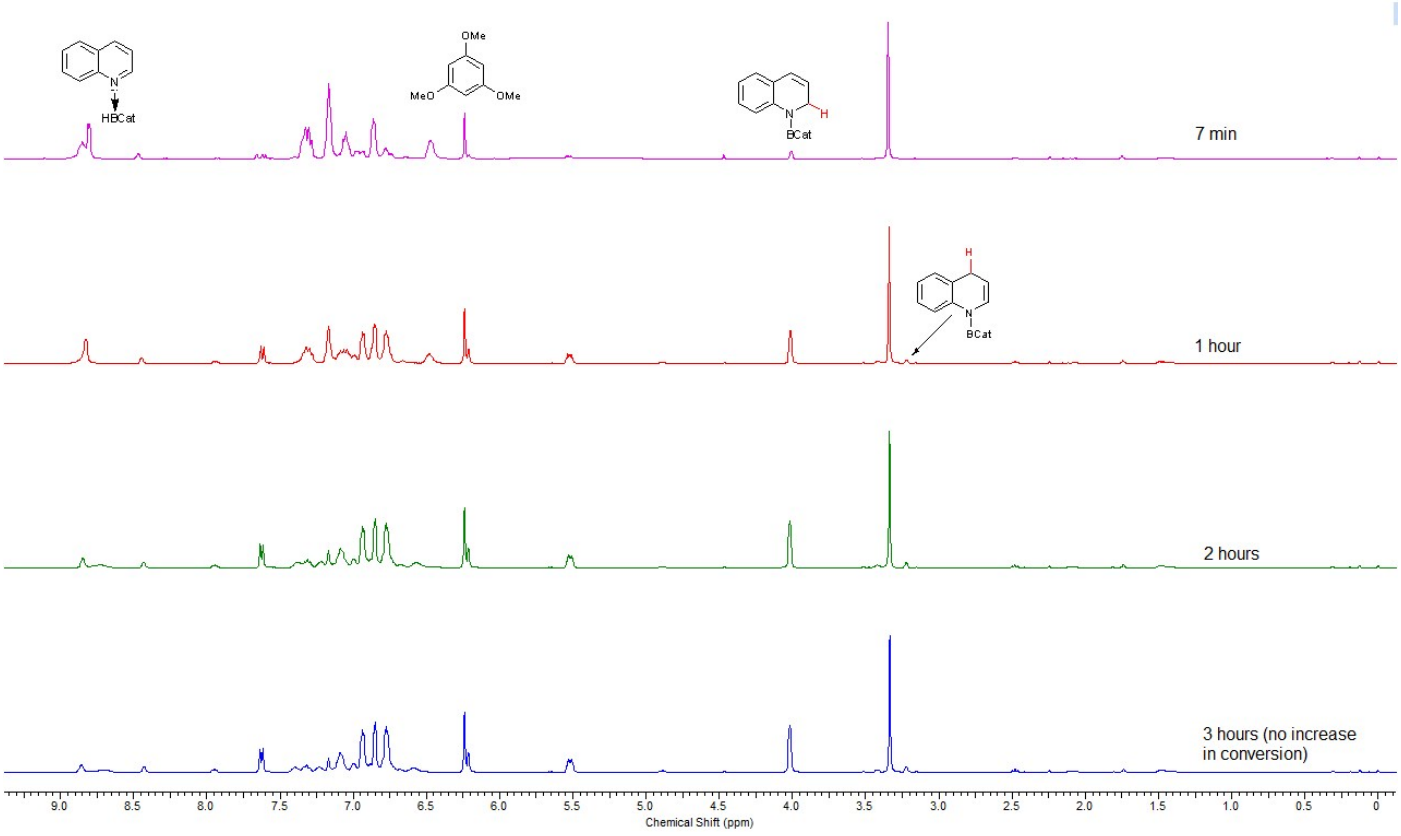

Figure S47. Hydroboration of quinoline (400 MHz, C_6D_6), 25°C, 3 hours, 3 mol% **3**

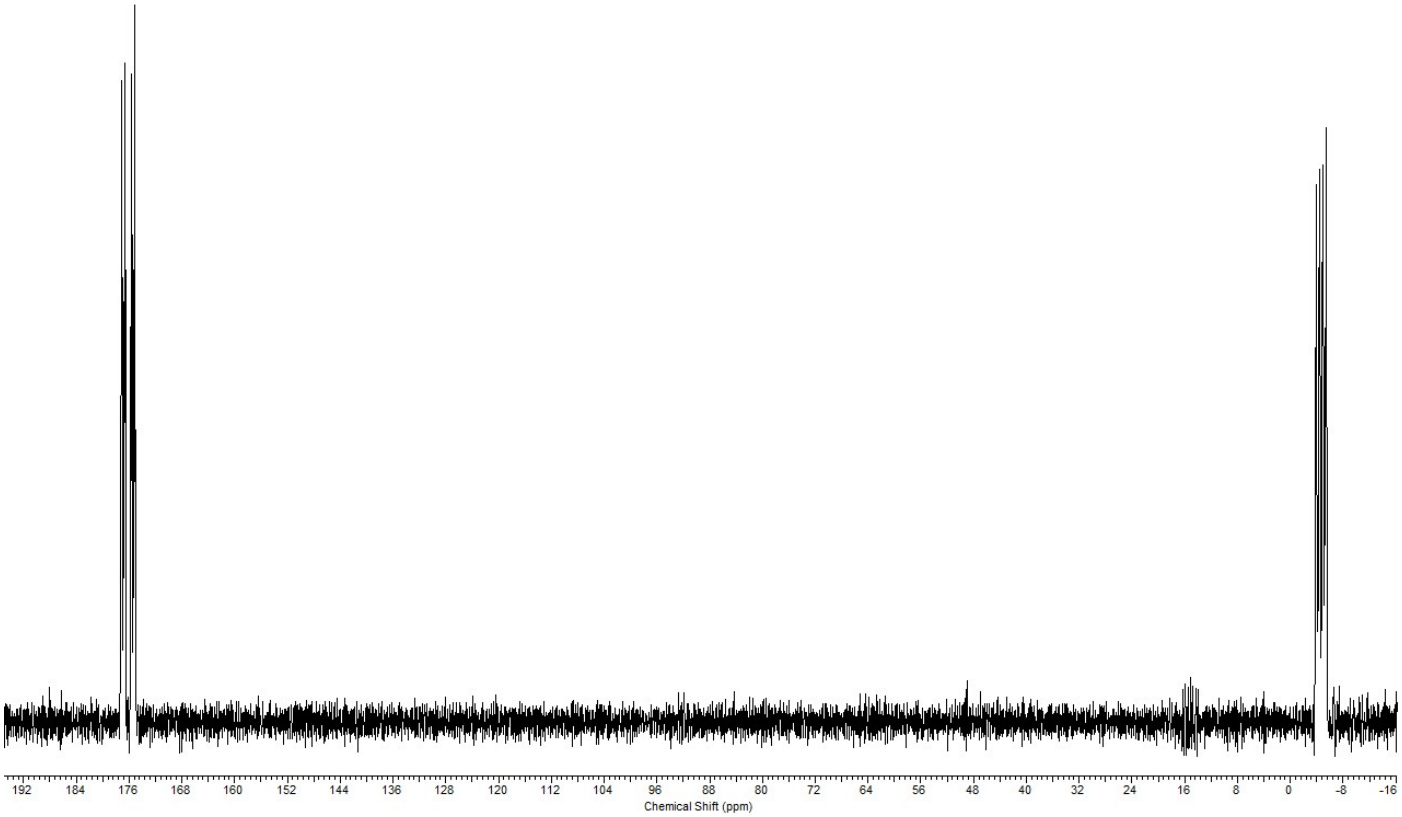

Figure S48. ^{31}P-NMR spectrum (C_6D_6) of the reaction between **3** and catecholborane (162 MHz, C_6D_6), ≈24h at 25°C

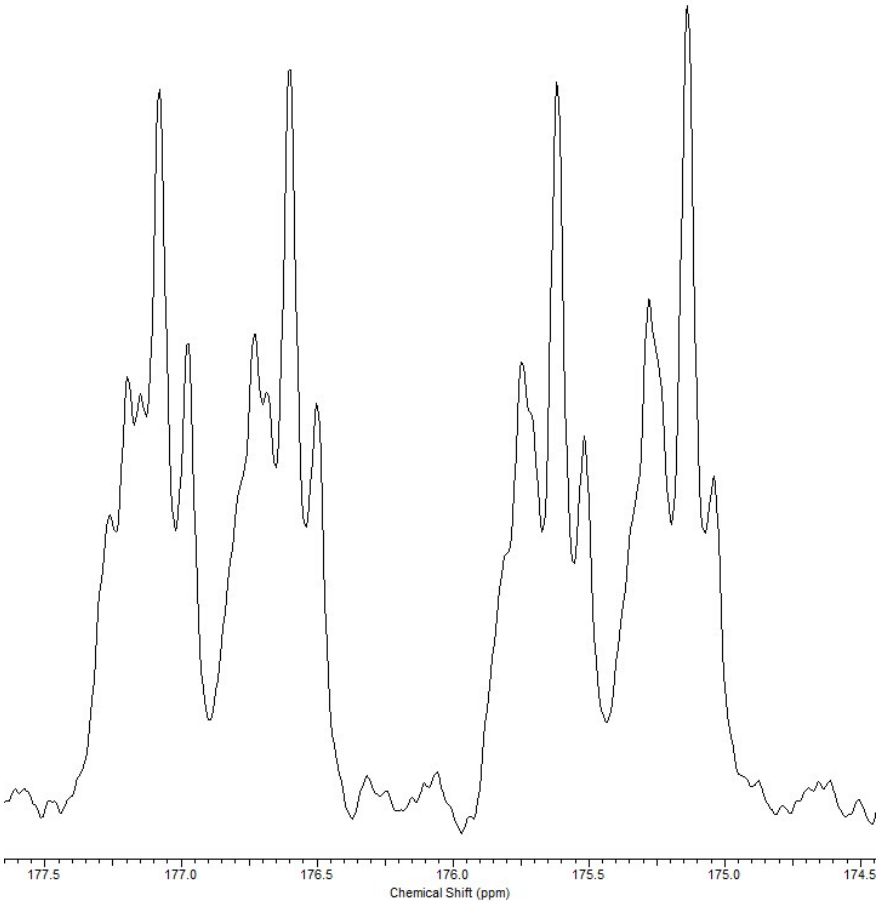

Figure S49. ^{31}P-NMR spectrum (phosphinine region) of the reaction between **3** and catecholborane, ≈24h at 25°C

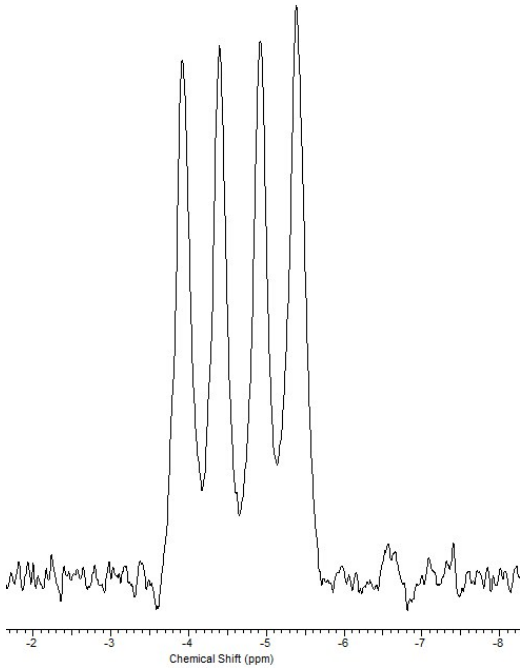

Figure S50. ^{31}P-NMR spectrum (phosphine region) of the reaction between **3** and catecholborane, ≈24h at 25°C

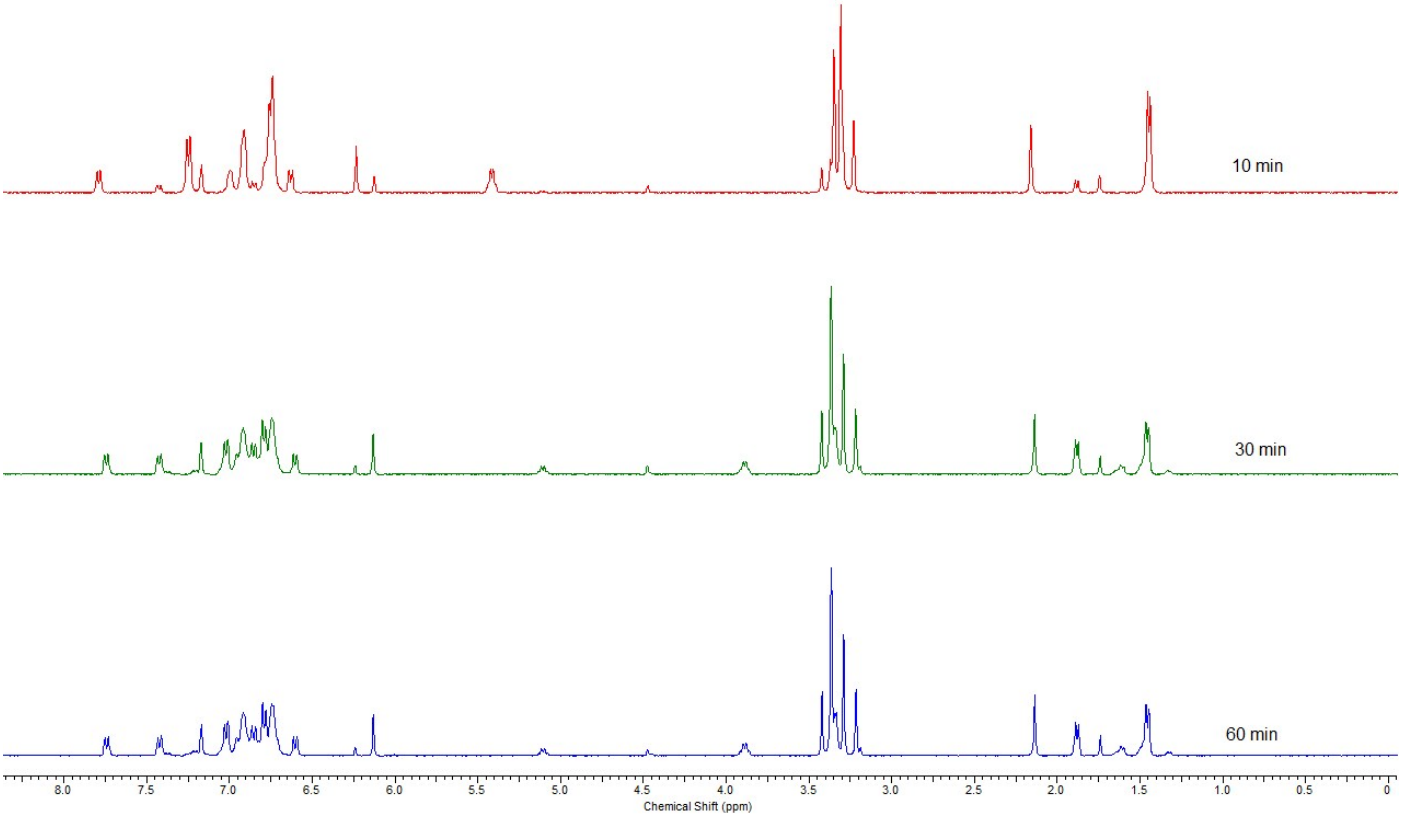

Figure S51. Hydroboration of 4'-methoxyacetophenone (400 MHz, C_6D_6), 25°C, 60 minutes, 0.1 mol% **3**

Hydroboration of ketones (repeat reactions)

To confirm the yields obtained, repeat reactions for the ketones were undertaken.

NMR-scale repeats gave results that fitted well with initial reactions. All results were calculated by integration against 1,3,5-trimethoxybenzene internal standard. For NMR data, see paper for link to Heriot-Watt University data repository.

Table S3. Results obtained from NMR-scale repeat reactions

	Yield (%)	
Substrate	**10 minutes**	**30 minutes**
4'-bromoacetophenone	83	99
4'-nitroacetophenone	83	98

To assess the viability of the reaction on a practical scale, the reaction was run at a 5 mmol scale for the 4 remaining ketones using the following procedure:

A Schlenk flask was charged with **3** (7.2 mg, 0.1 mol%) and a solution of catecholborane (606 mg, 5.05 mmol, 1.01 equiv.) in toluene (2 cm^3). The solution was stirred for two minutes for before the substrate (5 mmol, 1 equiv.) was added. The reaction was stirred for the required period of time before being concentrated *in-vacuo* by 50%. The yield was then calculated by recording the ^1H NMR spectrum and integrating the product signal against the starting material.

Table S4. Results obtained from scaled-up repeat reactions

Substrate	Time (min)	Yield (%)
Acetophenone	30	92
4'-fluoroacetophenone	30	93
4'-methylacetophenone	60	95
2'-methoxyacetophenone	30	92
4'-bromoacetophenone[a]	30	>99

[a]: Reaction run on a 6 mmol scale (1.194g substrate) scale.

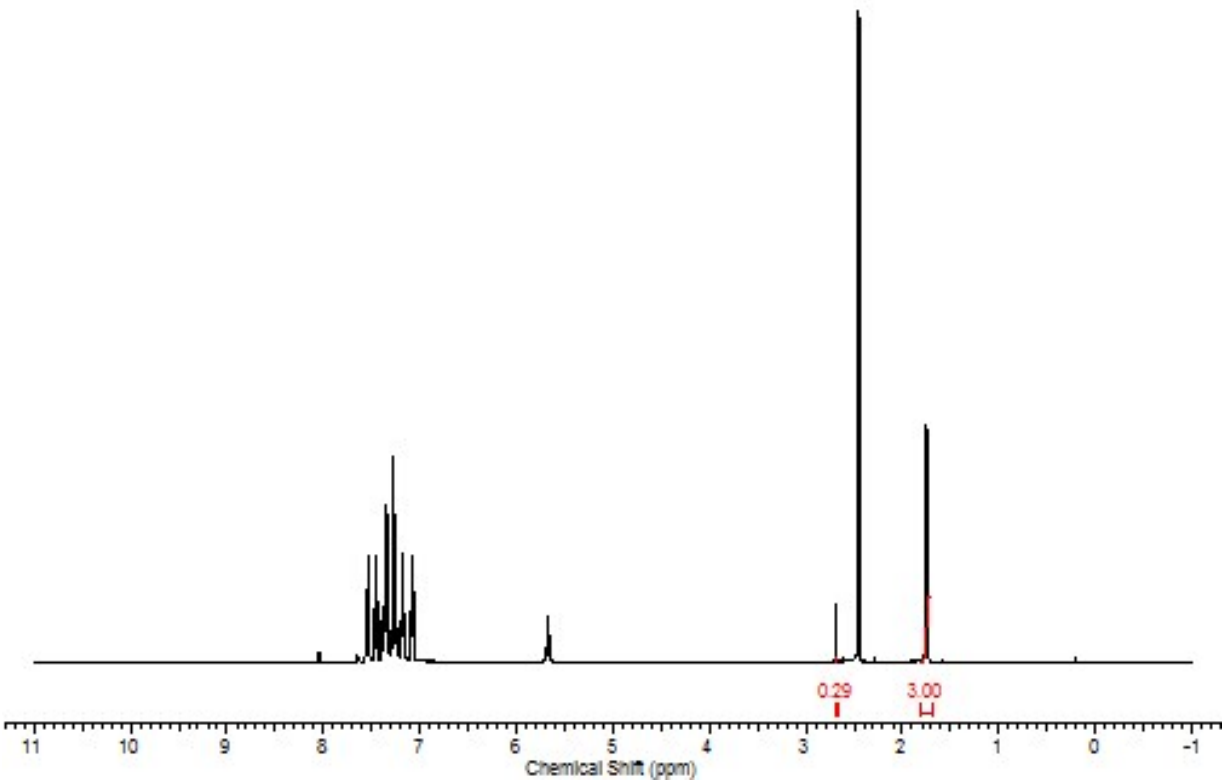

Figure S52. Hydroboration of acetophenone (5 mmol, 300 MHz, $CDCl_3$)

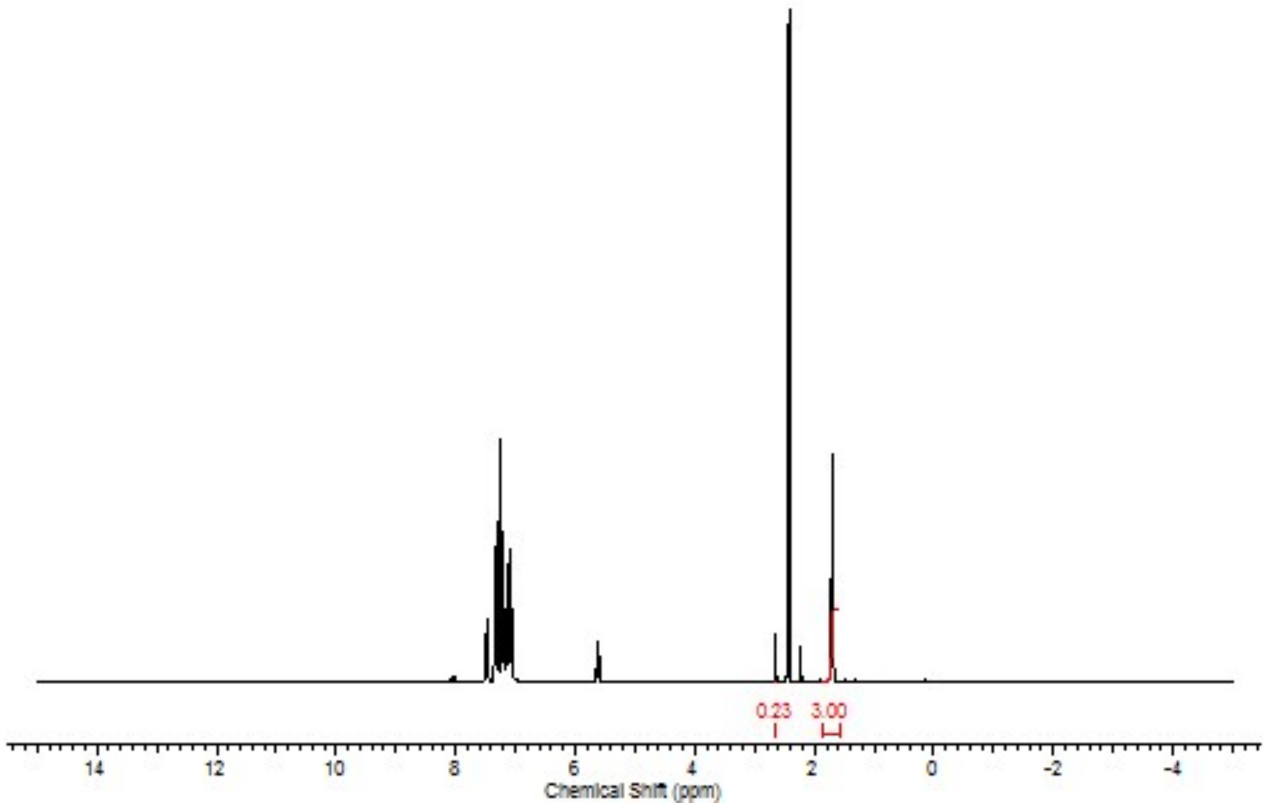

Figure S53. Hydroboration of 4'-fluoroacetophenone (5 mmol, 300 MHz, $CDCl_3$)

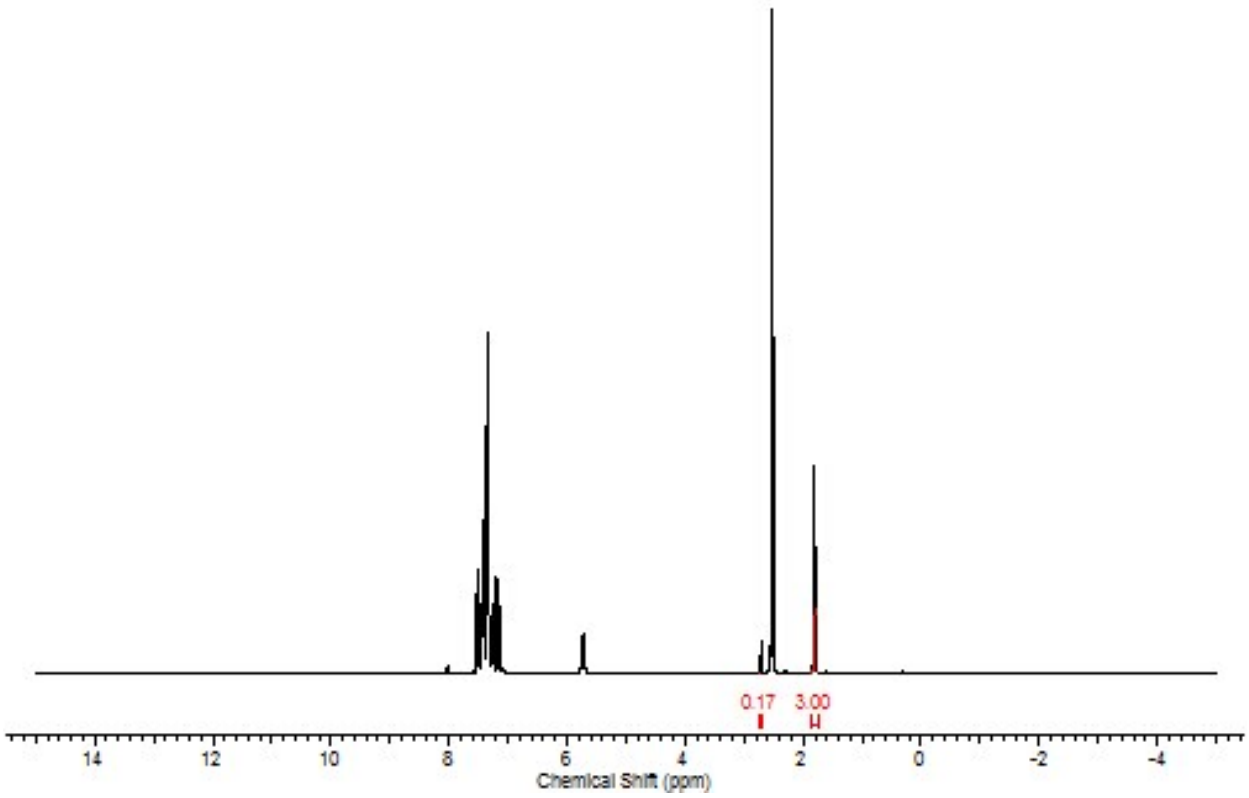

Figure S54. Hydroboration of 4'-methylacetophenone (5 mmol, 300 MHz, $CDCl_3$)

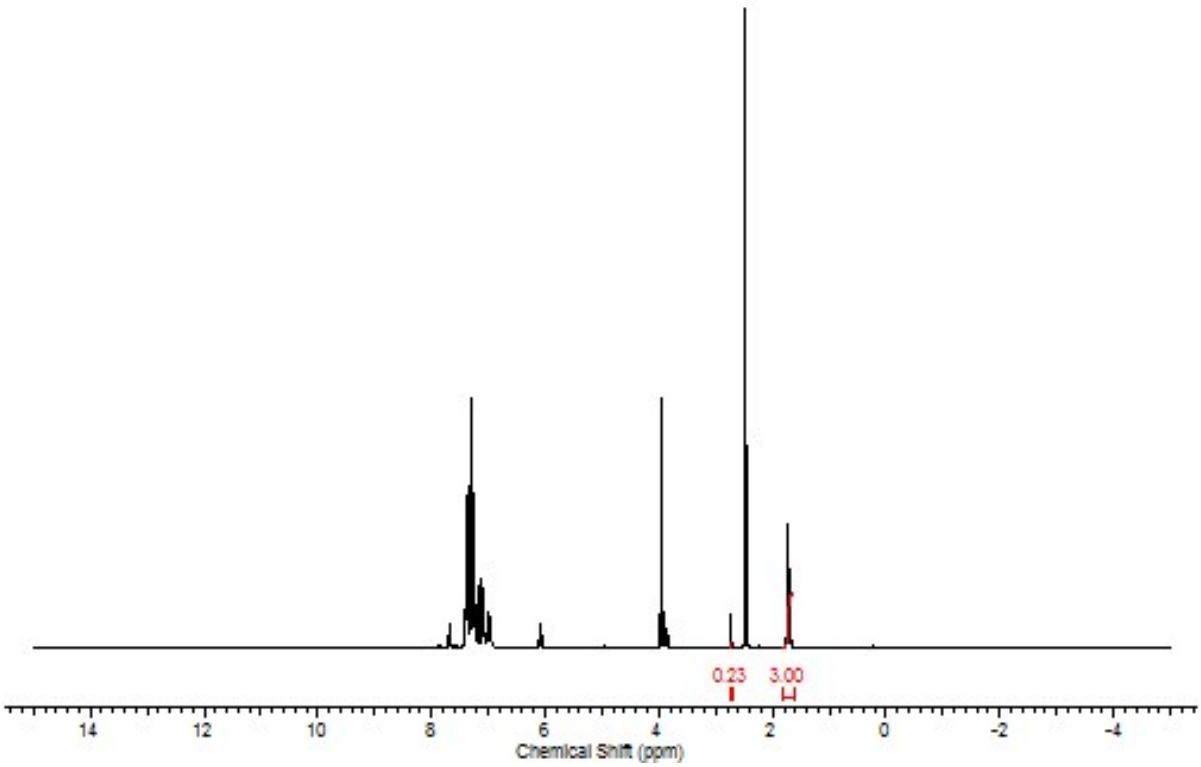

Figure S55. Hydroboration of 2'-methoxyacetophenone (5 mmol, 300 MHz, $CDCl_3$)

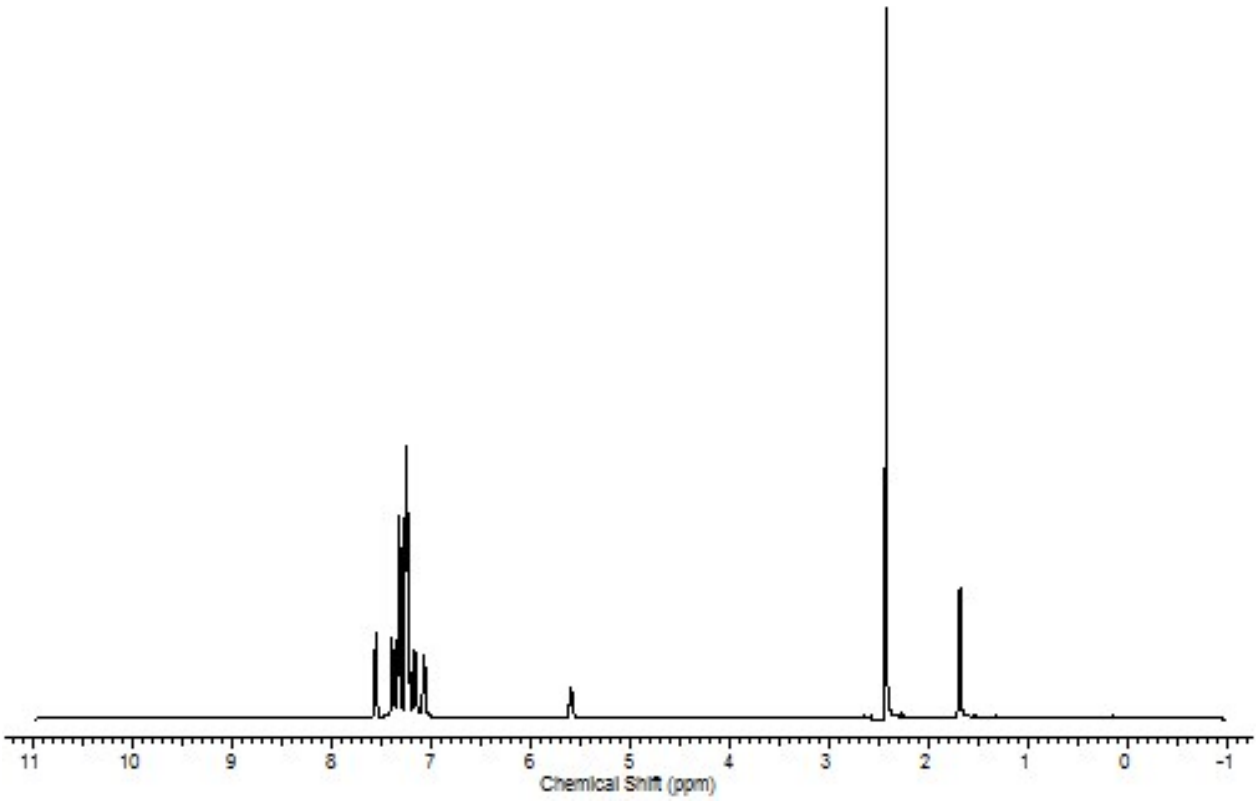

Figure-S55-Br. Hydroboration of 4'-bromoacetophenone (6 mmol, 300 MHz, $CDCl_3$)

Competition Reactions

To assess the selectivity of **3** as a catalyst for the hydroboration of ketones, a series of competition reactions were run using the standard NMR-scale methodology.

- **Run 1:** Hydroboration of 1-octene with **3**
- **Run 2:** Hydroboration of a 1:1 mixture (0.43 mmol each) of acetophenone and 1-octene (0.43 mmol HBCat)
- **Run 3:** Hydroboration of the same mixture with $[Rh(PPh_3)_3Cl]$

Table S5. Competition reaction results

	1-Octene Conversion (%)[a][b]			Acetophenone Conversion (%)[a]		
Run	**10 min**	**30 min**	**60 min**	**10 min**	**30 min**	**60 min**
1[c]	5	12	19	-	-	-
2	7	22	37	22	45	60
3	3	33	55	2	6	9

[a]: Conversion measured against 1,3,5-trimethoxybenzene internal standard.

[b]: For runs **2** and **3**, 1-octene consumption includes production of isomerised alkenes. Accurate integration not possible due to overlap with quartet from acetophenone hydroboration.

[c]: Left to run for 19 hours total. 73% consumed (23% alkene isomers).

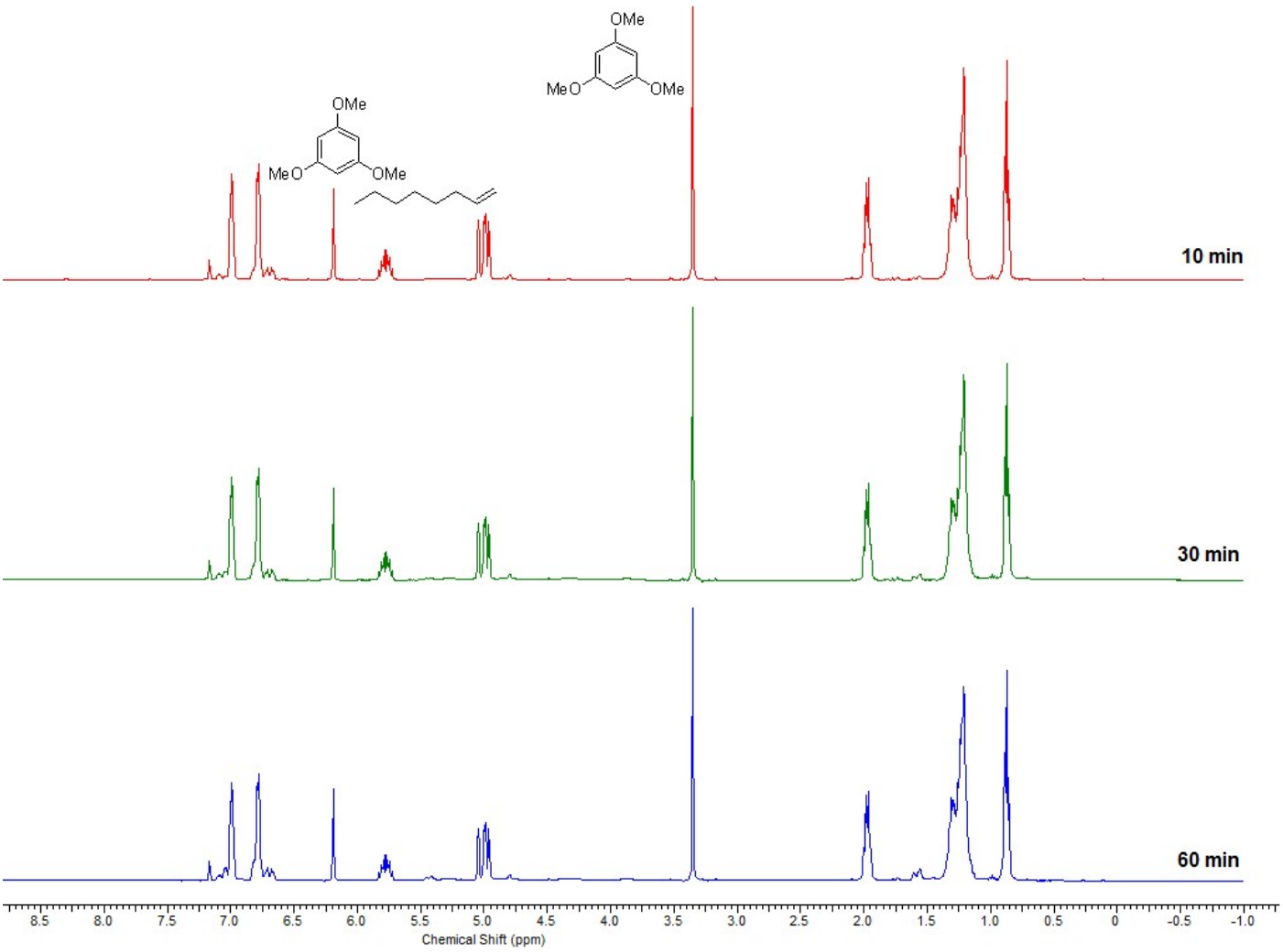

Figure S56. Hydroboration of 1-octene with **3** (400 MHz, C_6D_6)

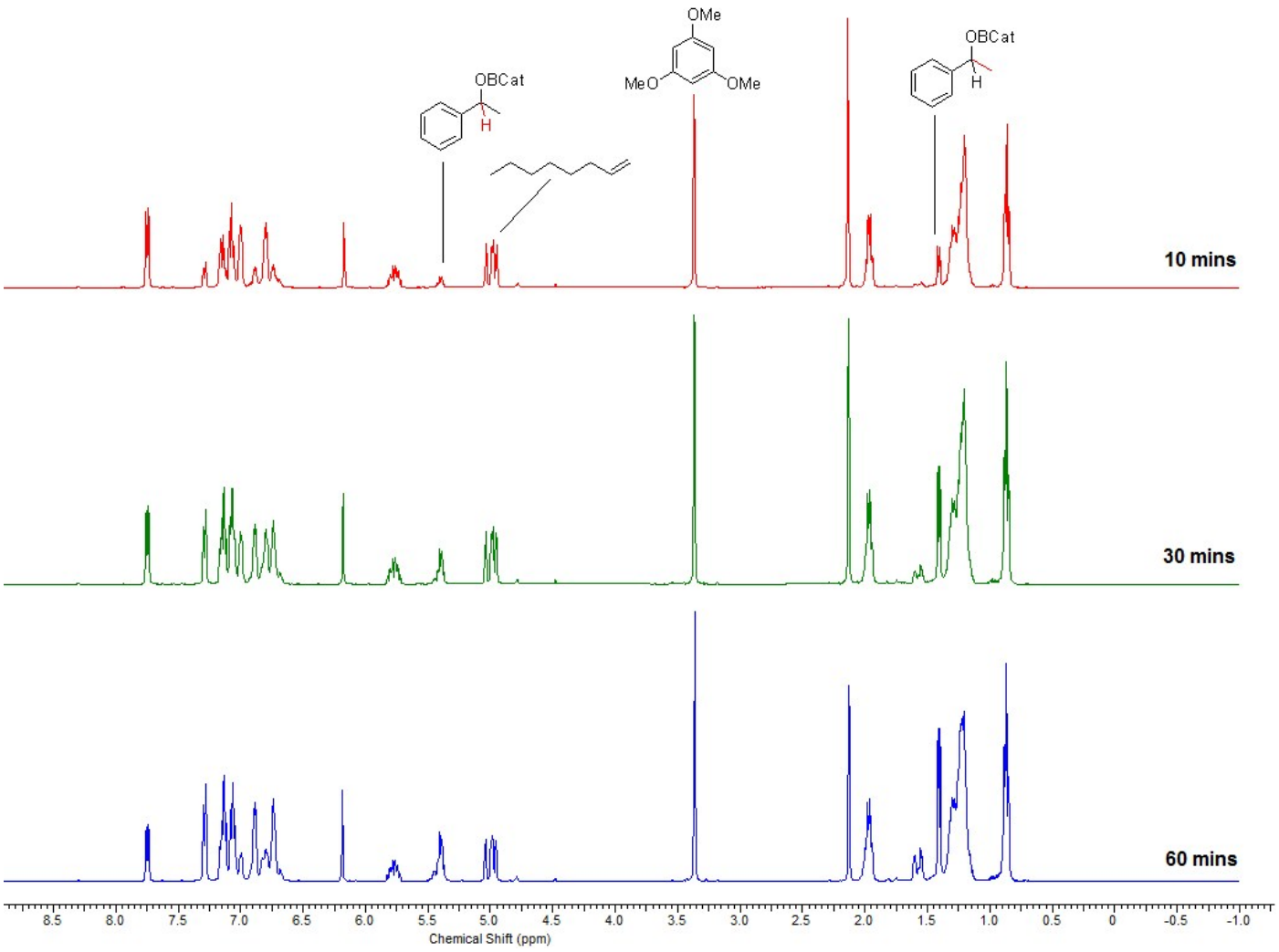

Figure S57. Hydroboration of 1-octene and acetophenone with **3** (400 MHz, C_6D_6)

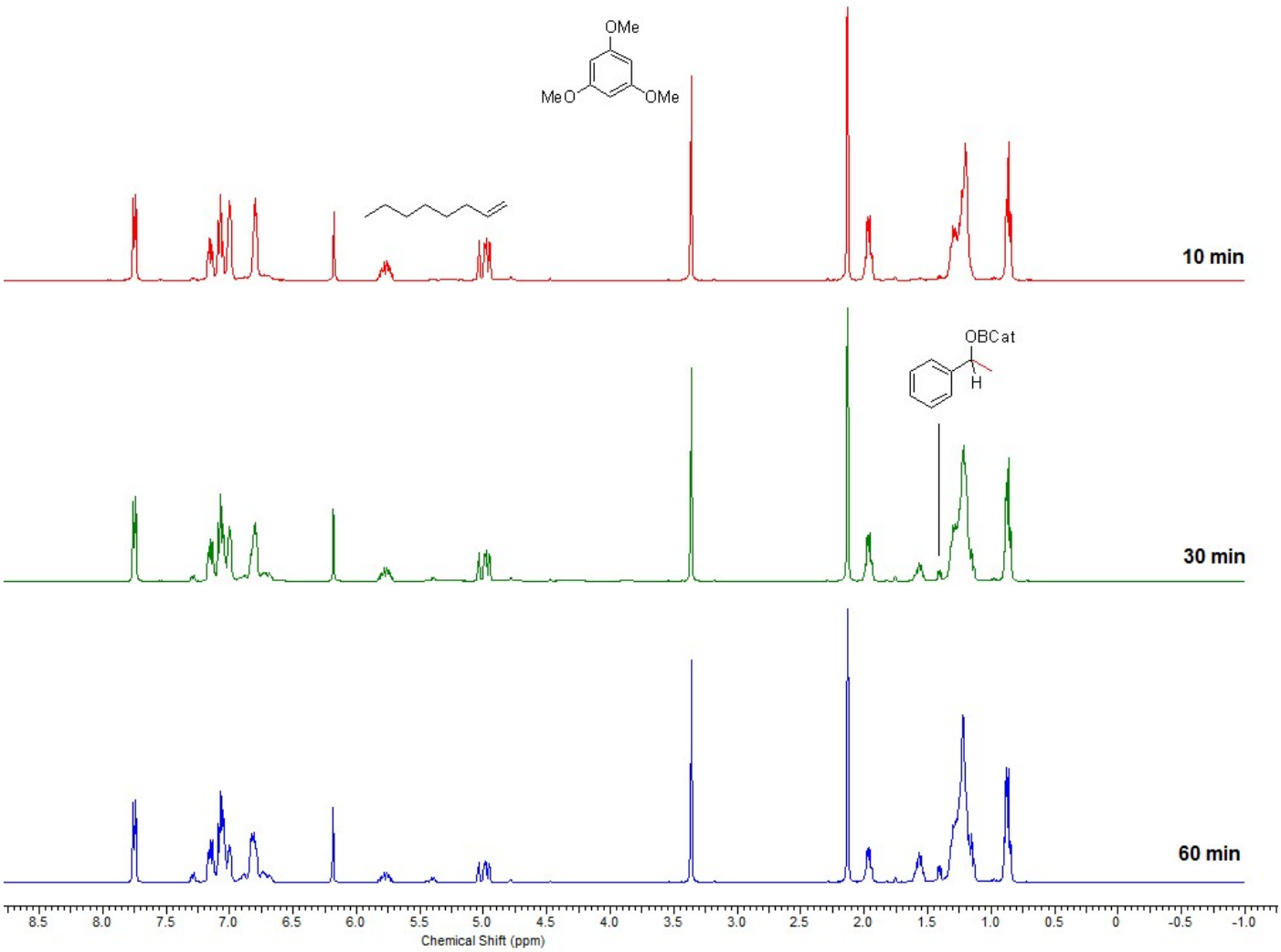

Figure S58. Hydroboration of 1-octene and acetophenone with $[Rh(PPh_3)_3Cl]$ (400 MHz, C_6D_6)

Extra Substrates

In order to assess the reactivity of other ketones, three other substrates (4-methylcyclohexanone, benzophenone and 4,4'-difluorobenzophenone) were investigated.

Initially 4-methylcyclohexanone was reacted with HBCat without a catalyst, and a 95% yield was obtained after 30 minutes. This agrees with the results of Männig and Nöth.[12] As such, the reaction was not repeated with a catalyst

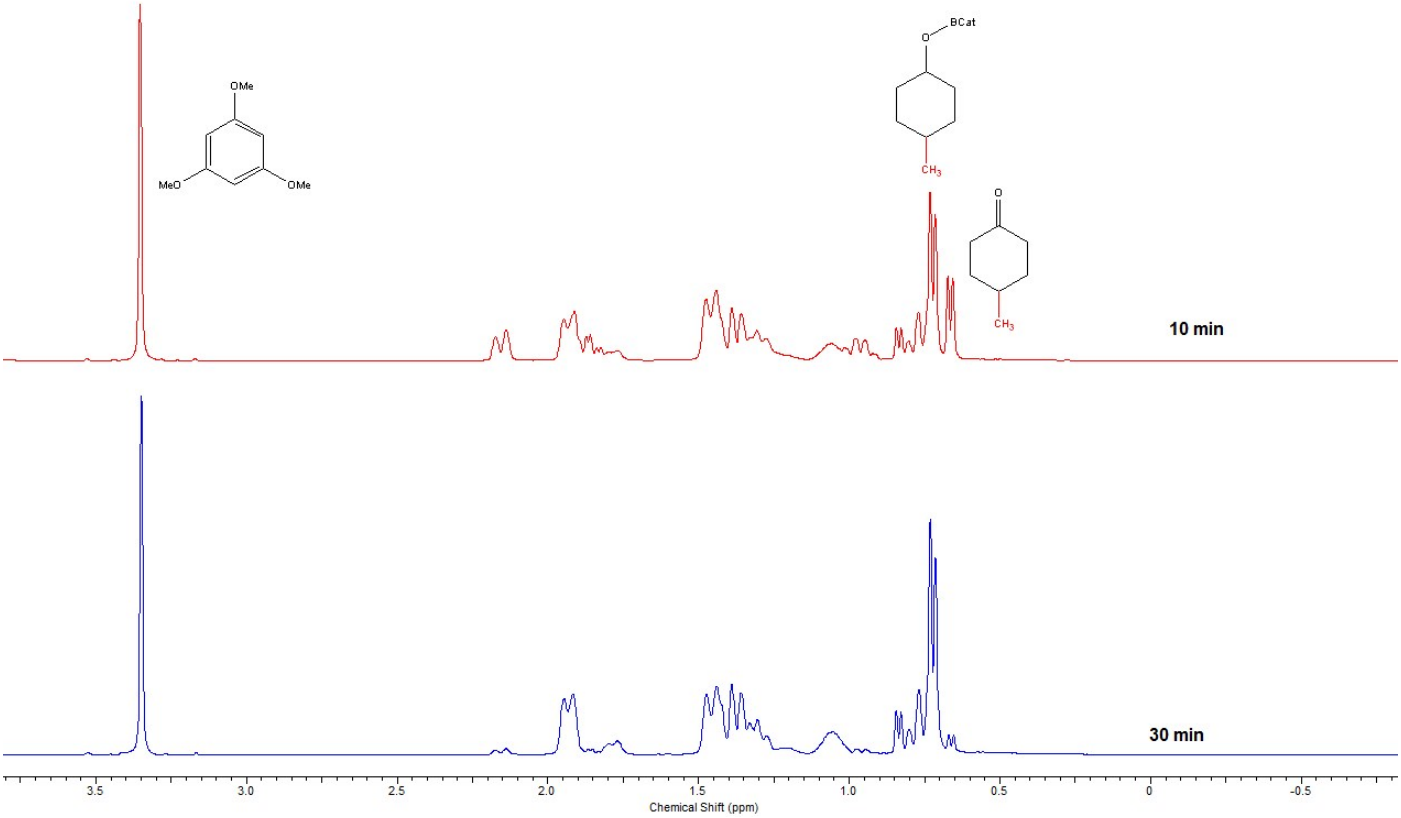

Figure S59. Hydroboration of 4-methylcyclohexanone (^{1}H alkyl region) – no catalyst (400 MHz, C_6D_6).

The catalytic hydroboration of benzophenone (Ph_2CO) was then investigated. No conversion was observed after 1 hour at 25°C using 0.1 mol% **3**, so the reaction was heated to 50°C using 1 mol% **3**, however, this resulted in the formation of multiple unknown products. In order to investigate whether the lack of reactivity under standard conditions was due to electronics or sterics, the reaction was repeated with electron-poor 4,4'-difluorobenzophenone. After one hour, a 7.5% yield was obtained, however when the reaction was repeated at 50°C for one hour using 1 mol% **3**, multiple products were also observed.

Table S6. Results obtained from the catalytic hydroboration of benzophenones

Substrate	25°C: Yield (%)[a]	50°C: Yield (%)[b]
Benzophenone	0	0[c]
4,4'-difluorobenzophenone	7.5	0[c]

[a]: 25°C for one hour, 0.1 mol% **3**. [b]: 50°C for one hour, 1 mol% **3**. [c]: multiple products detected.

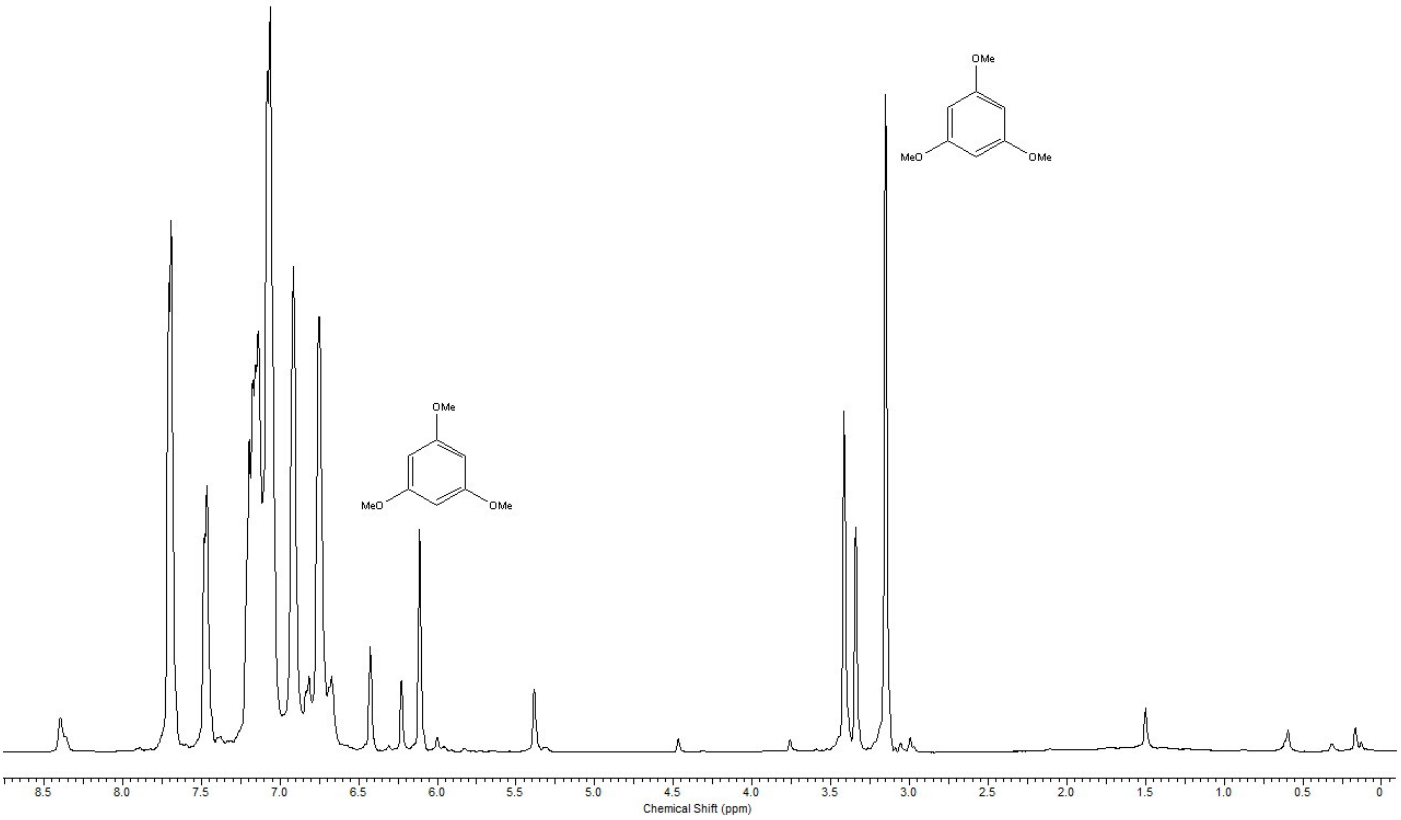

Figure S60. Hydroboration of benzophenone, 1h at 50°C, 1 mol% **3** (400 MHz, C_6D_6).

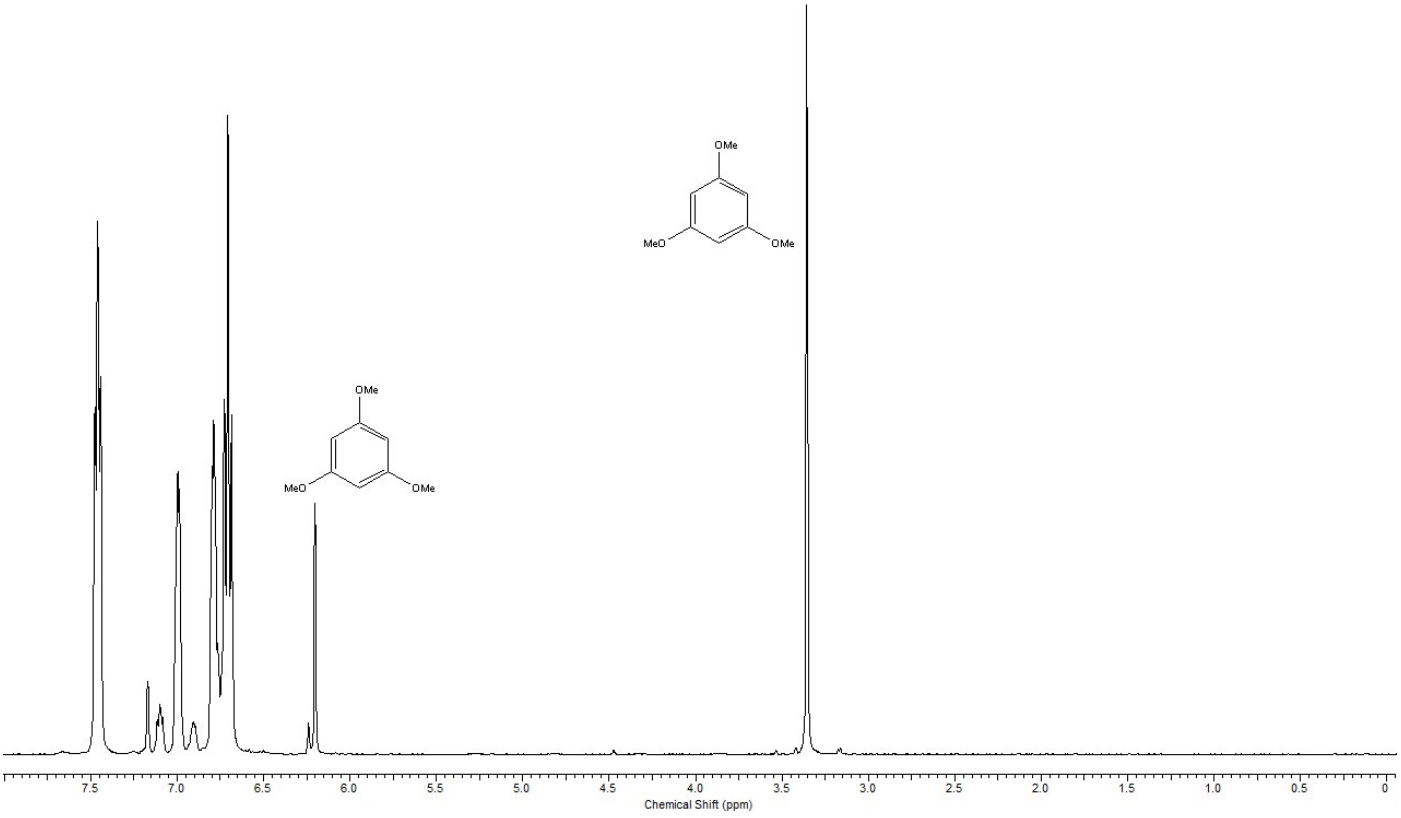

Figure S61A. Hydroboration of 4,4'-difluorobenzophenone, 1h at 25°C, 0.1 mol% **3** (400 MHz, C_6D_6).

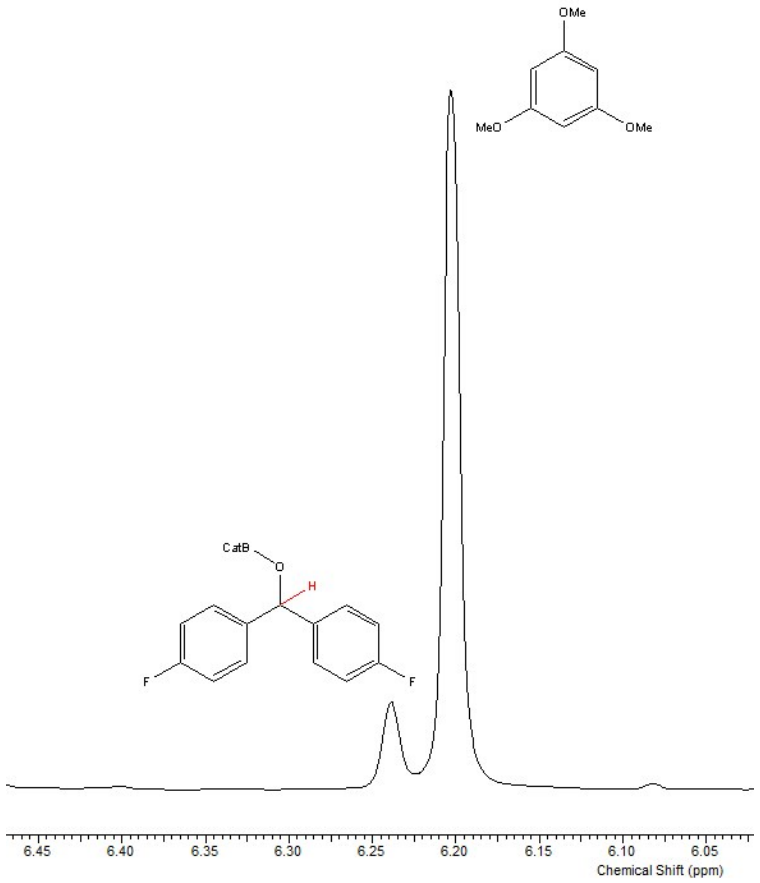

Figure S61A. Hydroboration of 4,4'-difluorobenzophenone, 1h at 25°C, 0.1 mol% **3**. Magnified ^{1}H NMR spectrum (400 MHz, C_6D_6)

Reaction Profile

To provide a clear picture of the reaction progression through a catalytic run, the percentage yields were plotted for the first 20 experiments recorded (5 min to 25 min) for 4'-methylacetophenone (as most other substrates proceeded too quickly to provide a useful plot).

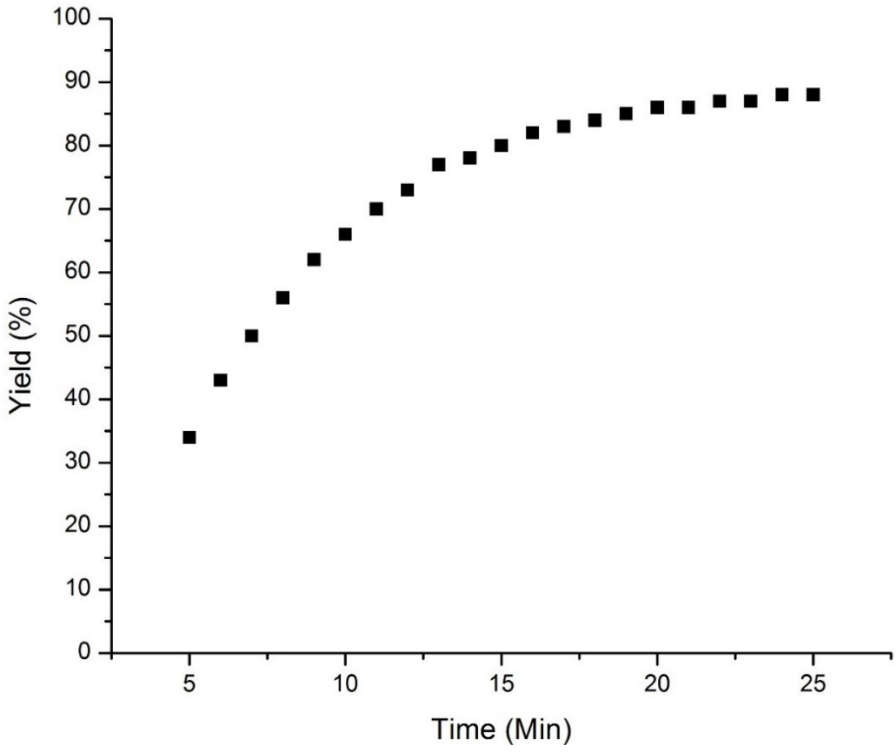

Figure S62. Reaction profile for the hydroboration of 4'-methylacetophenone

Hydrogenation Reactions

Experimental Procedure

Under air, a 250 cm^3 Schlenk flask was charged with substrate (1 mmol), **3** (29 mg, 2 mol%) and fluorobenzene (2 cm^3). The flask was then subjected to three freeze-pump-thaw cycles. On the third cycle, the flask was sealed under high-vacuum and hydrogen admitted *via* a balloon. The solution was allowed to thaw and stirred vigorously under a hydrogen atmosphere for the time indicated in **Table S3**. The flask was then opened to air and a known amount of 1,3,5-trimethoxybenzene (as an internal standard) added. An aliquot of the solution was then analysed by ^{1}H-NMR spectroscopy to determine the yield of alkane.

Table S7. Results of hydrogenation of Alkenes (reaction not optimised)

Substrate	Time (h)	Yield (%)
Styrene	22	>99%
Cyclohexene	17	>99%

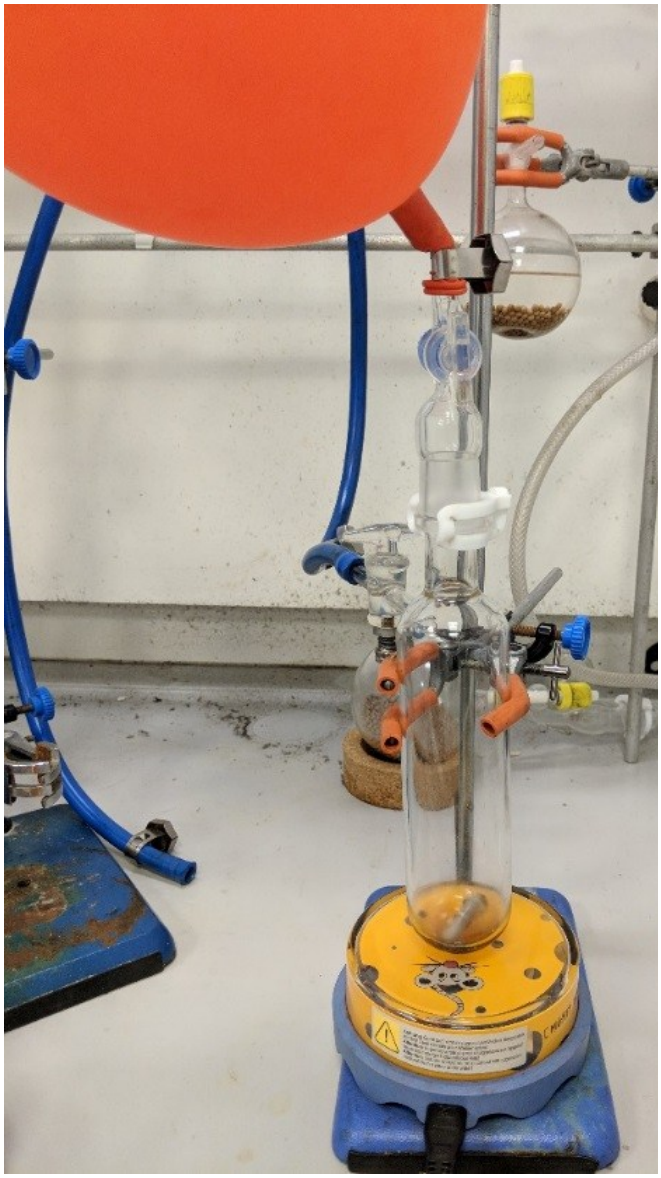

Figure S60. Hydrogenation setup

Crude Product NMR Spectra

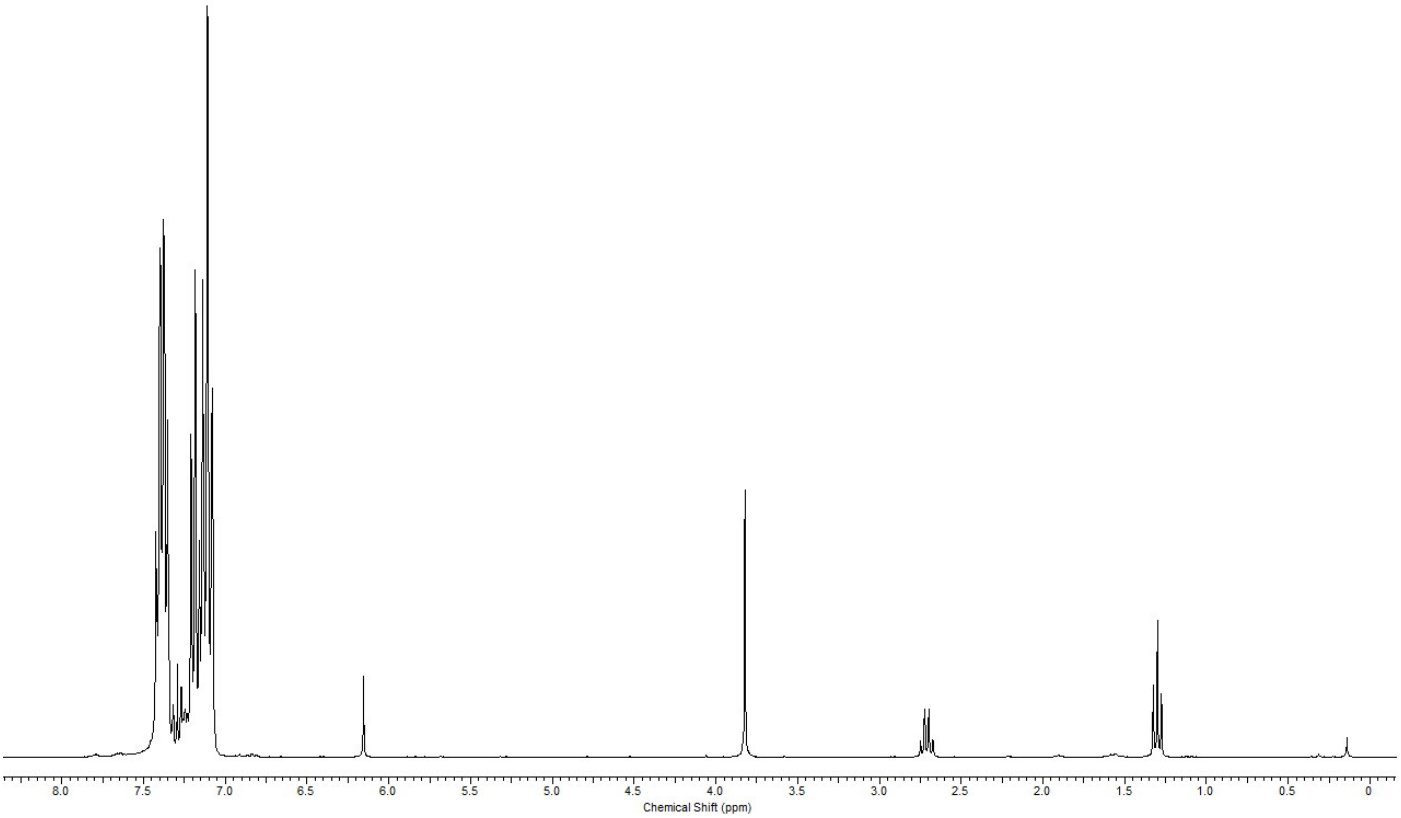

Figure S63. Hydrogenation of styrene, 25°C, 22 hours, 2 mol% **3** (300 MHz, $CDCl_3$)

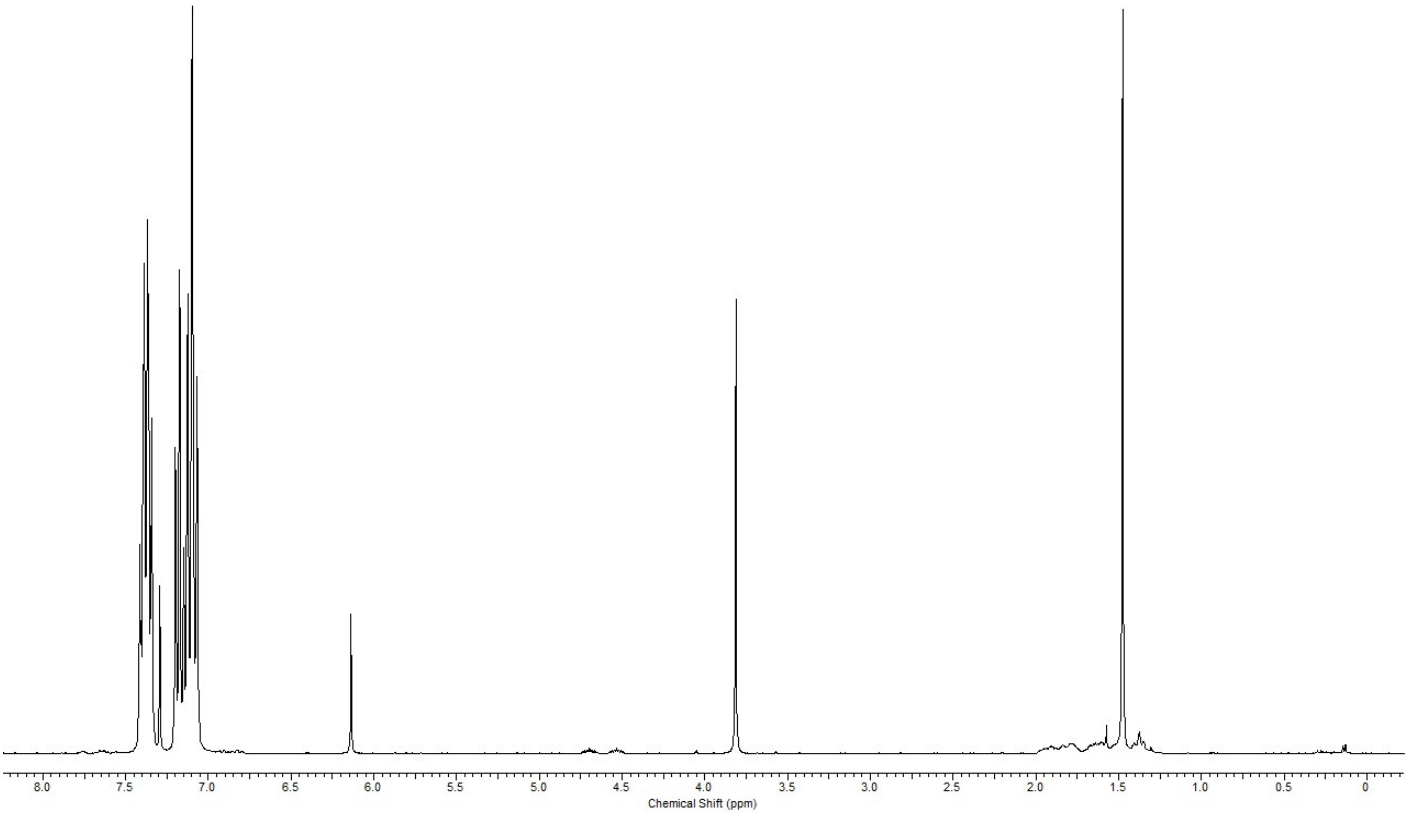

Figure S64. Hydrogenation of cyclohexene, 25°C, 17 hours, 2 mol% **3** (300 MHz, $CDCl_3$)

Monodentate Phosphinine Ligands

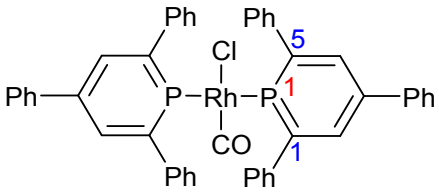

Rh(1)-P(1): 2.281(1), P(1)-C(1): 1.717(5), P(1)-C(5): 1.722(5), C(1)-P(1)-C(5): 105.8(2)°, ν(CO): 1999 cm^{-1}

Figure S65.[13]

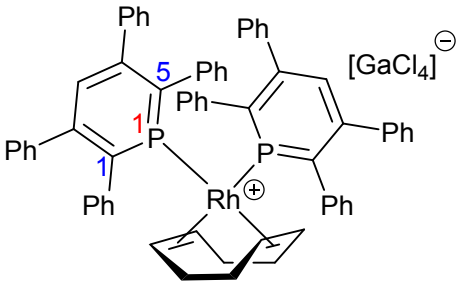

Rh(1)-P(1): 2.301(1), P(1)-C(1): 1.738(5), P(1)-C(5): 1.738(5), C(1)-P(1)-C(5): 106.4(2)°

Figure S66.[14]

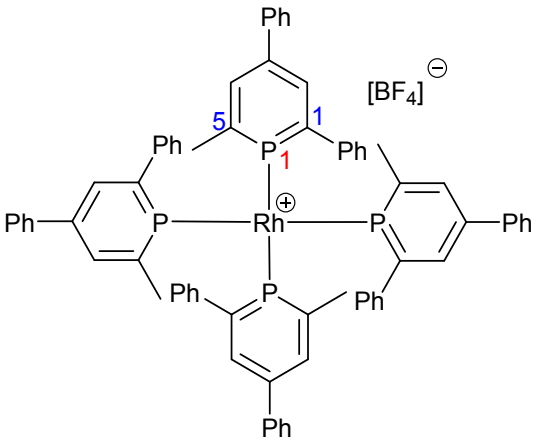

Rh(1)-P(1): 2.292(1), P(1)-C(1): 1.735(3), P(1)-C(5): 1.720(4), C(1)-P(1)-C(5): 105.7(2)°

Figure S67.[15]

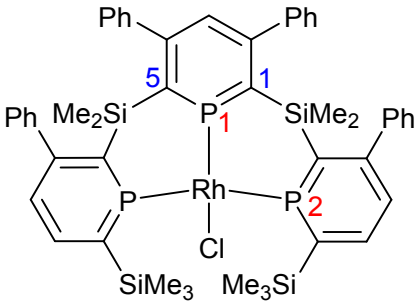

Rh(1)-P(1): 2.1626(9), Rh(1)-P(2): 2.2704(9), P(1)-C(1): 1.737(3), P(1)-C(5): 1.722(2), C(1)-P(1)-C(5): 109.1(1)°
P(1)-Rh(1)-P(2): 90.65(3)°

Figure S68.[16]

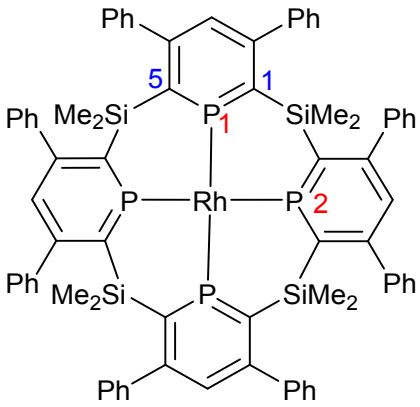

Rh(1)-P(1): 2.26(1), Rh(1)-P(2): 2.24(2), P(1)-C(1): 1.72(3), P(1)-C(5): 1.78(5), C(1)-P(1)-C(5): 105(2)°,
P(1)-Rh(1)-P(2): 88.3(5)°

Figure S69.[17]

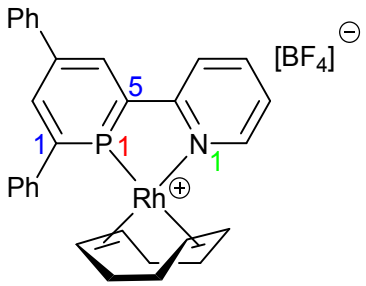

Rh(1)-P(1): 2.2250(7), Rh(1)-N(1): 2.159(3), P(1)-C(1): 1.729(3), P(1)-C(5): 1.721(3), C(1)-P(1)-C(5): 105.3(1)°,
P(1)-Rh(1)-N(1): 79.77(7)°

Figure S70.[18]

NMR simulations

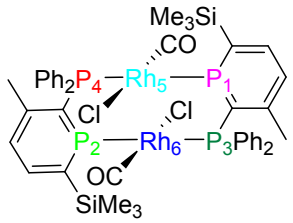

2

Nucleus	δ	Width / Hz	J_1 / Hz	J_2 / Hz	J_3 / Hz	J_4 / Hz	J_5 / Hz
1	250.628	19.41					
2	250.628	19.41	0.00				
3	25.521	13.08	137.33	*-430.25*			
4	25.521	13.08	*-430.25*	137.33			
5	0.000	5.00	**-143.57**	3.28	3.00	**-138.70**	
6	0.000	5.00	3.28	**-143.57**	**-138.70**	3.00	0.00

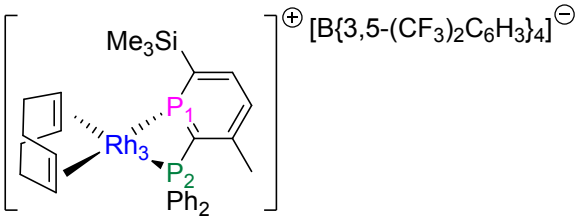

3

Nucleus	δ	Width / Hz	J_1 / Hz	J_2 / Hz
1 (a)	189.53	9		
2 (b)	-6.673	9	15.95	
3 (c)	0.000		-122.89	-148.24

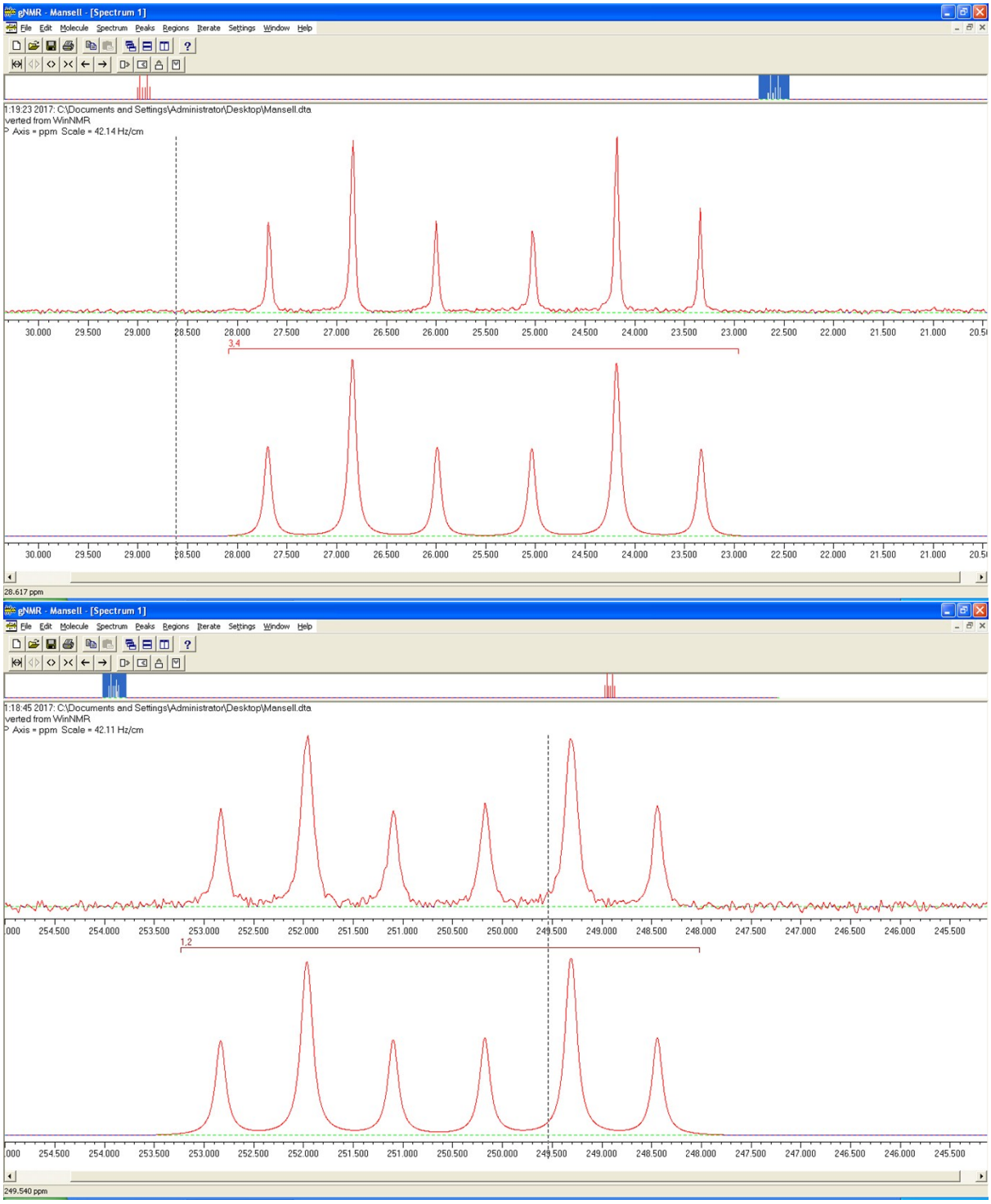

Figure S71. NMR simulation results for **2**: Experimental (top traces) and simulated (bottom traces) spectra for the phosphine and phosphinine regions of **2**.

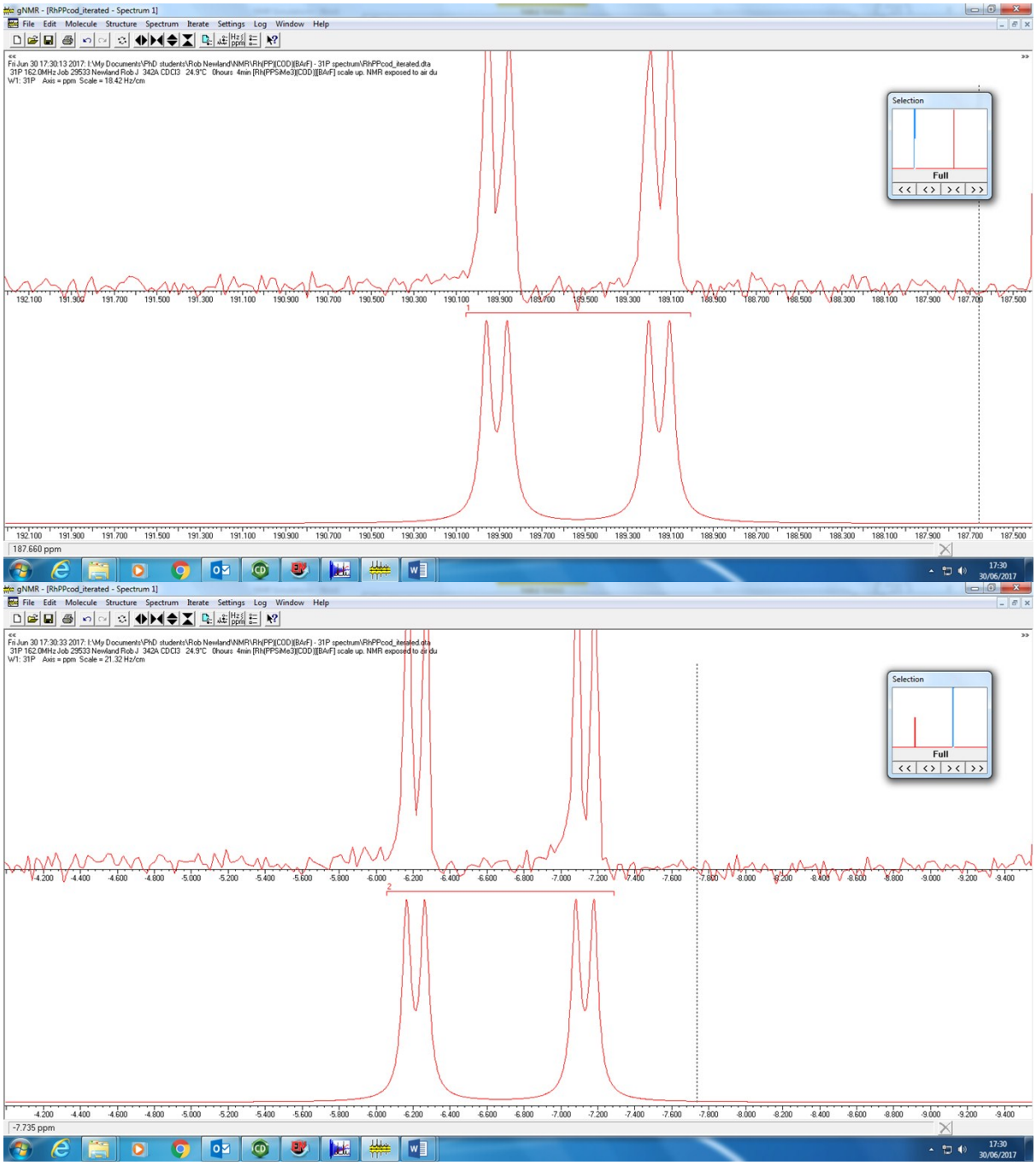

Figure S72. NMR simulation results for **3**: Experimental (top traces) and simulated (bottom traces) spectra for the phosphinine and phosphine regions of **3**.

References

1. R. J. Newland, M. F. Wyatt, R. L. Wingad and S. M. Mansell, *Dalton Trans.*, 2017, **46**, 6172-6176.
2. R. Cramer, J. A. McCleverty and J. Bray, in *Inorg. Synth.*, John Wiley & Sons, Inc., 2007, pp. 14-18.
3. D. L. Reger, T. D. Wright, C. A. Little, J. J. S. Lamba and M. D. Smith, *Inorg. Chem.*, 2001, **40**, 3810-3814.
4. J. A. Osborn, G. Wilkinson and J. J. Mrowca, in *Inorg. Synth.*, John Wiley & Sons, Inc., 2007, pp. 67-71.
5. G. Giordano, R. H. Crabtree, R. M. Heintz, D. Forster and D. E. Morris, in *Inorg. Synth.*, John Wiley & Sons, Inc., 2007, pp. 88-90.
6. S. C. Ensign, E. P. Vanable, G. D. Kortman, L. J. Weir and K. L. Hull, *J. Am. Chem. Soc.*, 2015, **137**, 13748-13751.
7. Z.-d. Mou, N. Deng, F. Zhang, J. Zhang, J. Cen and X. Zhang, *Eur. J. Med. Chem.*, 2017, **138**, 72-82.
8. Bruker AXS Inc., Madison, Wisconsin, USA, 2009
9. G. Sheldrick, *Acta Crystallogr., Sect. A: Found. Crystallogr.*, 2008, **64**, 112-122.
10. O. V. Dolomanov, L. J. Bourhis, R. J. Gildea, J. A. K. Howard and H. Puschmann, *J. Appl. Crystallogr.*, 2009, **42**, 339-341.
11. A. Y. Khalimon, P. Farha, L. G. Kuzmina and G. I. Nikonov, *Chem. Commun.*, 2012, **48**, 455-457.
12. D. Männig and H. Nöth, *Angewandte Chemie International Edition in English*, 1985, **24**, 878-879.
13. B. Breit, R. Winde, T. Mackewitz, R. Paciello and K. Harms, *Chem.-Eur. J.*, 2001, **7**, 3106-3121.
14. M. Doux, L. Ricard, F. Mathey, Pascal L. Floch and N. Mézailles, *Eur. J. Inorg. Chem.*, 2003, **2003**, 687-698.
15. B. Breit, R. Winde and K. Harms, *J. Chem. Soc., Perkin Trans. 1*, 1997, 2681-2682.
16. N. Mézailles, N. Avarvari, L. Ricard, F. Mathey and P. Le Floch, *Inorg. Chem.*, 1998, **37**, 5313-5316.
17. N. Avarvari, N. Mézailles, L. Ricard, P. L. Floch and F. Mathey, *Science*, 1998, **280**, 1587-1589.
18. A. C. Carrasco, E. A. Pidko, A. M. Masdeu-Bulto, M. Lutz, A. L. Spek, D. Vogt and C. Muller, *New J. Chem.*, 2010, **34**, 1547-1550.